Climate4you update February 2019

Contents:

February 2019 global surface air temperature overview

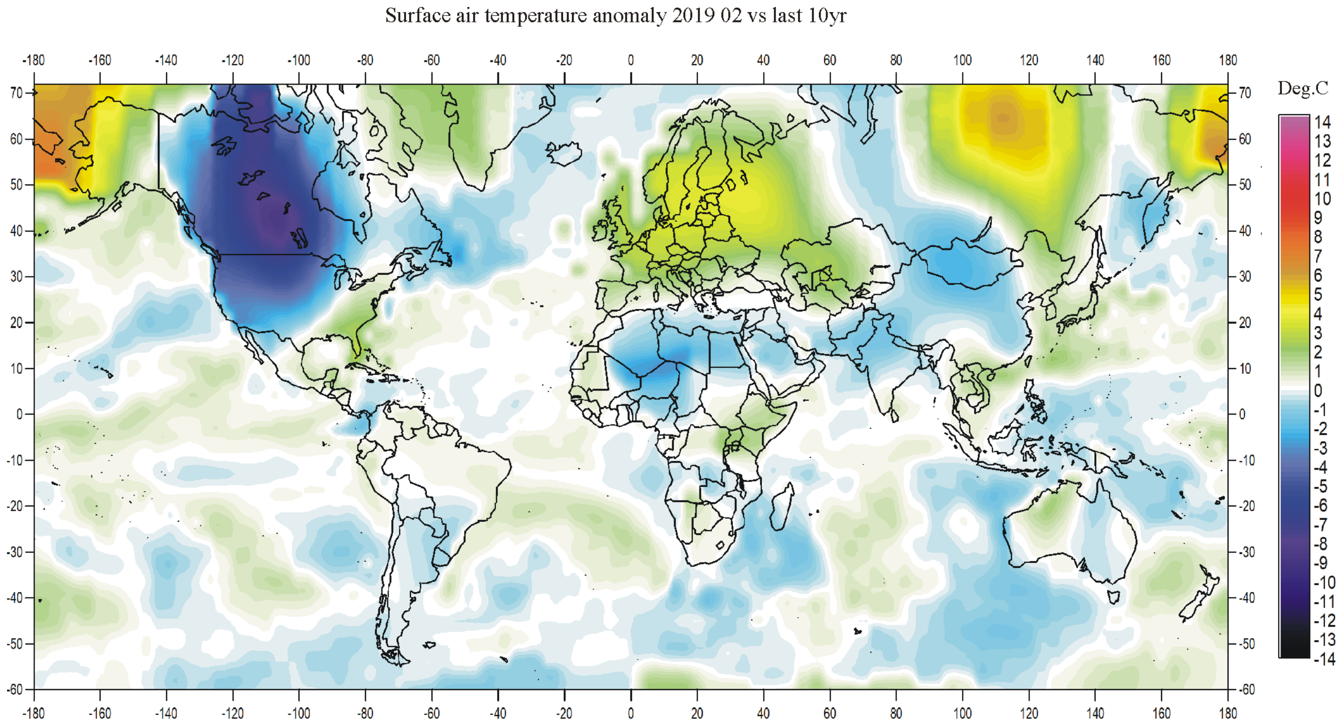

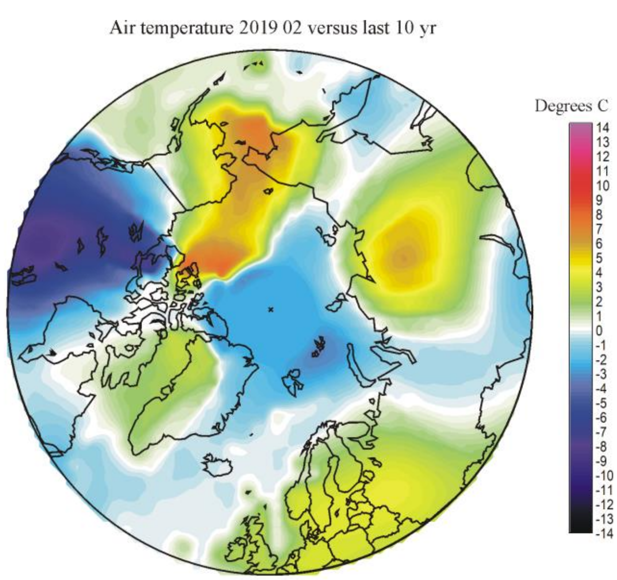

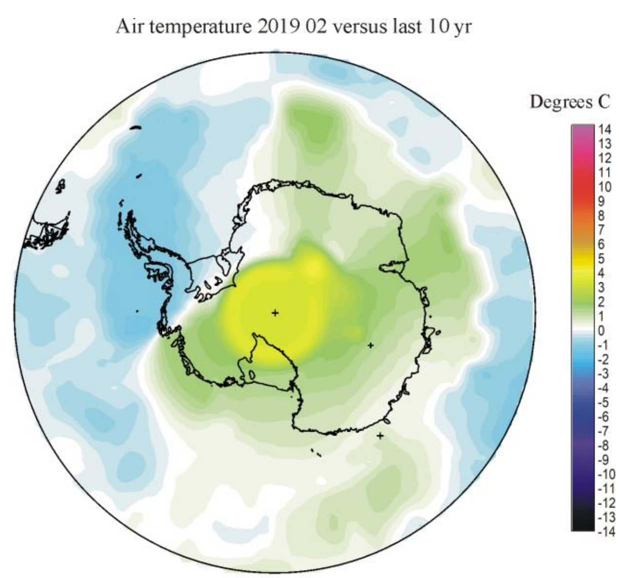

February 2019 surface air temperature compared to the average of the last 10 years. Green-yellow-red colours indicate areas with higher temperature than the 10-year average, while blue colours indicate lower than average temperatures. Data source: [Goddard Institute for Space Studies](#) (GISS) using Hadl_Reyn_v2 ocean surface temperatures.

Comments to the February 2019 global surface air temperature overview

General: This newsletter contains graphs showing a selection of key meteorological variables for the past month. *All temperatures are given in degrees Celsius*.

In the above maps showing the geographical pattern of surface air temperatures, *the last previous 10 years are used as reference period*.

The rationale for comparing with this recent period instead of the official WMO 'normal' period 1961-1990, is that the latter period is affected by the cold period 1945-1980. Most comparisons with this time period will automatically appear as warm, and it will be difficult to decide if modern surface air temperatures are increasing or decreasing. Comparing instead with the last previous 10 years overcomes this problem and displays the modern dynamics of ongoing change. This decadal approach also corresponds well to the typical memory horizon for many people.

In addition, the GISS temperature data used for preparing the above diagrams display distinct temporal instability for data before the turn of the century (see p. 7). Any comparison with the WMO 'normal' period 1961-1990 is therefore influenced by ongoing monthly mainly administrative changes. An unstable value is clearly not suited as reference value. Simply comparing with the last previous 10 years makes more sense and is more useful. See also the additional reflections on page 46.

The different air temperature records have been divided into three quality classes, QC1, QC2 and QC3, respectively, as described on page 7.

In many diagrams shown in this newsletter the thin line represents the monthly global average value, and the thick line indicate a simple running average, in most cases a simple moving 37-month average, nearly corresponding to a three-year average. The 37-month average is calculated from values covering a range from 18 months before to 18 months after, with equal weight given to all individual months.

The year 1979 has been chosen as starting point in many diagrams, as this roughly corresponds to both the beginning of satellite observations and the onset of the late 20th century warming period. However, several of the data series have a much longer record length, which may be inspected in greater detail on www.climate4you.com.

February 2019 global surface air temperatures

General: For February 2019 GISS supplied 15924 interpolated surface air data points; all values are used to produce the diagrams shown on page 2. According to the GISS data, the average global monthly temperature anomaly was slightly higher than in the previous month. However, the overall decrease of global surface air temperatures since the 2016-17 El Niño global temperature peak persists, as illustrated by the diagrams on p. 4-6.

The Northern Hemisphere anomality pattern was characterised by large regional contrasts. Most of North America were cold compared to the previous 10 years, especially Canada. Also, northern Africa was relatively cold. In contrast, much of Europe, parts of Siberia and Alaska was relatively warm. Central Arctic remained relatively cold. However, the GISS surface air temperatures north of 80° N still appears to have an issue with interpolation, resulting in an unrealistic circular anomaly pattern.

Near the Equator temperatures were largely near the 10-year average. In the Pacific, however, temperatures were somewhat above average, signifying the initial phase of a weak (?) new El Niño episode (see p. 22).

The Southern Hemisphere temperatures were near or below the average for the previous 10 years. Especially the ocean SW and S of Australia was relatively cold. Also, much of South America remained relatively cold. In contrast, the oceans around New Zealand were relatively warm. In the Antarctica, much of the continent was relatively warm, except for the Antarctic Peninsula. South of 80°S the GISS anomaly pattern is influenced by an interpolation artefact.

Temperature quality class 1: Lower troposphere temperature from satellites, updated to February 2019

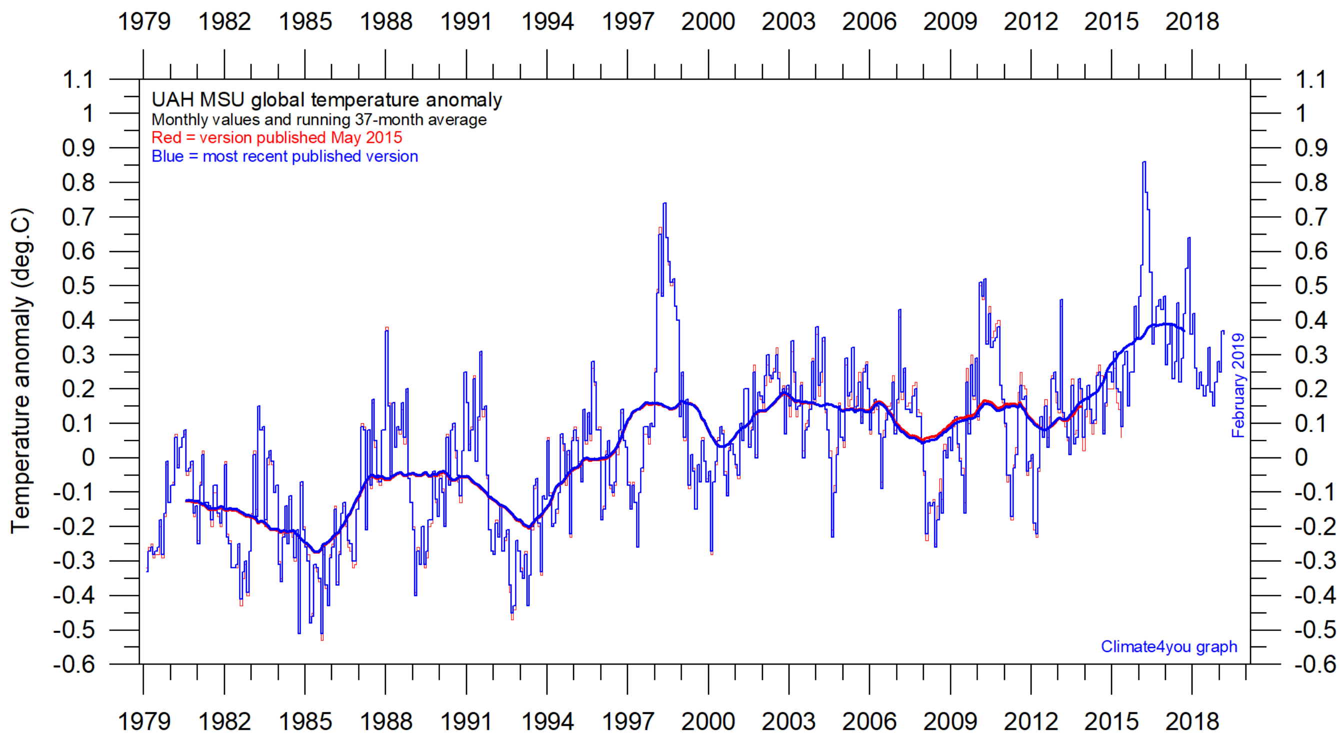

Global monthly average lower troposphere temperature (thin line) since 1979 according to University of Alabama at Huntsville, USA. The thick line is the simple running 37-month average.

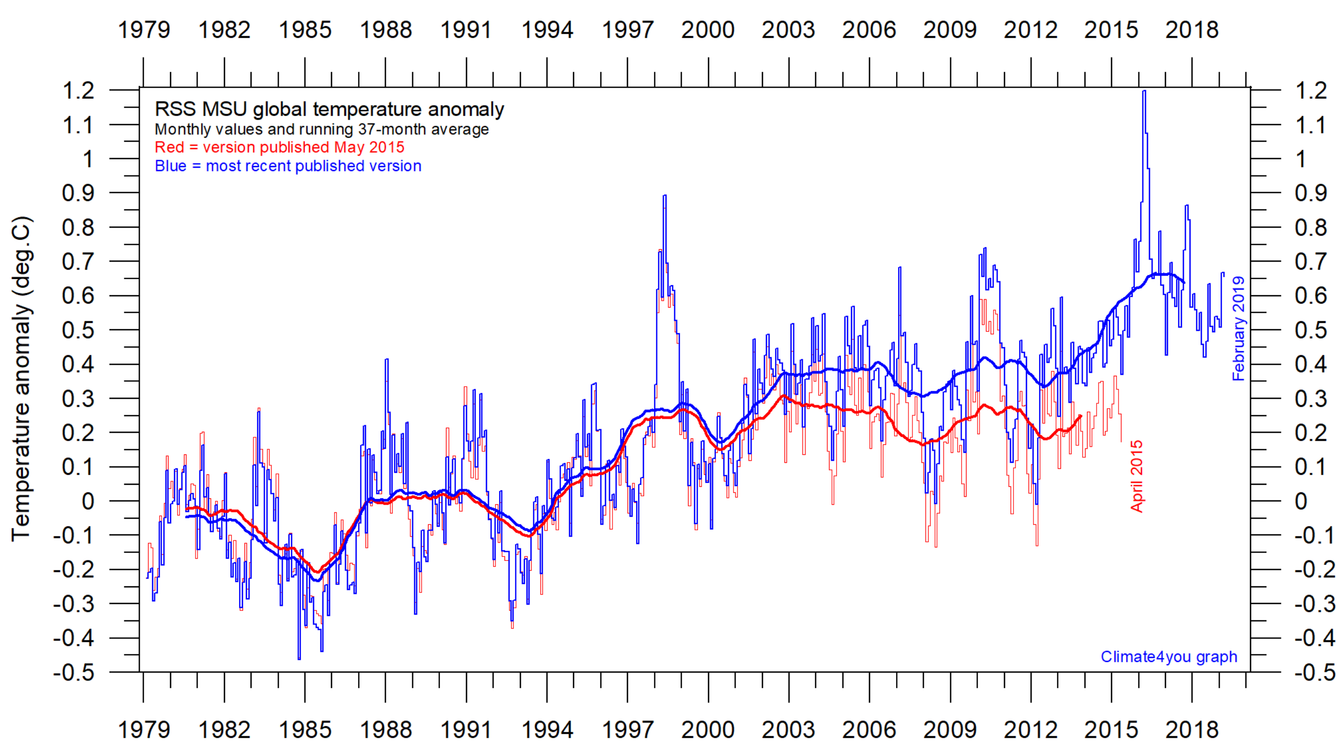

Global monthly average lower troposphere temperature (thin line) since 1979 according to according to Remote Sensing Systems (RSS), USA. The thick line is the simple running 37-month average.

Temperature quality class 2: HadCRUT global surface air temperature, updated to January 2019

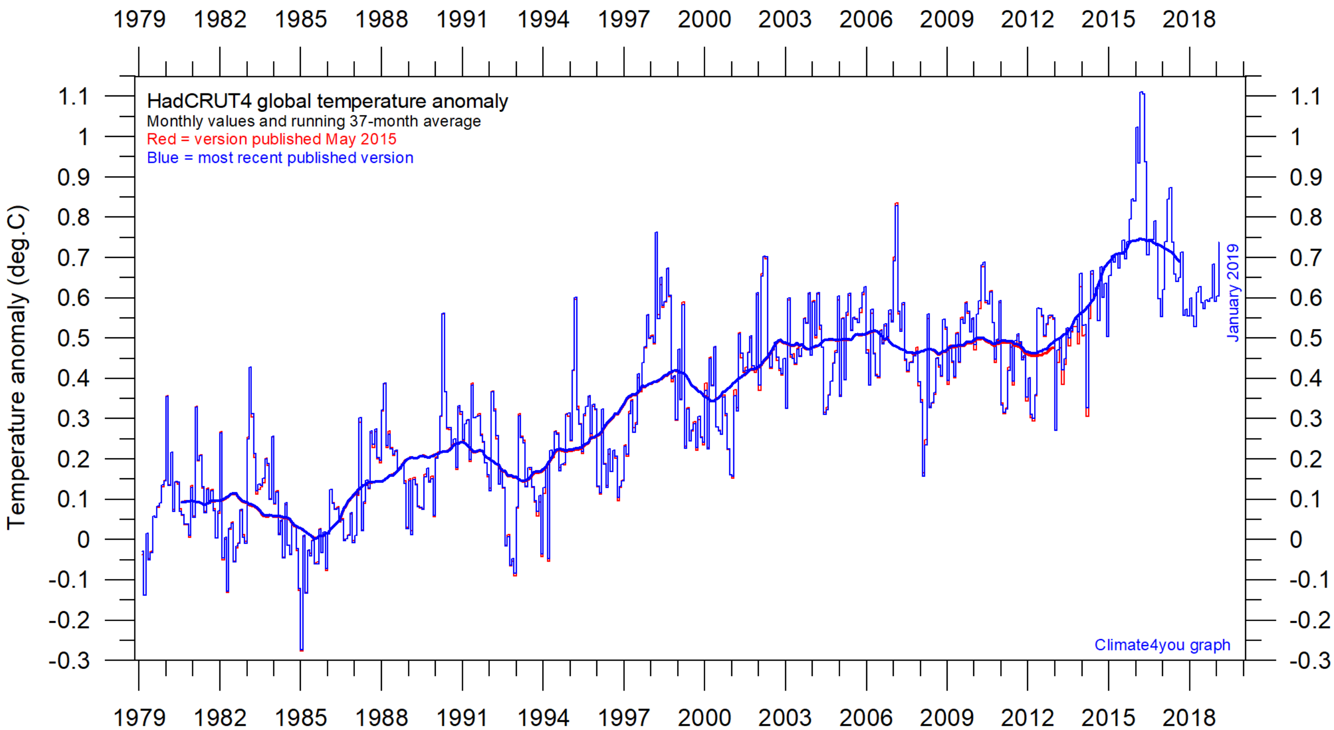

Global monthly average surface air temperature (thin line) since 1979 according to according to the Hadley Centre for Climate Prediction and Research and the University of East Anglia's [Climatic Research Unit](#) ([CRU](#)), UK. The thick line is the simple running 37-month average.

Temperature quality class 3: GISS and NCDC global surface air temperature, updated to February 2019

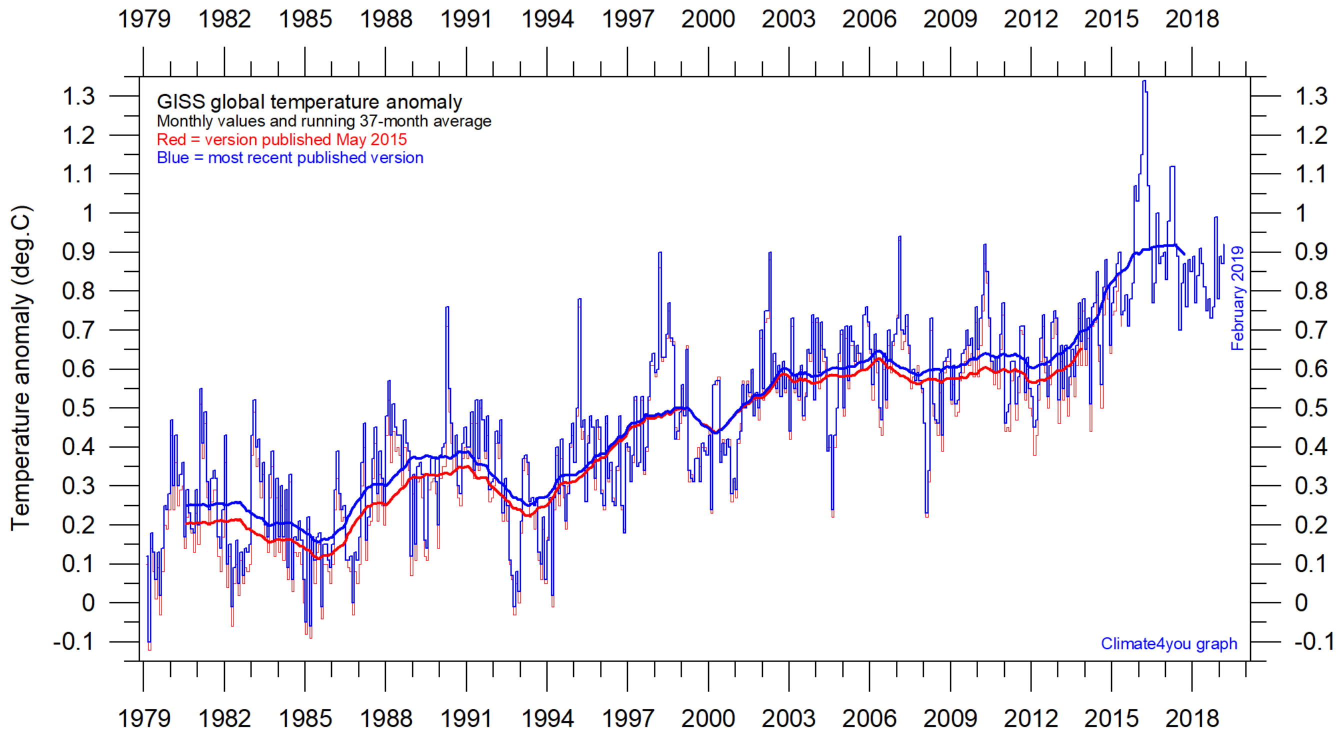

Global monthly average surface air temperature (thin line) since 1979 according to according to the [Goddard Institute for Space Studies](#) (GISS), at Columbia University, New York City, USA, using ERSST_v4 ocean surface temperatures. The thick line is the simple running 37-month average.

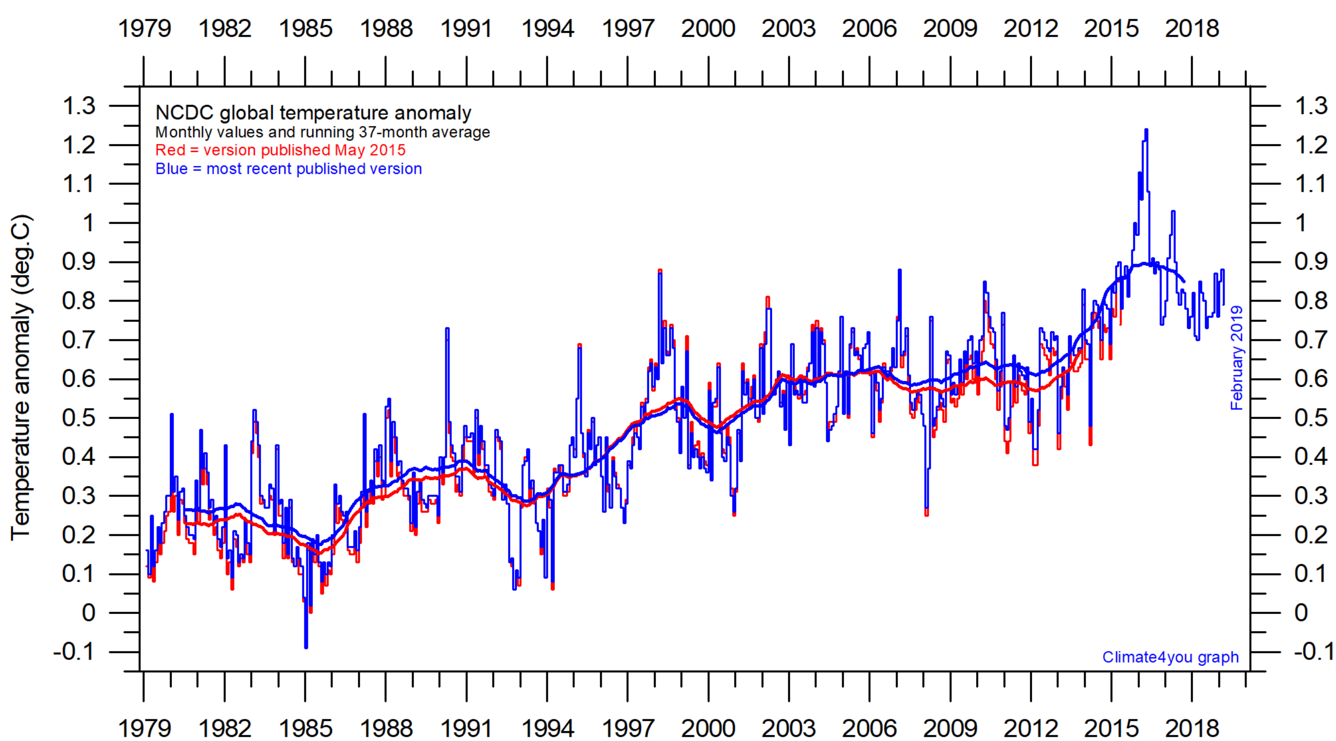

Global monthly average surface air temperature since 1979 according to according to the [National Climatic Data Center](#) (NCDC), USA. The thick line is the simple running 37-month average.

A note on data record stability and -quality:

The temperature diagrams shown above all have 1979 as starting year. This roughly marks the beginning of the recent episode of global warming, after termination of the previous episode of global cooling from about 1940. In addition, the year 1979 also represents the starting date for the satellite-based global temperature estimates (UAH and RSS). For the three surface air temperature records (HadCRUT, NCDC and GISS), they begin much earlier (in 1850 and 1880, respectively), as can be inspected on www.climate4you.com.

For all three surface air temperature records, but especially NCDC and GISS, administrative changes to anomaly values are quite often introduced, even for observations many years back in time. Some changes may be due to the delayed addition of new station data or change of station location, while others probably have their origin in changes of the technique adopted to calculate average values. It is clearly impossible to evaluate the validity of such administrative changes for the outside user of these records; it is only possible to note that such changes appear very often (se example diagram next page).

In addition, the three surface records represent a blend of sea surface data collected by moving ships or by other means, plus data from land stations of partly unknown quality and unknown degree of representativeness for their region. Many of the land stations also has been moved geographically during their period of operation, their instrumentation have been changed, and they are influenced by changes in their near surroundings (vegetation, buildings, etc.).

The satellite temperature records also have their problems, but these are generally of a more technical nature and therefore correctable. In addition, the temperature sampling by satellites is more regular and complete on a global basis than that represented by the surface records. It is also important that the sensors on satellites measure temperature directly by emitted radiation, while most surface temperature measurements are indirect, using electronic resistance.

Everybody interested in climate science should gratefully acknowledge the efforts put into maintaining the different temperature databases referred to in the present newsletter. At the same time, however, it is also important to realise that all temperature records cannot be of equal scientific quality. The simple fact that they to some degree differ shows that they cannot all be correct.

On this background, and for practical reasons, Climate4you operates with three quality classes (1-3) for global temperature records, with 1 representing the highest quality level:

Quality class 1: The satellite records (UAH and RSS).

Quality class 2: The HadCRUT surface record.

Quality class 3: The NCDC and GISS surface records.

The main reason for discriminating between the three surface records is the following:

While both NCDC and GISS often experience quite large administrative changes (see example on p.8), and therefore essentially are unstable temperature records, the changes introduced to HadCRUT are fewer and smaller. For obvious reasons, as the past does not change, any record undergoing continuing changes cannot describe the past correctly all the time. Frequent and large corrections in a database also signal a fundamental doubt about what is likely to represent the correct values.

You can find more on the issue of lack of temporal stability on www.climate4you.com (go to: *Global Temperature*, followed by *Temporal Stability*).

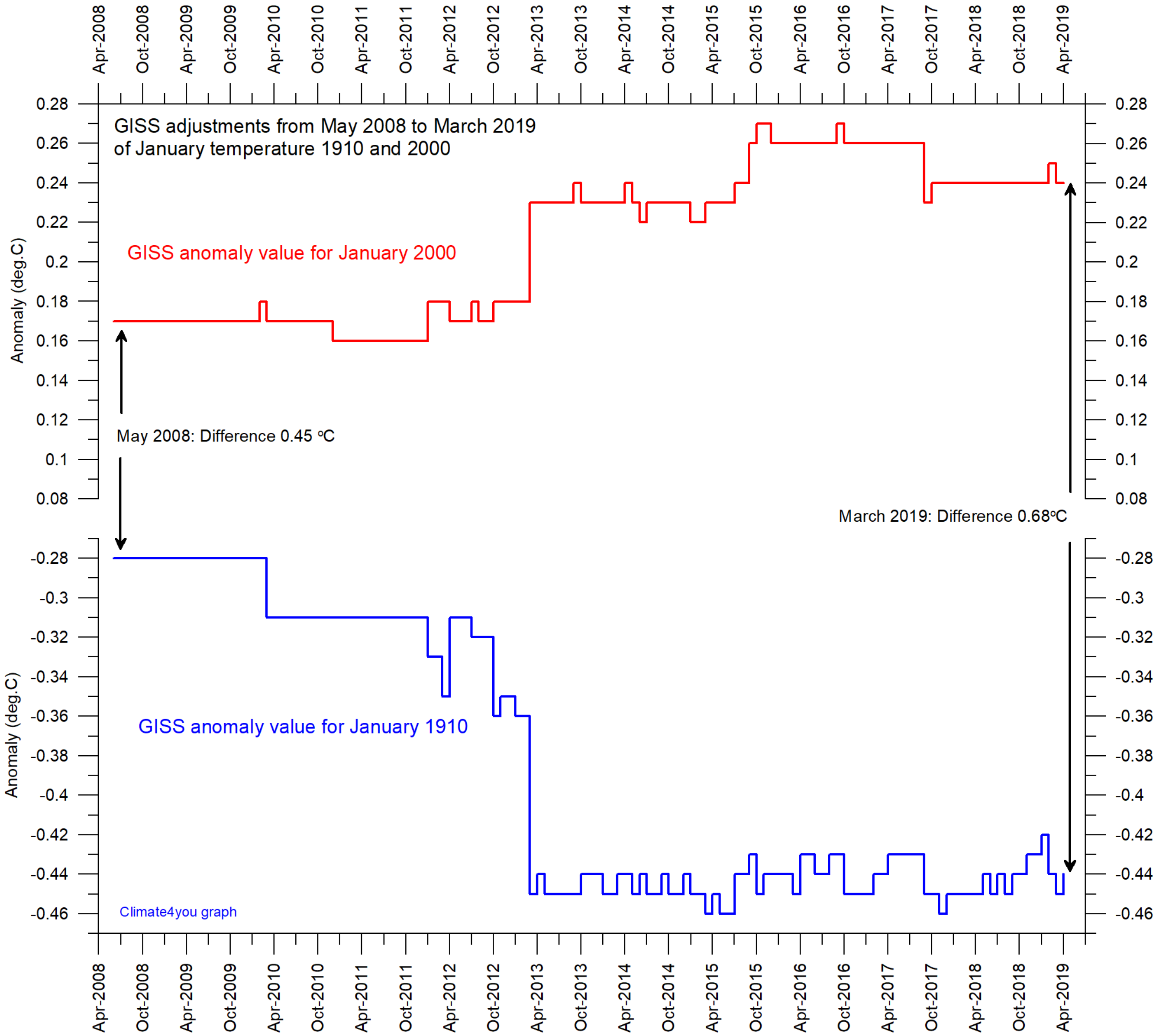

Diagram showing the adjustments made since May 2008 by the [Goddard Institute for Space Studies](#) (GISS), USA, in published anomaly values for the months January 1910 and January 2000.

<u>Note:</u> The administrative upsurge of the temperature increase from January 1915 to January 2000 has grown from 0.45 (reported May 2008) to 0.68°C (reported March 2019). This represents an about 51% administrative temperature increase over this period, meaning that more than half of the apparent global temperature increase from January 1910 to January 2000 (as reported by GISS) is due to administrative changes of the original data since May 2008.

[Comparing global surface air temperature and lower troposphere satellite temperatures; updated to January 2019]

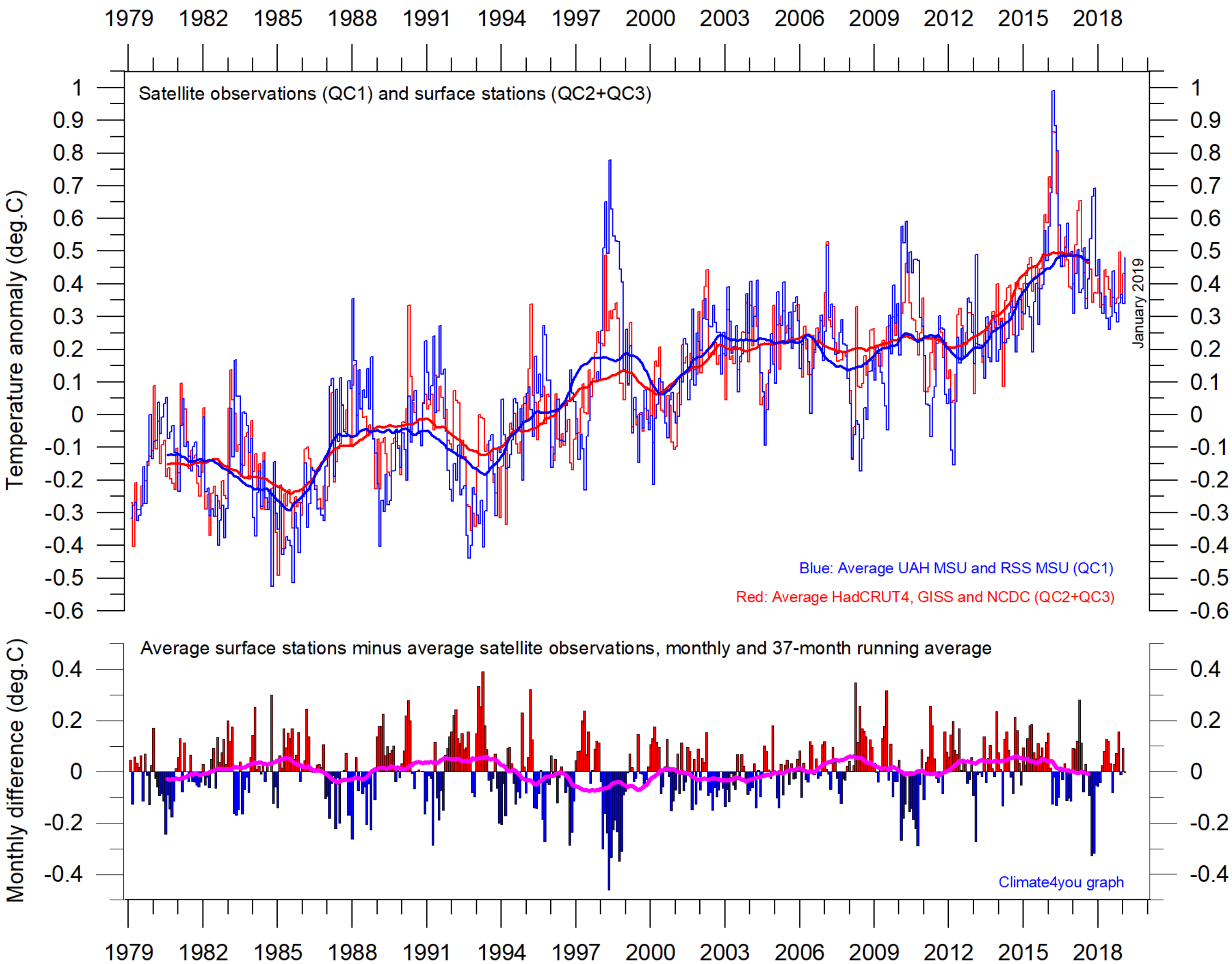

Plot showing the average of monthly global surface air temperature estimates ([HadCRUT4], [GISS] and [NCDC]) and satellite-based temperature estimates ([RSS MSU] and [UAH MSU]). The thin lines indicate the monthly value, while the thick lines represent the simple running 37-month average, nearly corresponding to a running 3-yr average. The lower panel shows the monthly difference between average surface air temperature and satellite temperatures. As the base period differs for the different temperature estimates, they have all been normalised by comparing to the average value of 30 years from January 1979 to December 2008.

Global air temperature linear trends updated to January 2019

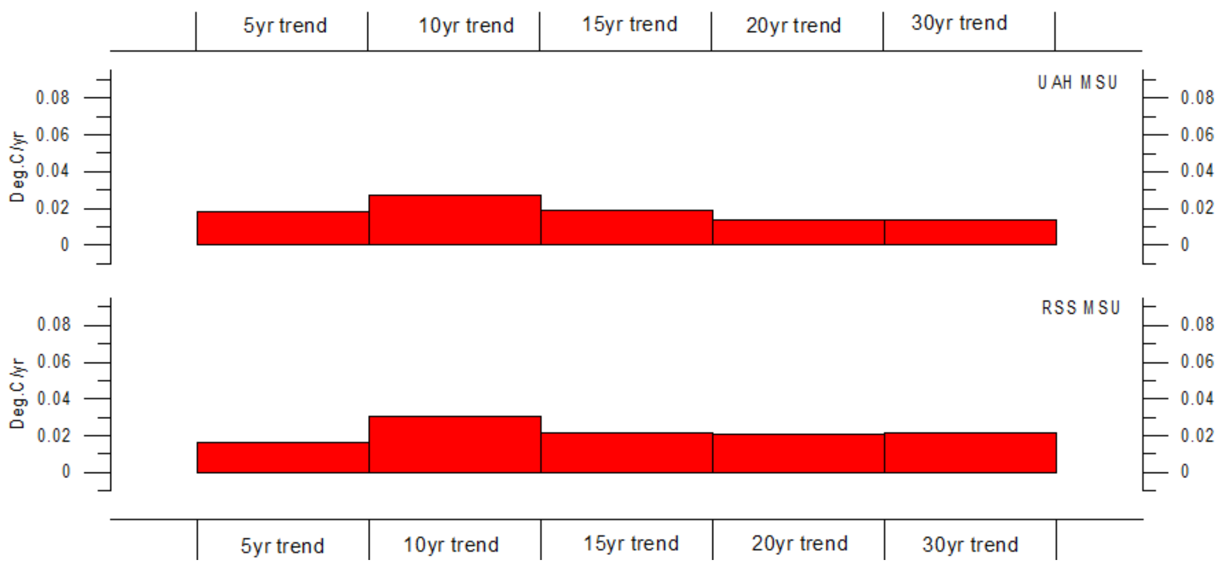

Diagram showing the latest 5, 10, 20 and 30-yr linear annual global temperature trend, calculated as the slope of the linear regression line through the data points, for two satellite-based temperature estimates (UAH MSU and RSS MSU).

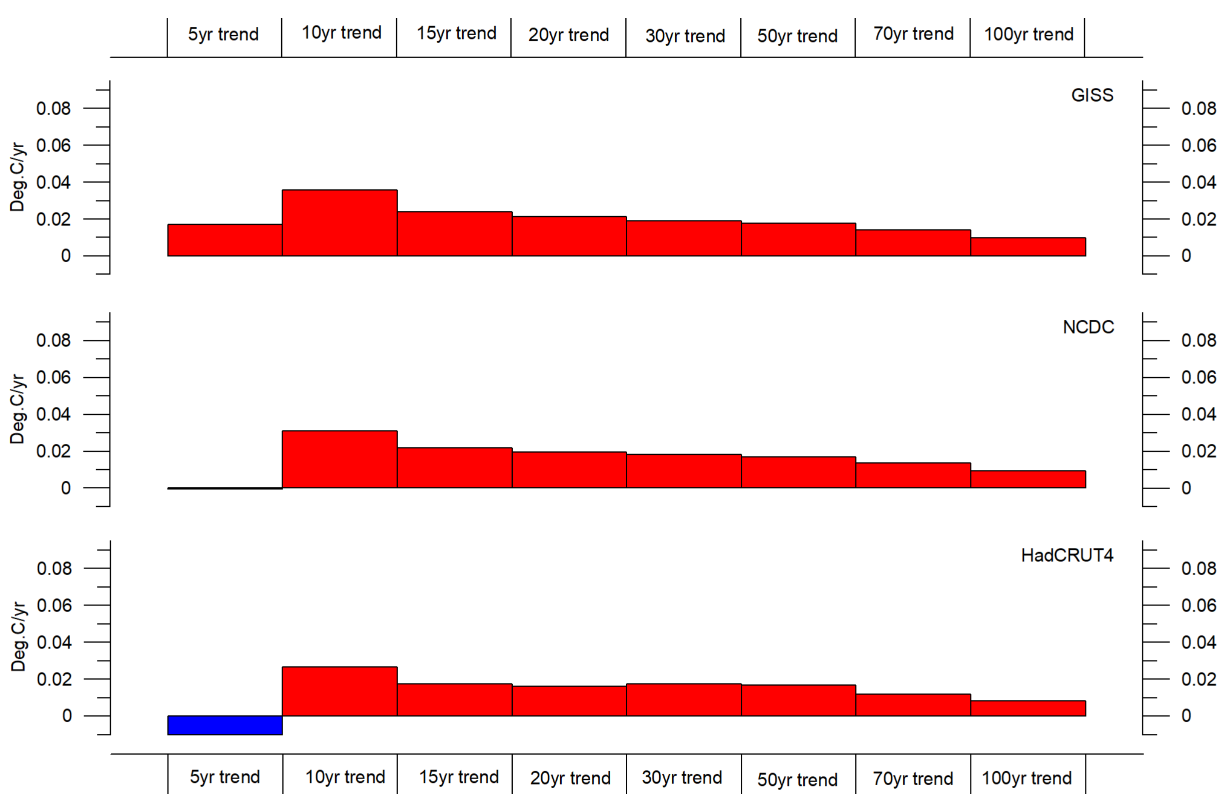

Diagram showing the latest 5, 10, 20, 30, 50, 70 and 100-year linear annual global temperature trend, calculated as the slope of the linear regression line through the data points, for three surface-based temperature estimates (GISS, NCDC and HadCRUT4).

All in one, Quality Class 1, 2 and 3; updated to January 2019

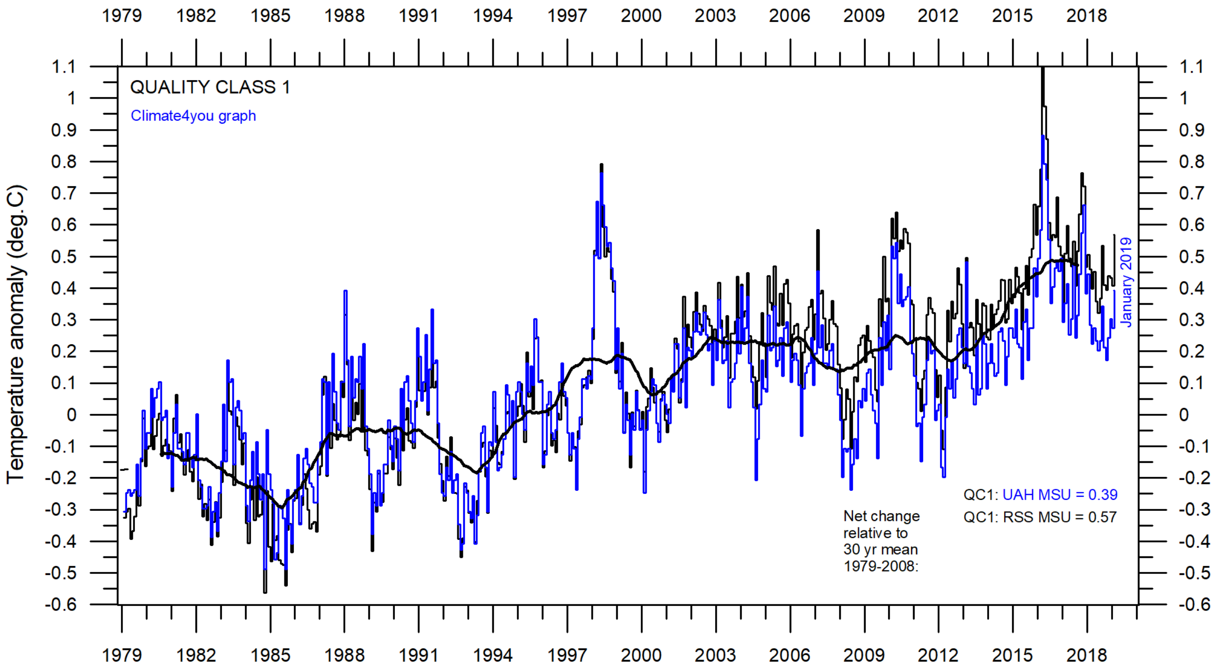

Superimposed plot of Quality Class 1 (UAH and RSS) global monthly temperature estimates. As the base period differs for the individual temperature estimates, they have all been normalised by comparing with the average value of the initial 120 months (30 years) from January 1979 to December 2008. The heavy black line represents the simple running 37 month (c. 3 year) mean of the average of both temperature records. The numbers shown in the lower right corner represent the temperature anomaly relative to the individual 1979-2008 averages.

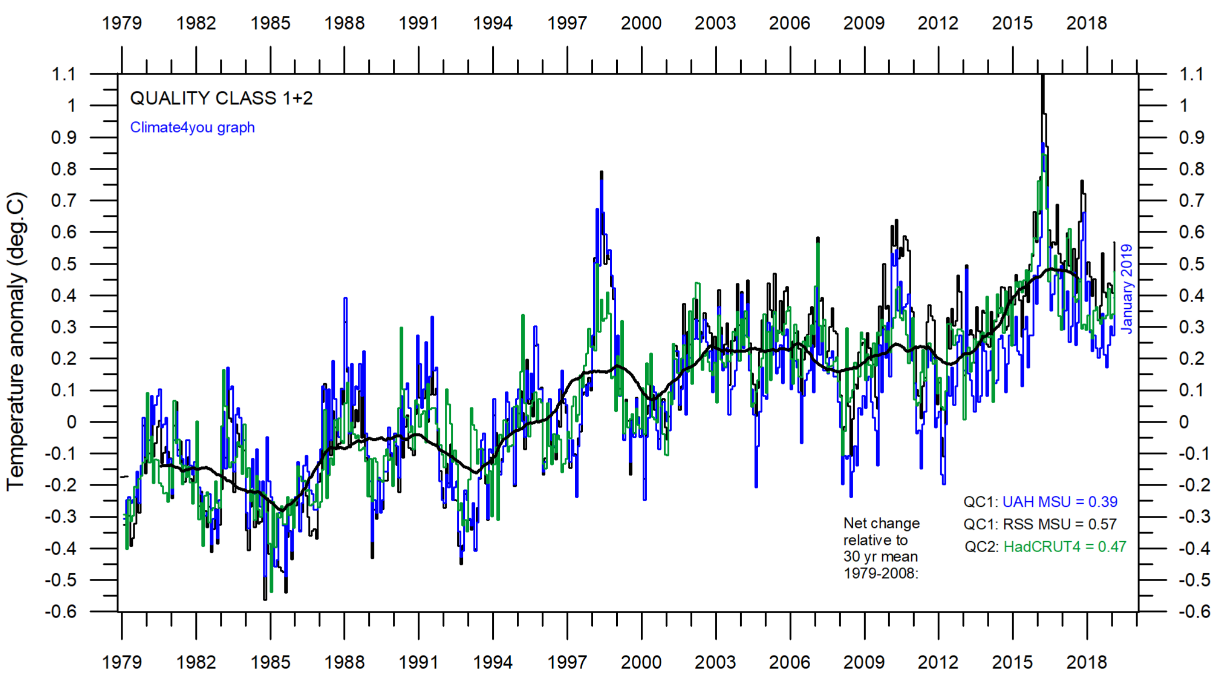

Superimposed plot of Quality Class 1 and 2 (UAH, RSS and HadCRUT4) global monthly temperature estimates. As the base period differs for the individual temperature estimates, they have all been normalised by comparing with the average value of the initial 120 months (30 years) from January 1979 to December 2008. The heavy black line represents the simple running 37 month (c. 3 year) mean of the average of all three temperature records. The numbers shown in the lower right corner represent the temperature anomaly relative to the individual 1979-2008 averages.

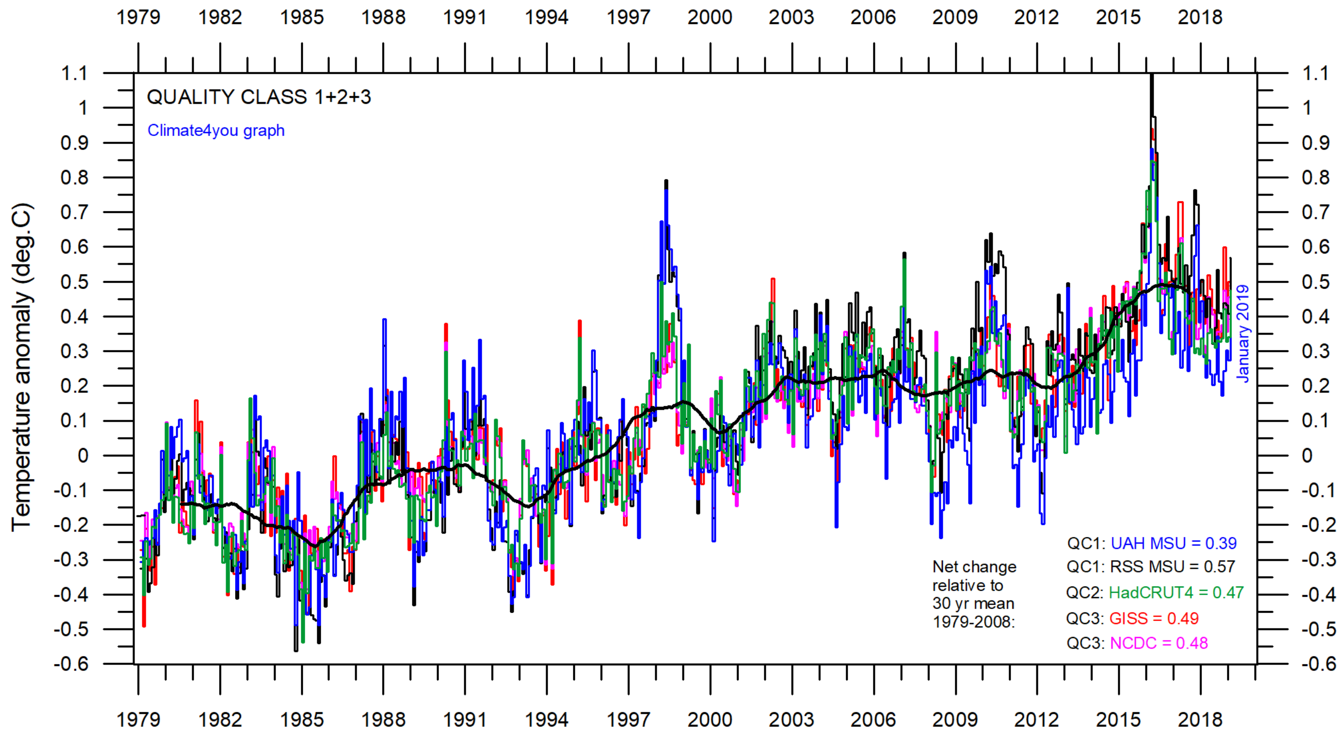

Superimposed plot of Quality Class 1, 2 and 3 global monthly temperature estimates (UAH, RSS, HadCRUT4, GISS and NCDC). As the base period differs for the individual temperature estimates, they have all been normalised by comparing with the average value of the initial 120 months (30 years) from January 1979 to December 2008. The heavy black line represents the simple running 37 month (c. 3 year) mean of the average of all five temperature records. The numbers shown in the lower right corner represent the temperature anomaly relative to the individual 1979-2008 averages.

Please see notes on page 7 relating to the above three quality classes.

Satellite- and surface-based temperature estimates are derived from different types of measurements, and that comparing them directly as done in the diagrams above therefore may be questionable.

However, as both types of estimate often are discussed together, the above diagrams may nevertheless be of interest. In fact, the different types of temperature estimates appear to agree as to the overall temperature variations on a 2-3-year scale, although on a shorter time scale there are often considerable differences between the individual records. However, since about 2003 the surface records are slowly drifting towards higher temperatures than the combined satellite record (see p. 9).

The average of all five global temperature estimates presently shows an overall stagnation, at least since 2002-2003. There has been no significant increase in global air temperature since 1998, which however was affected by the oceanographic El Niño event. Also, the recent (2015-16) strong El Niño event probably represents a relatively short-lived spike on a longer development. The coming years will show if this is the case or not. Neither has there been a temperature decrease since about 2002-2003. See also diagram on page 47.

The present temperature stagnation does not exclude the possibility that global temperatures will begin to increase significantly again later. On the other hand, it also remains a possibility that Earth just now is passing an overall temperature peak, and that global temperatures will begin to decrease during the coming years. Again, time will show which of these possibilities is correct.

Global sea surface temperature, updated to February 2019

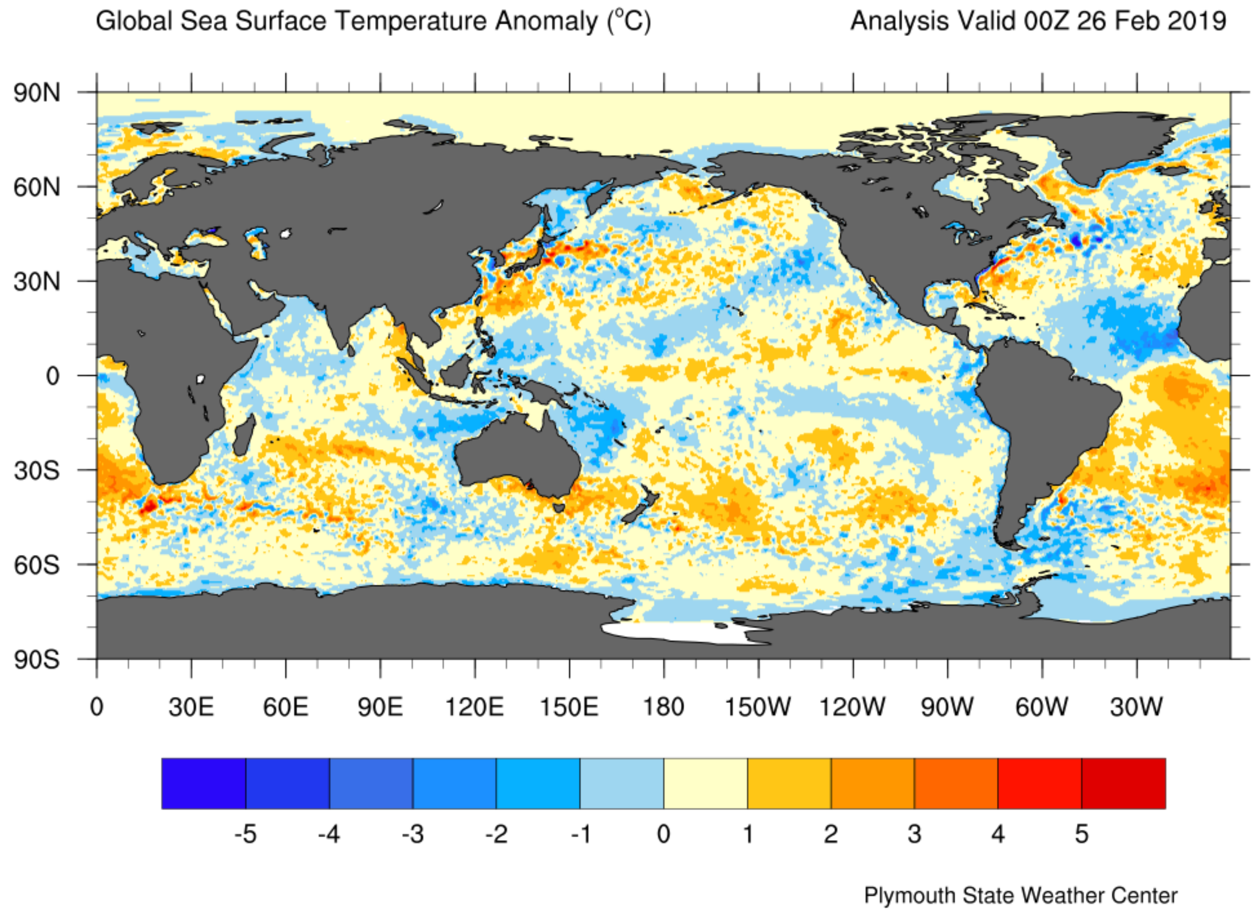

Sea surface temperature anomaly on 26 February 2019. Map source: Plymouth State Weather Center. Reference period: 1977-1991.

Because of the large surface areas near Equator, the temperature of the surface water in these regions is especially important for the global atmospheric temperature (p. 4-6). In fact, 50% of planet Earth's surface area is located within 30°N and 30°S.

A mixture of relatively warm and cold water dominates much of the oceans near the Equator. In addition, parts of the North Atlantic are cooling, while the South Atlantic is warming. All this will be influencing global air temperatures in the months to come.

However, the significance of any short-term cooling or warming reflected in air temperatures should not be overstated. Whenever Earth experiences cold La Niña or warm El Niño episodes (Pacific Ocean) major heat exchanges takes place between the Pacific Ocean and the atmosphere above, eventually showing up in estimates of the global air temperature.

However, this does not reflect similar changes in the total heat content of the atmosphere-ocean system. In fact, global net changes can be small and such heat exchanges may mainly reflect redistribution of energy between ocean and atmosphere. What matters is the overall temperature development when seen over several years.

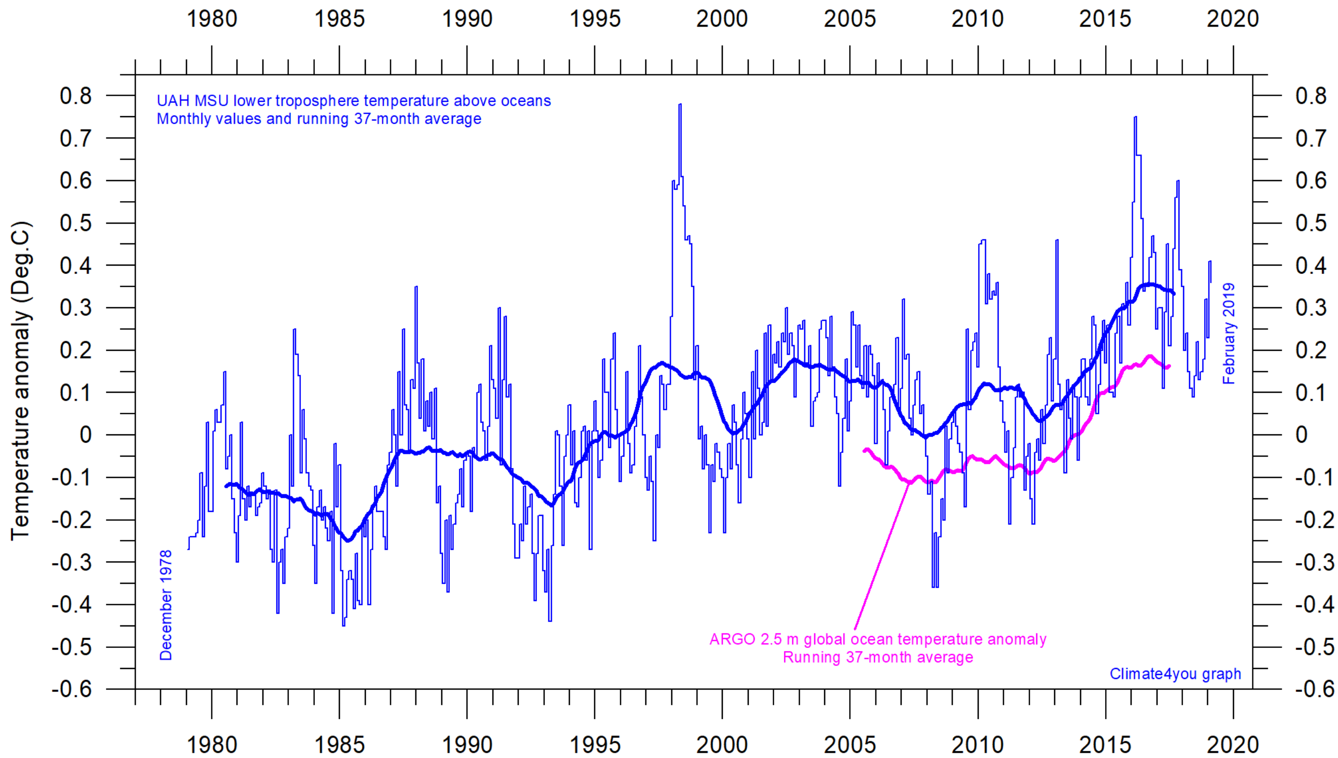

Global monthly average lower troposphere temperature over oceans (thin line) since 1979 according to [University of Alabama]() at Huntsville, USA. The thick line is the simple running 37-month average. Insert: Argo global ocean temperature anomaly from floats.

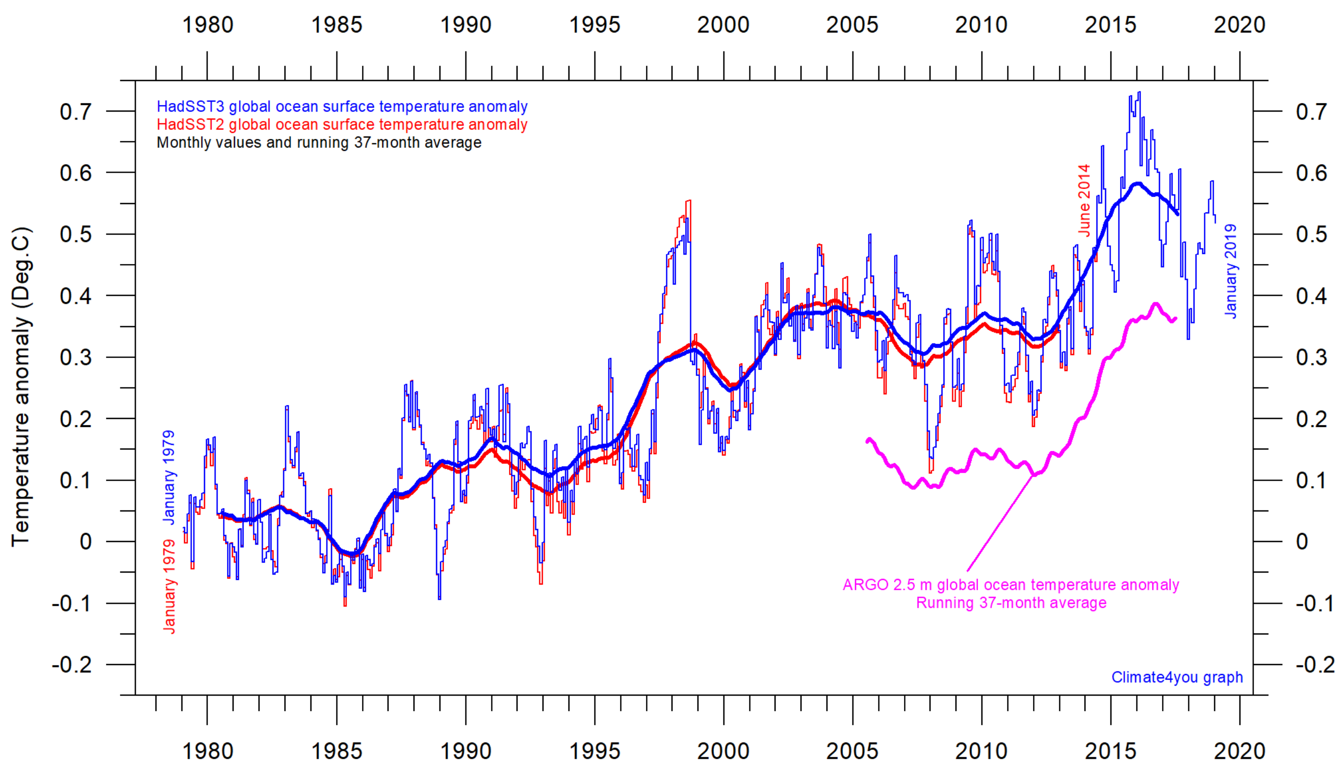

Global monthly average sea surface temperature since 1979 according to University of East Anglia's [Climatic Research Unit]() ([CRU]()), UK. Base period: 1961-1990. The thick line is the simple running 37-month average. Insert: Argo global ocean temperature anomaly from floats.

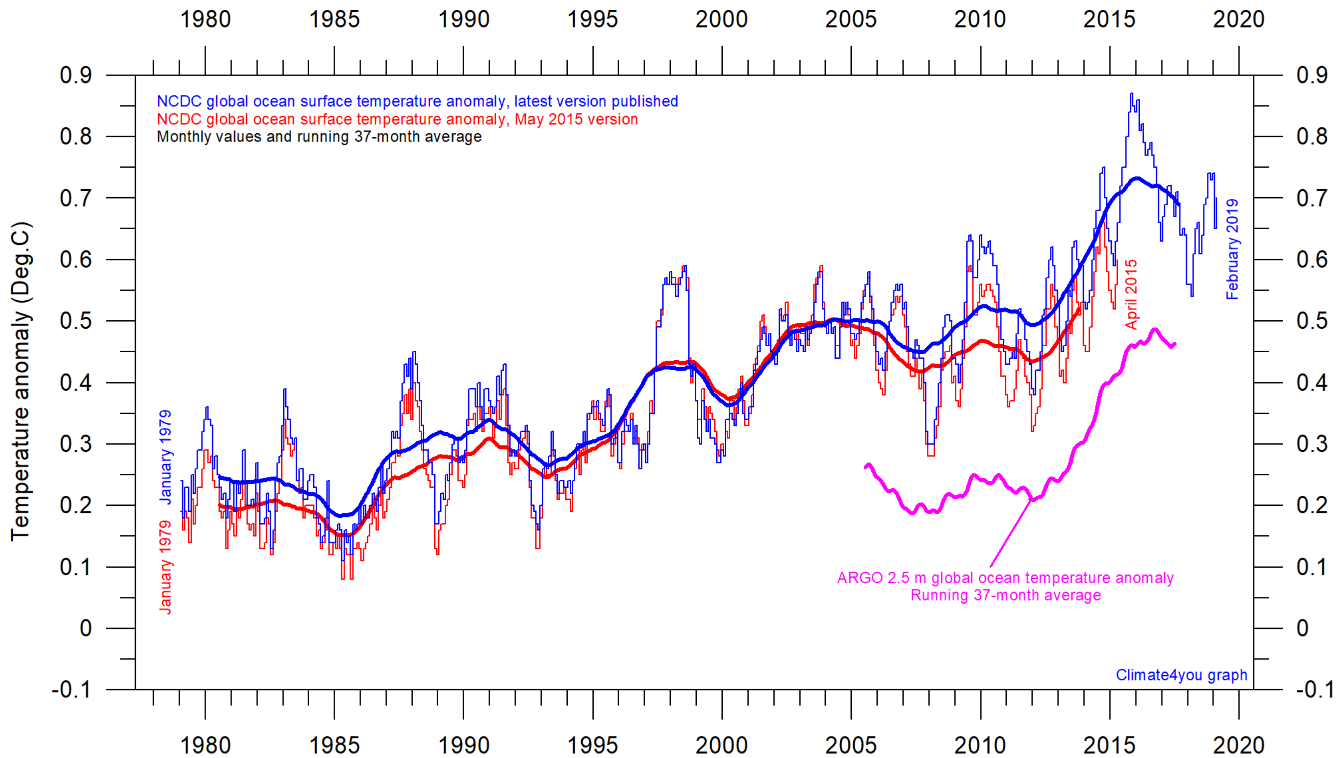

Global monthly average sea surface temperature since 1979 according to the National Climatic Data Center (NCDC), USA. Base period: 1901-2000. The thick line is the simple running 37-month average. Insert: Argo global ocean temperature anomaly from floats.

June 18, 2015: *NCDC has introduced several rather large administrative changes to their sea surface temperature record. The overall result is to produce a record giving the impression of a continuous temperature increase, also in the 21st century. As the oceans cover about 71% of the entire surface of planet Earth, the effect of this administrative change is clearly seen in the NCDC record for global surface air temperature (p. 6).*

Ocean temperature in uppermost 100 m, updated to December 2018

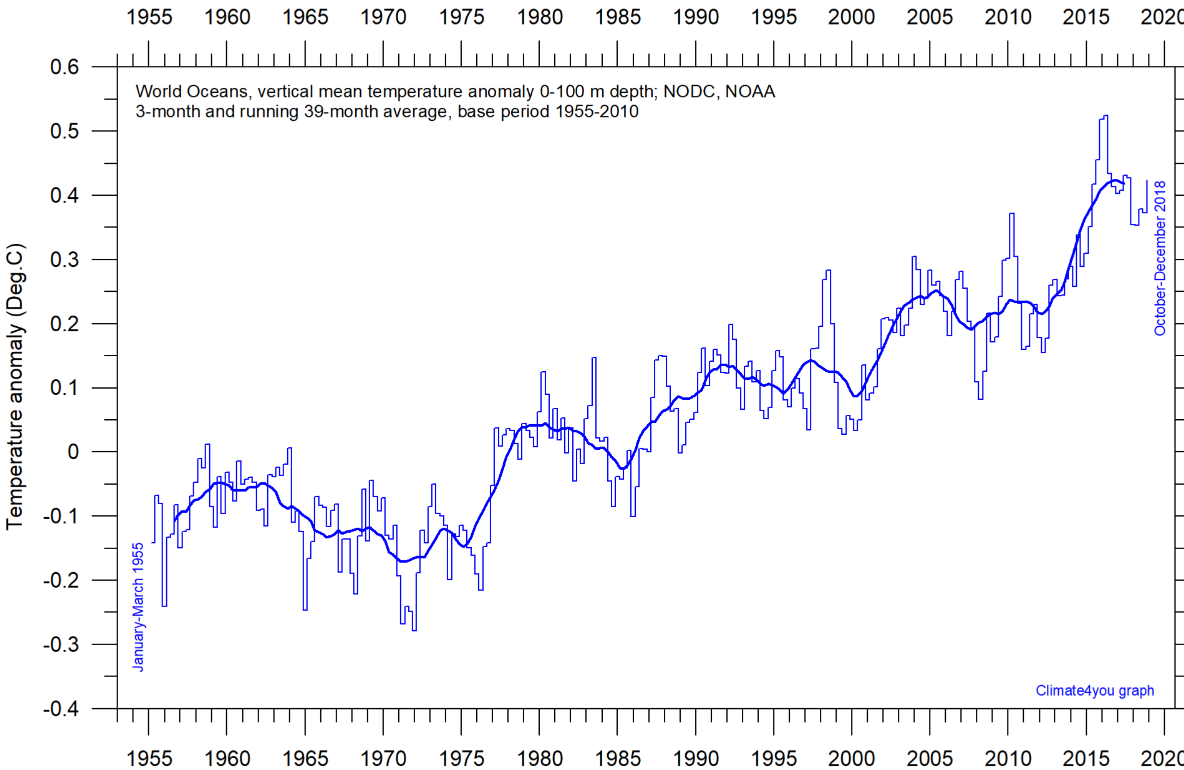

World Oceans vertical average temperature 0-100 m depth since 1955. The thin line indicates 3-month values, and the thick line represents the simple running 39-month (c. 3 year) average. Data source: [NOAA National Oceanographic Data Center](#) (NODC). Base period 1955-2010.

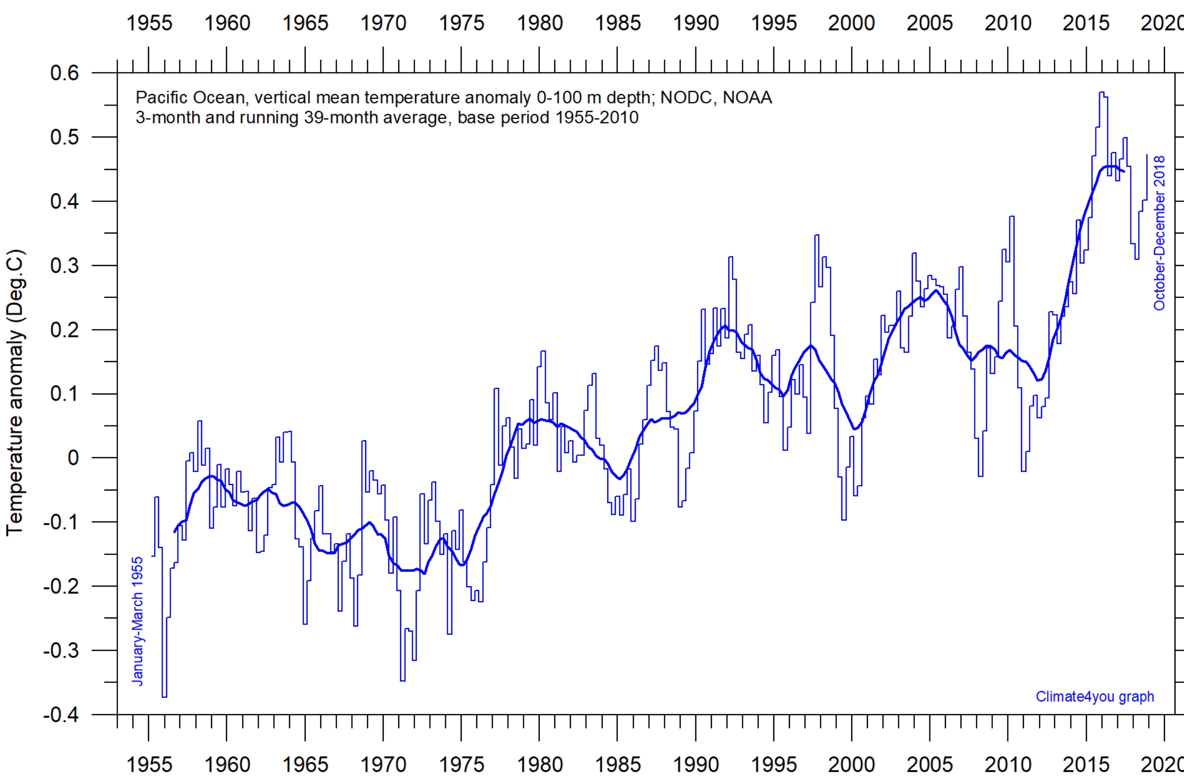

Pacific Ocean vertical average temperature 0-100 m depth since 1955. The thin line indicate 3-month values, and the thick line represents the simple running 39-month (c. 3 year) average. Data source: [NOAA National Oceanographic Data Center](#) (NODC). Base period 1955-2010.

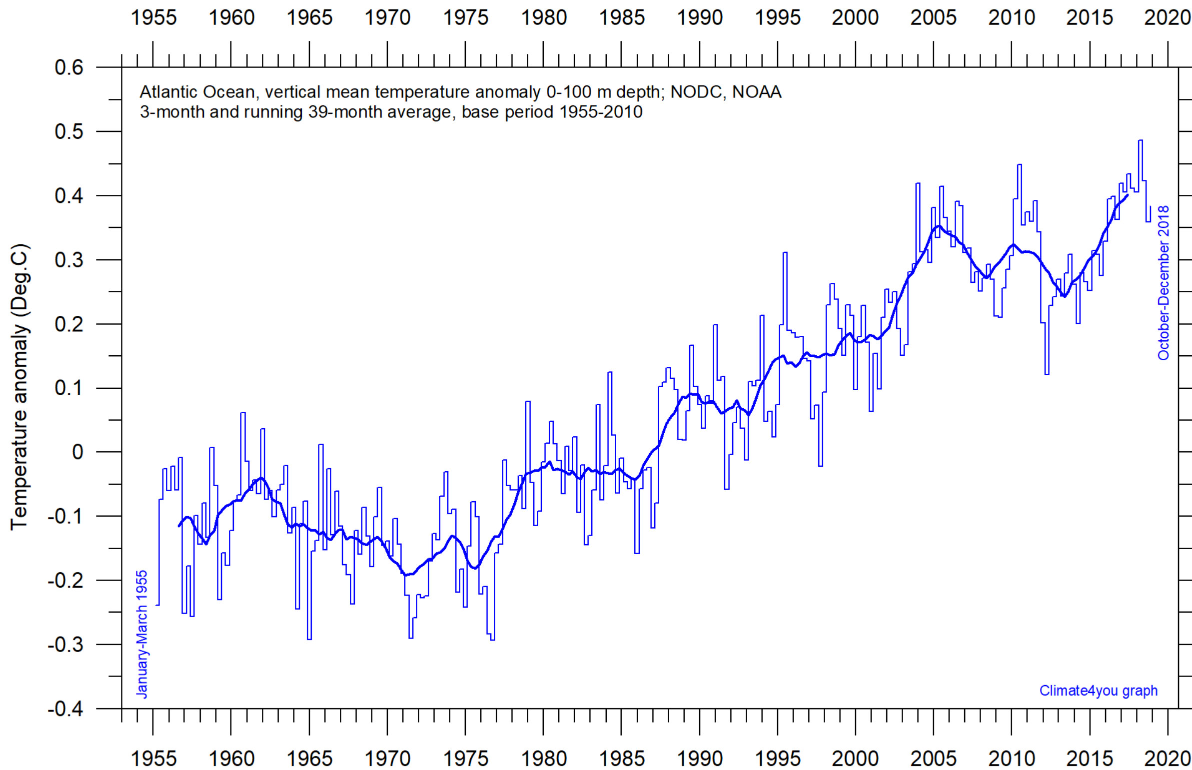

Atlantic Ocean vertical average temperature 0-100 m depth since 1955. The thin line indicate 3-month values, and the thick line represents the simple running 39-month (c. 3 year) average. Data source: [NOAA National Oceanographic Data Center] (NODC). Base period 1955-2010.

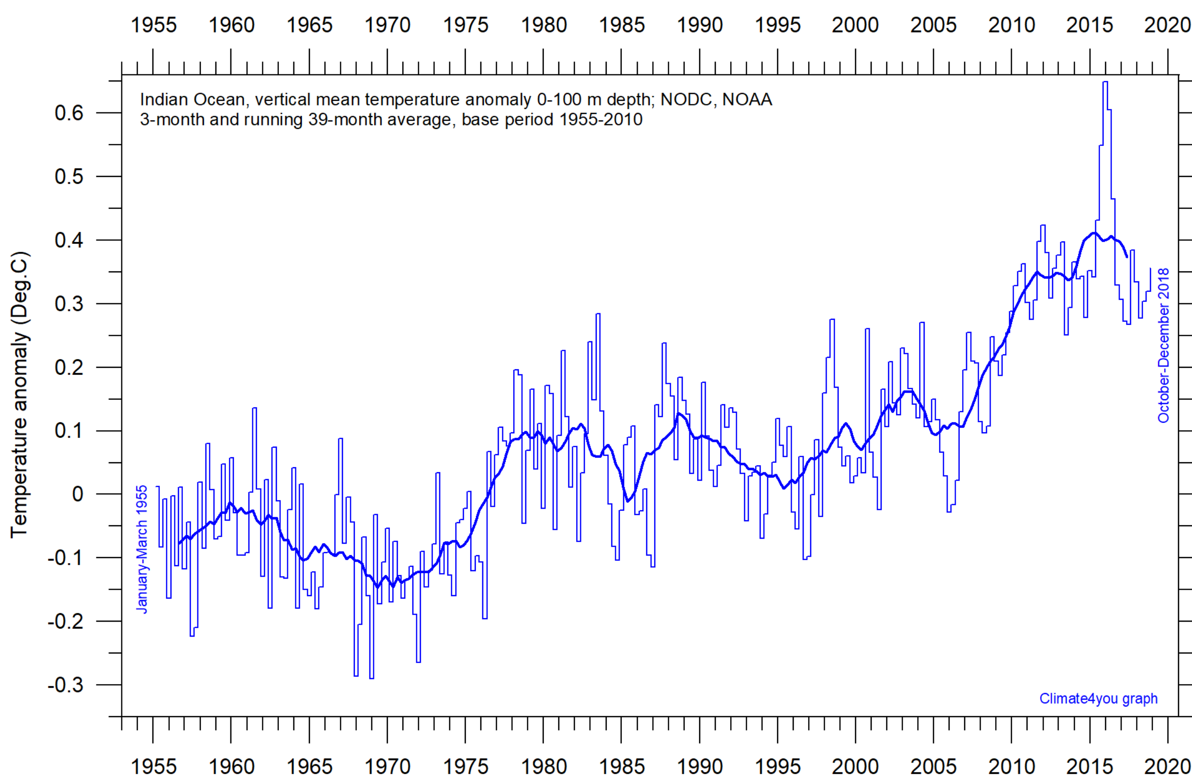

Indian Ocean vertical average temperature 0-100 m depth since 1955. The thin line indicate 3-month values, and the thick line represents the simple running 39-month (c. 3 year) average. Data source: [NOAA National Oceanographic Data Center] (NODC). Base period 1955-2010.

North Atlantic heat content uppermost 700 m, updated to September 2018

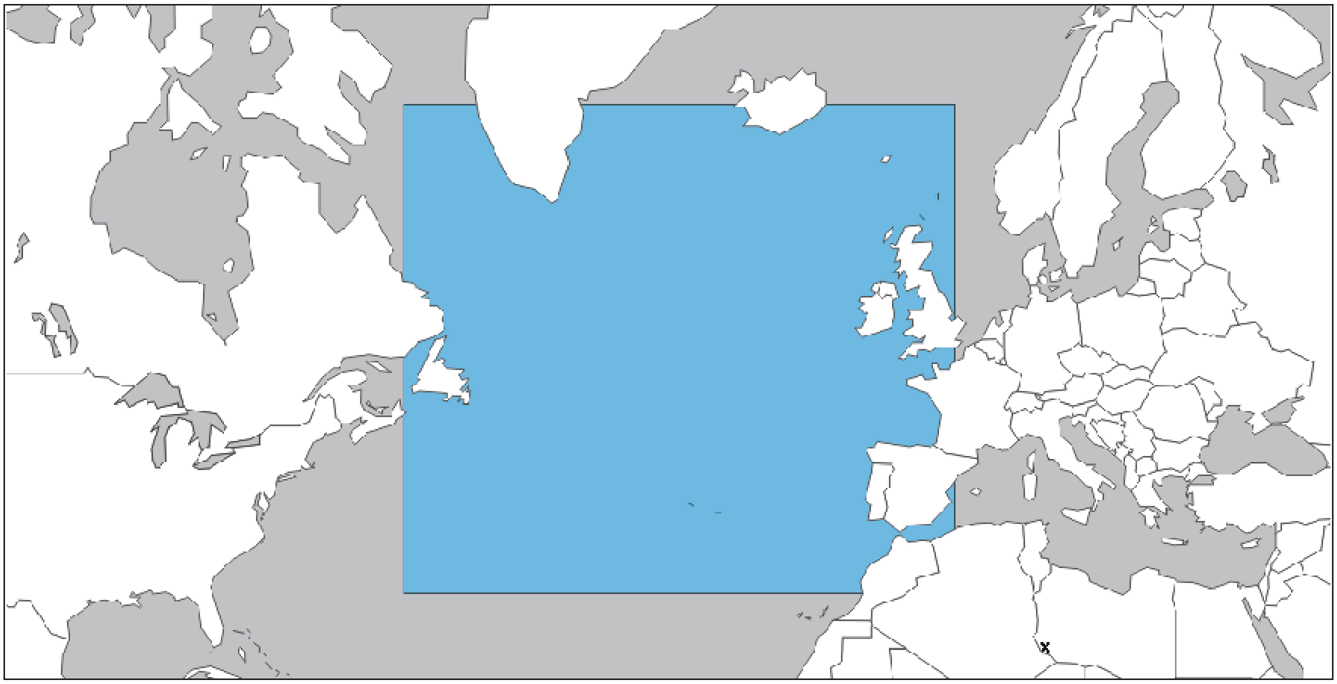

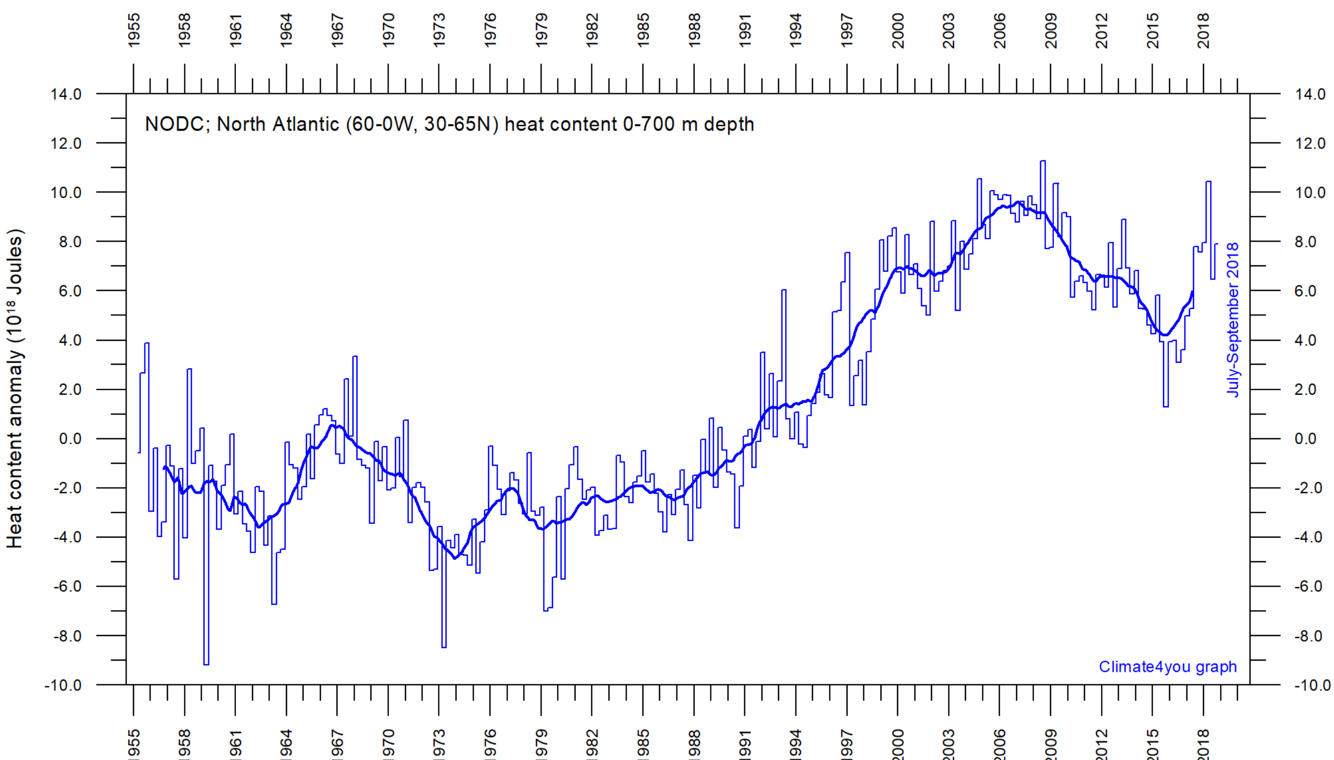

Global monthly heat content anomaly (10^{18} Joules) in the uppermost 700 m of the North Atlantic (60-0W, 30-65N; see map above) *ocean since January 1955. The thin line indicates monthly values, and the thick line represents the simple running 37-month (c. 3 year) average. Data source: [National Oceanographic Data Center](#) (NODC).*

North Atlantic temperatures 0-800 m depth along 59ºN, 30-0W, updated to December 2018

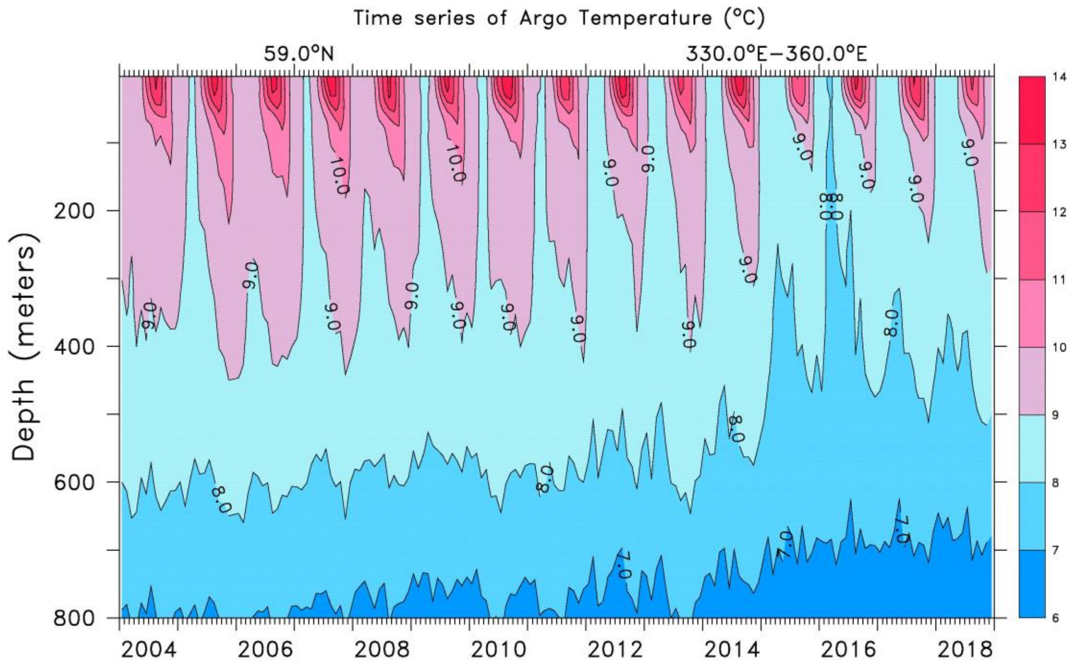

Time series depth-temperature diagram along 59 N across the North Atlantic Current from 30ºW to 0ºW, from surface to 800 m depth. Source: Global Marine Argo Atlas. See also the diagram below.

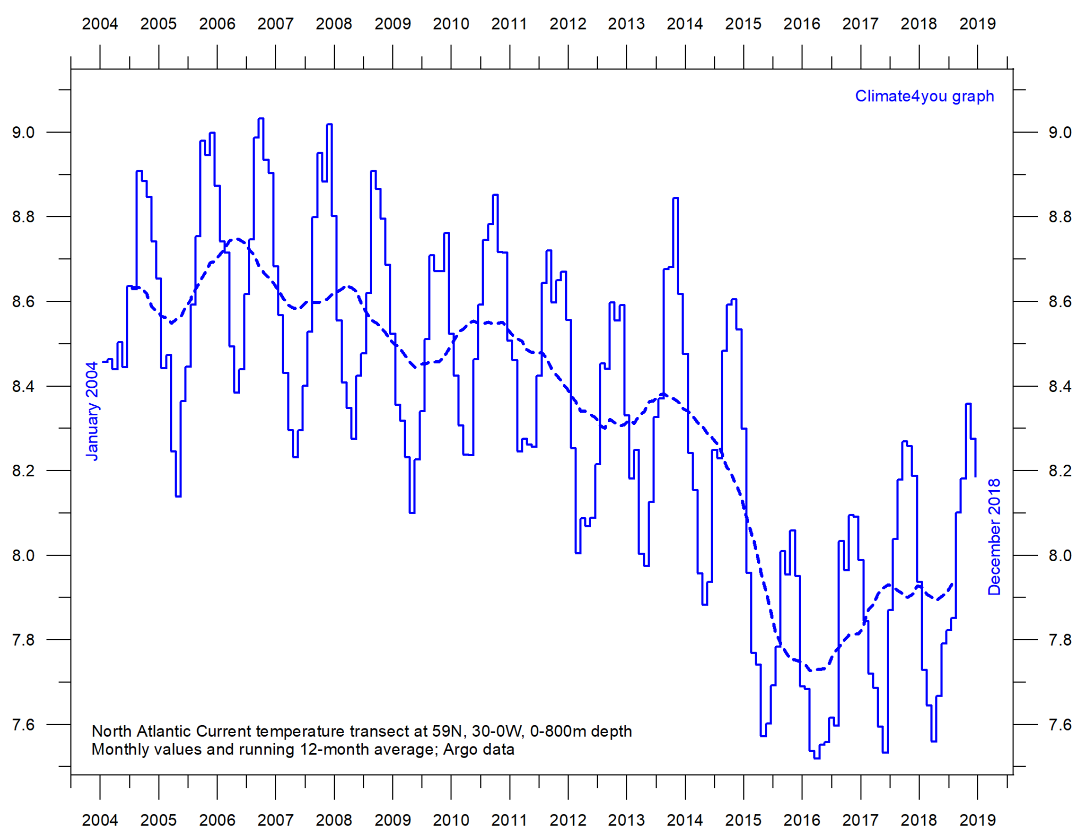

Average temperature along 59 N, 30-0W, 0-800m depth, corresponding to the main part of the North Atlantic Current, using Argo-data. Source: Global Marine Argo Atlas. Additional information can be found in: Roemmich, D. and J. Gilson, 2009. The 2004-2008 mean and annual cycle of temperature, salinity, and steric height in the global ocean from the Argo Program. Progress in Oceanography, 82, 81-100.

Global ocean temperature 0-1900 m depth summary, updated to December 2018

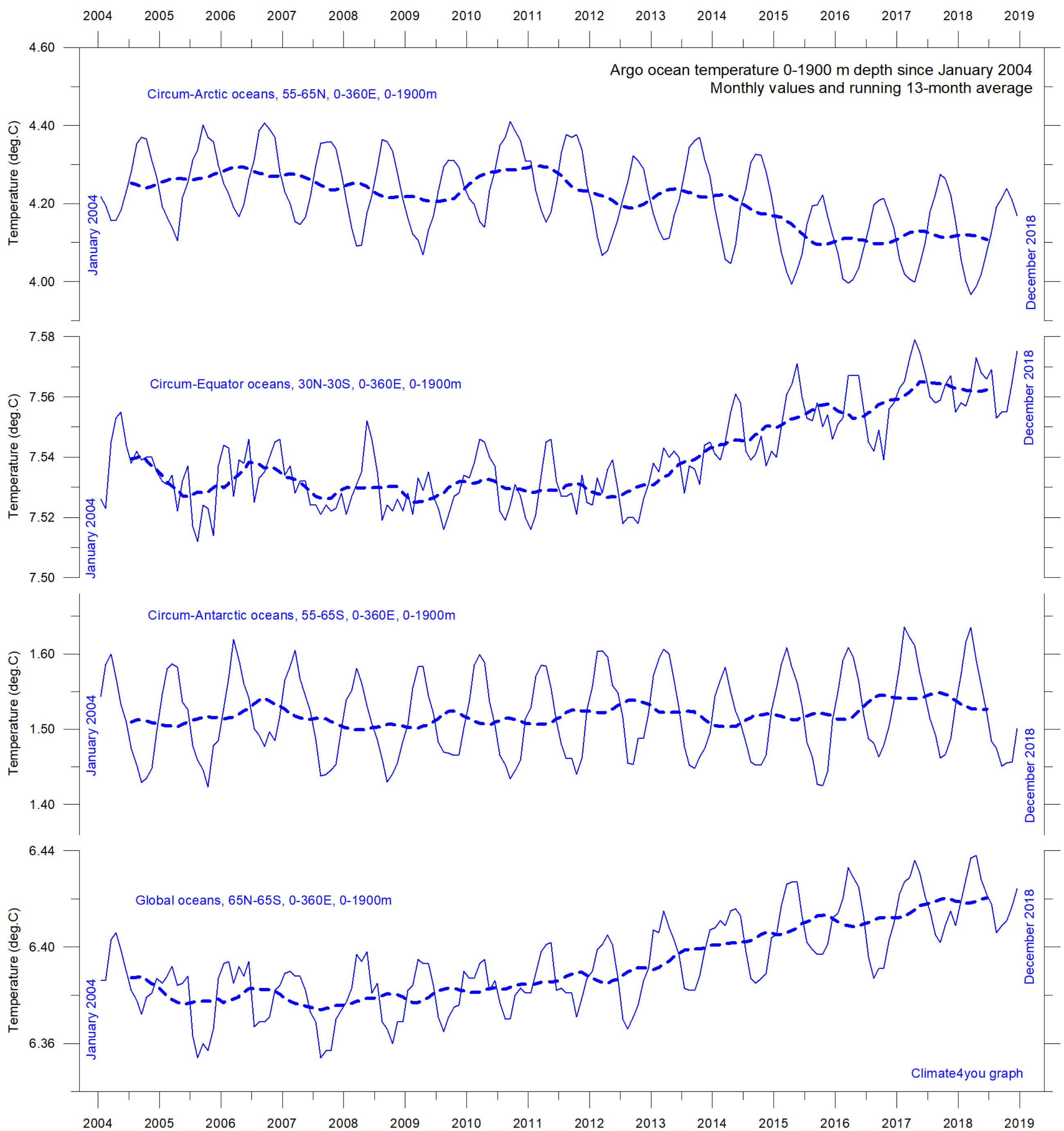

Summary of average temperature in uppermost 1900 m in different parts of the global oceans, using [Argo](#)-data. Source: [Global Marine Argo Atlas](#). Additional information can be found in: Roemmich, D. and J. Gilson, 2009. The 2004-2008 mean and annual cycle of temperature, salinity, and steric height in the global ocean from the Argo Program. [Progress in Oceanography](#), 82, 81-100.

Global ocean net temperature change since 2004 at different depths, updated to December 2018

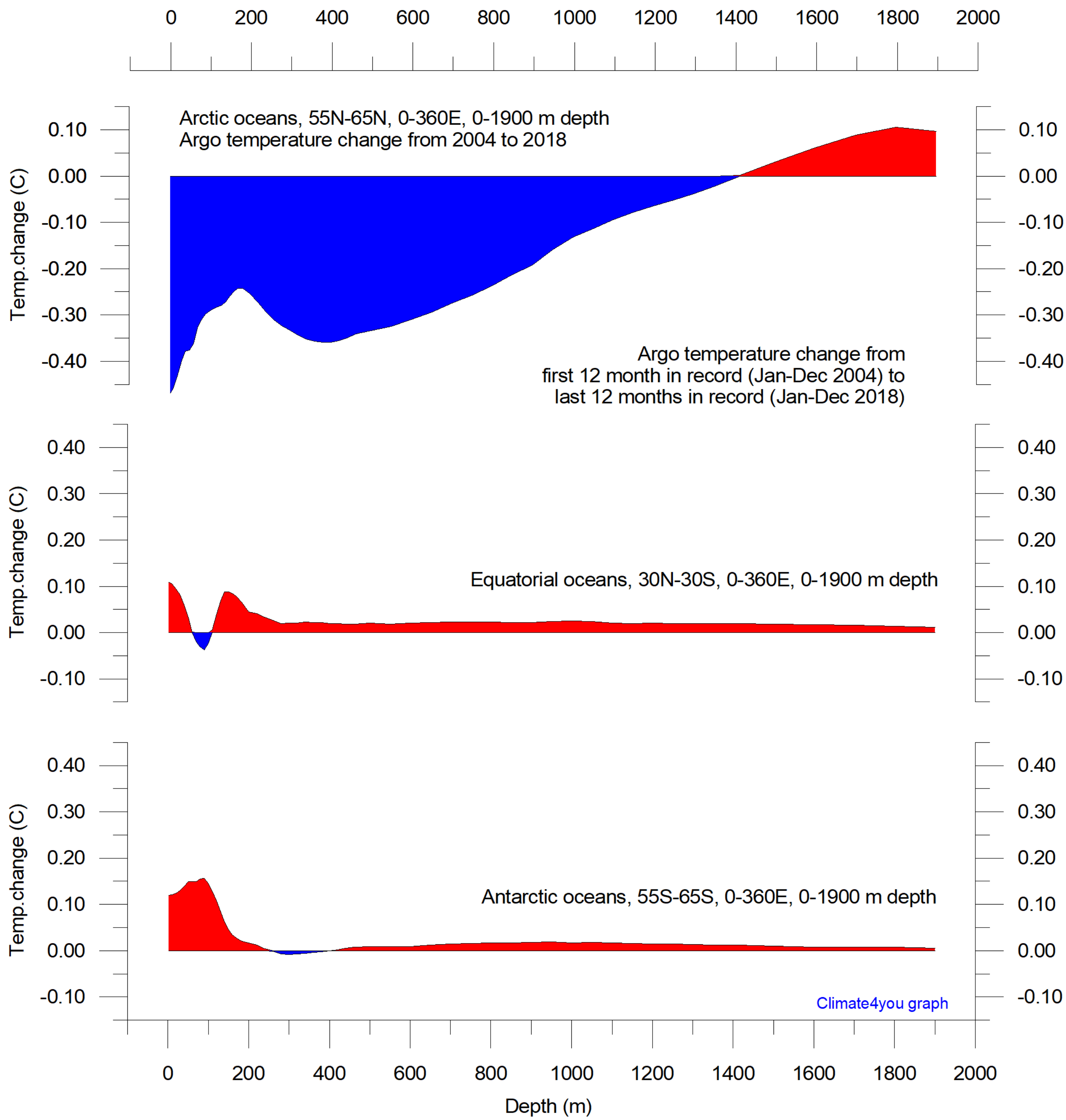

Net temperature change since 2004 from surface to 1900 m depth in different parts of the global oceans, using Argo-data. Source: Global Marine Argo Atlas. Additional information can be found in: Roemmich, D. and J. Gilson, 2009. The 2004-2008 mean and annual cycle of temperature, salinity, and steric height in the global ocean from the Argo Program. Progress in Oceanography, 82, 81-100. Please note that due to the spherical form of Earth, northern and southern latitudes represent only small ocean volumes, compared to latitudes near the Equator.

La Niña and El Niño episodes, updated to February 2019

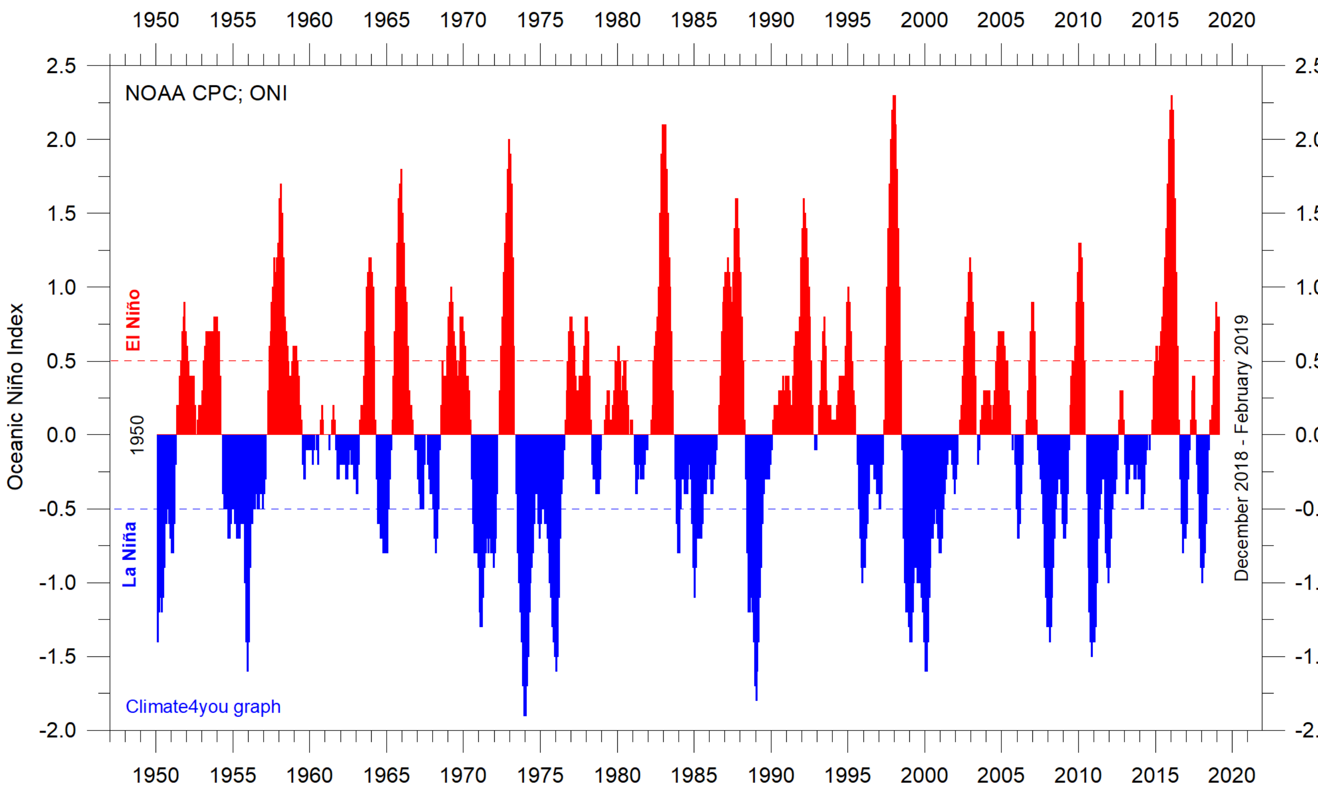

Warm (>+0.5°C) and cold (<0.5°C) episodes for the Oceanic Niño Index (ONI), defined as 3 month running mean of ERSSTv4 SST anomalies in the Niño 3.4 region (5°N-5°S, 120°-170°W)]. For historical purposes cold and warm episodes are defined when the threshold is met for a minimum of 5 consecutive over-lapping seasons. Anomalies are centred on 30-yr base periods updated every 5 years.

Troposphere and stratosphere temperatures from satellites, updated to February 2019

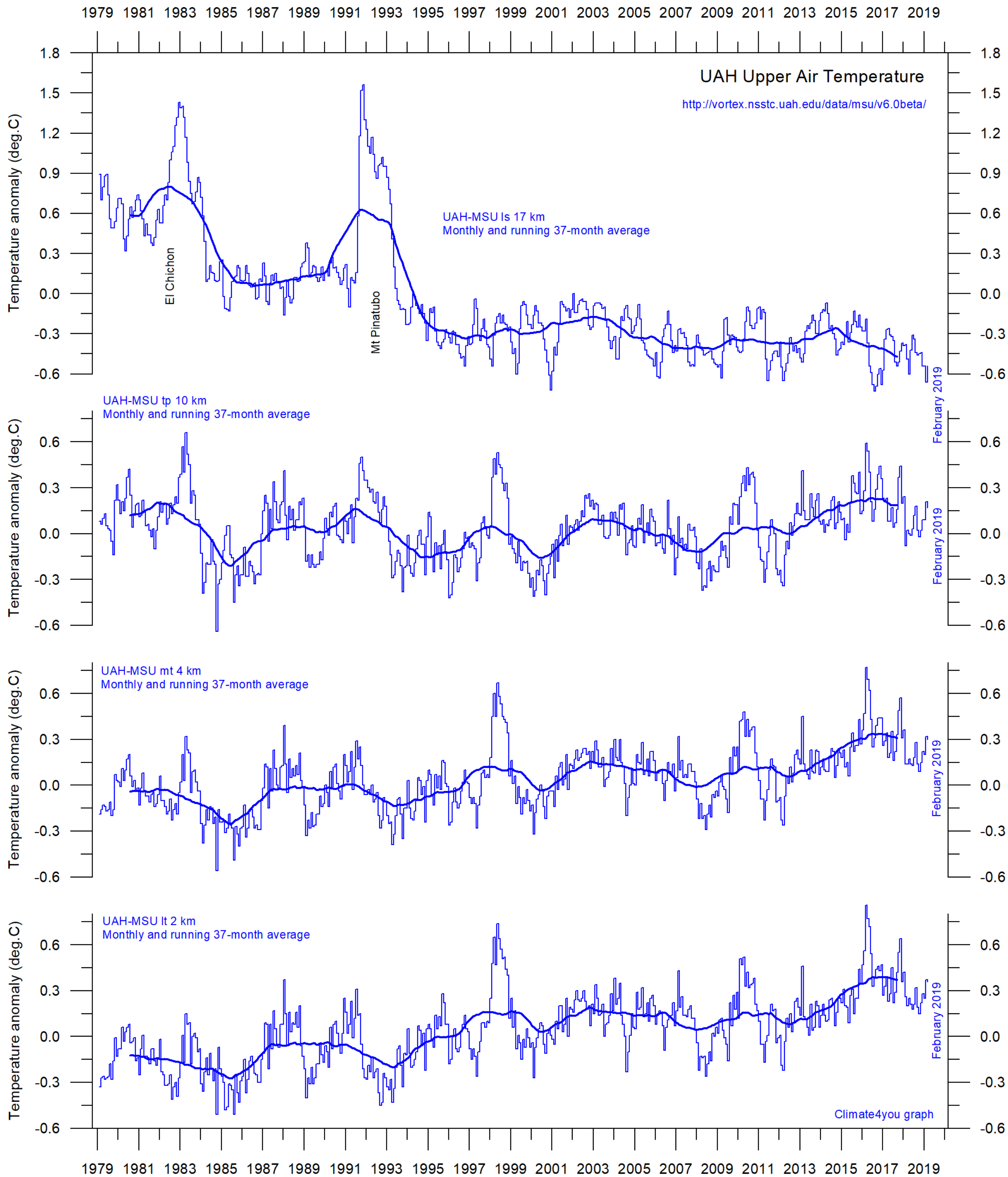

Global monthly average temperature in different according to University of Alabama at Huntsville, USA. The thin lines represent the monthly average, and the thick line the simple running 37-month average, nearly corresponding to a running 3-year average.

Zonal lower troposphere temperatures from satellites, updated to February 2019

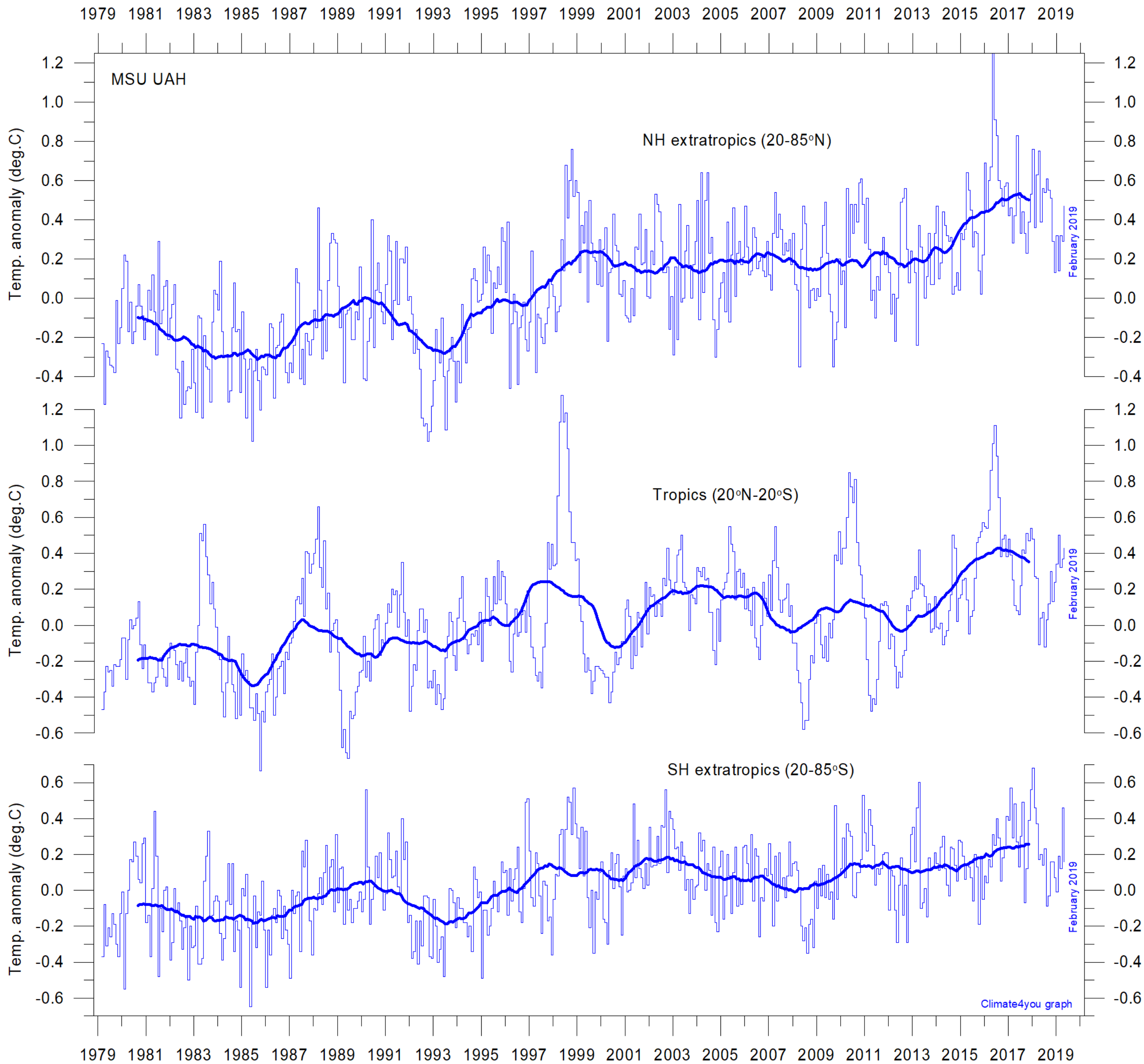

Global monthly average lower troposphere temperature since 1979 for the tropics and the northern and southern extratropics, according to University of Alabama at Huntsville, USA. Thin lines show the monthly temperature. Thick lines represent the simple running 37-month average, nearly corresponding to a running 3-year average. Reference period 1981-2010.

Arctic and Antarctic lower troposphere temperature, updated to February 2019

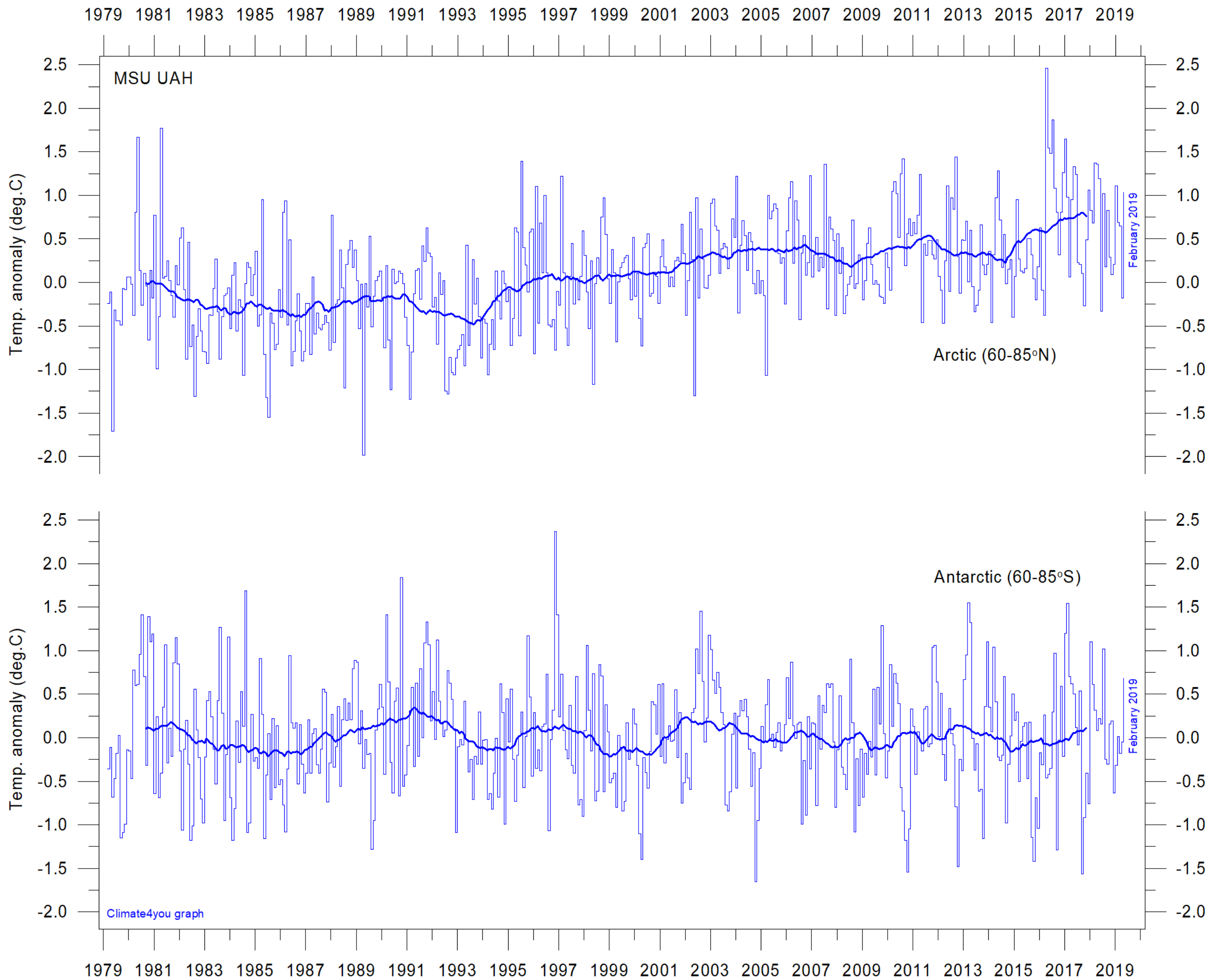

Global monthly average lower troposphere temperature since 1979 for the North Pole and South Pole regions, based on satellite observations ([University of Alabama]() at Huntsville, USA). Thin lines show the monthly temperature. The thick line is the simple running 37-month average, nearly corresponding to a running 3-year average. Reference period 1981-2010.

Temperature over land versus over oceans, updated to February 2019

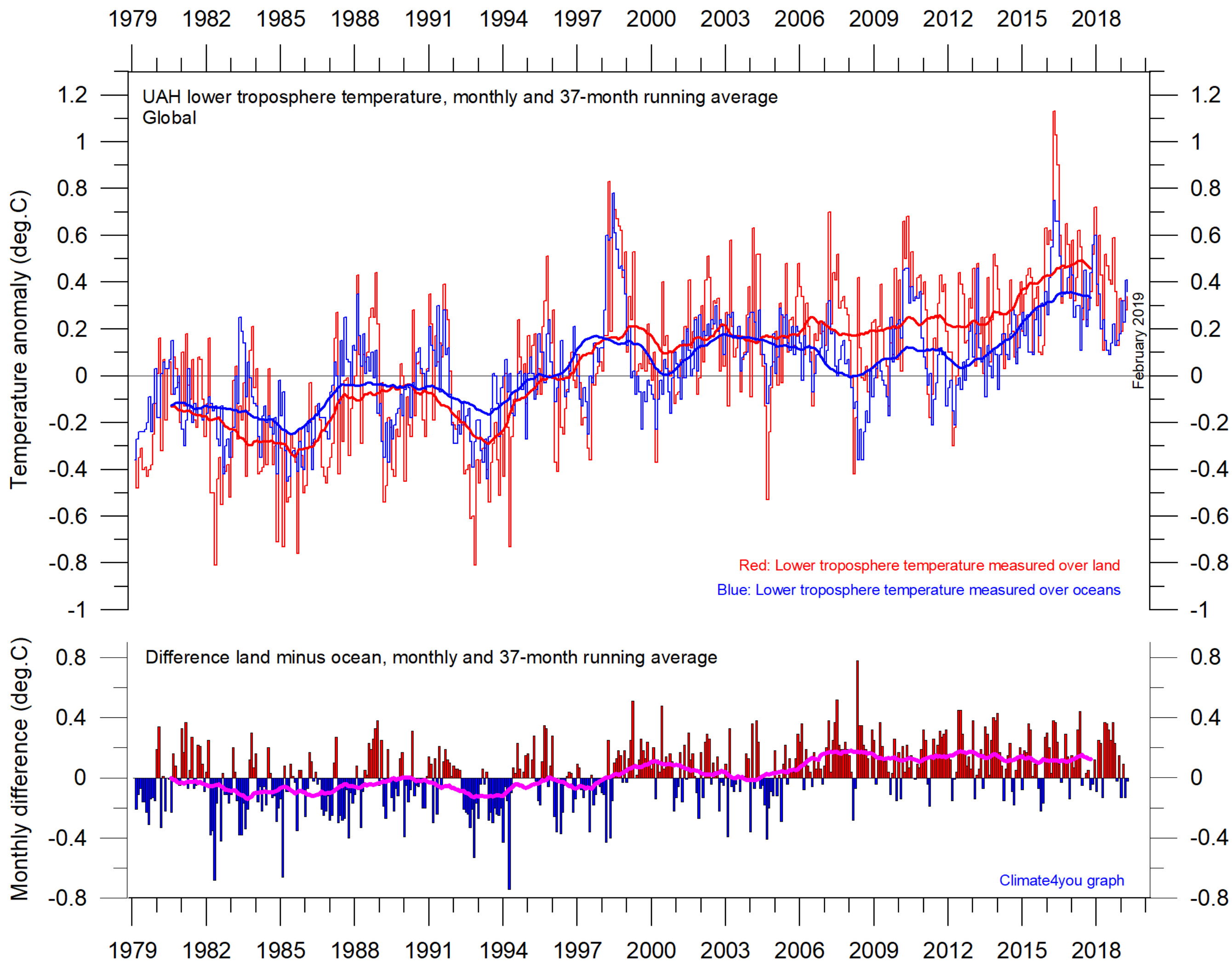

Global monthly average lower troposphere temperature since 1979 measured over land and oceans, respectively, according to University of Alabama at Huntsville, USA. Thick lines are the simple running 37-month average, nearly corresponding to a running 3-year average. Reference period 1981-2010.

Note: Since 1979, the lower troposphere over land has warmed much more than over oceans, suggesting that the overall warming mainly is derived from incoming solar radiation.

[Arctic and Antarctic surface air temperature, updated to January 2019]

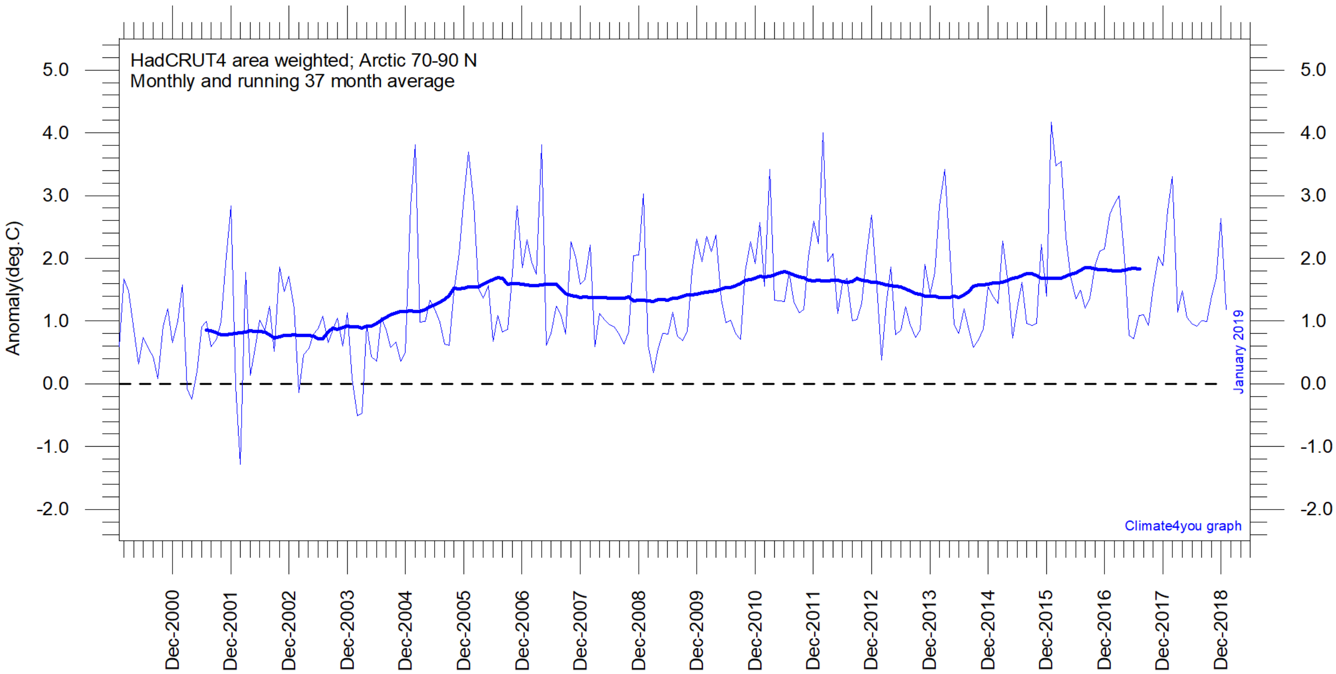

Diagram showing area weighted Arctic (70-90°N) monthly surface air temperature anomalies ([HadCRUT4]) since January 2000, in relation to the WMO [normal period] 1961-1990. The thin line shows the monthly temperature anomaly, while the thicker line shows the running 37-month (c. 3 year) average.

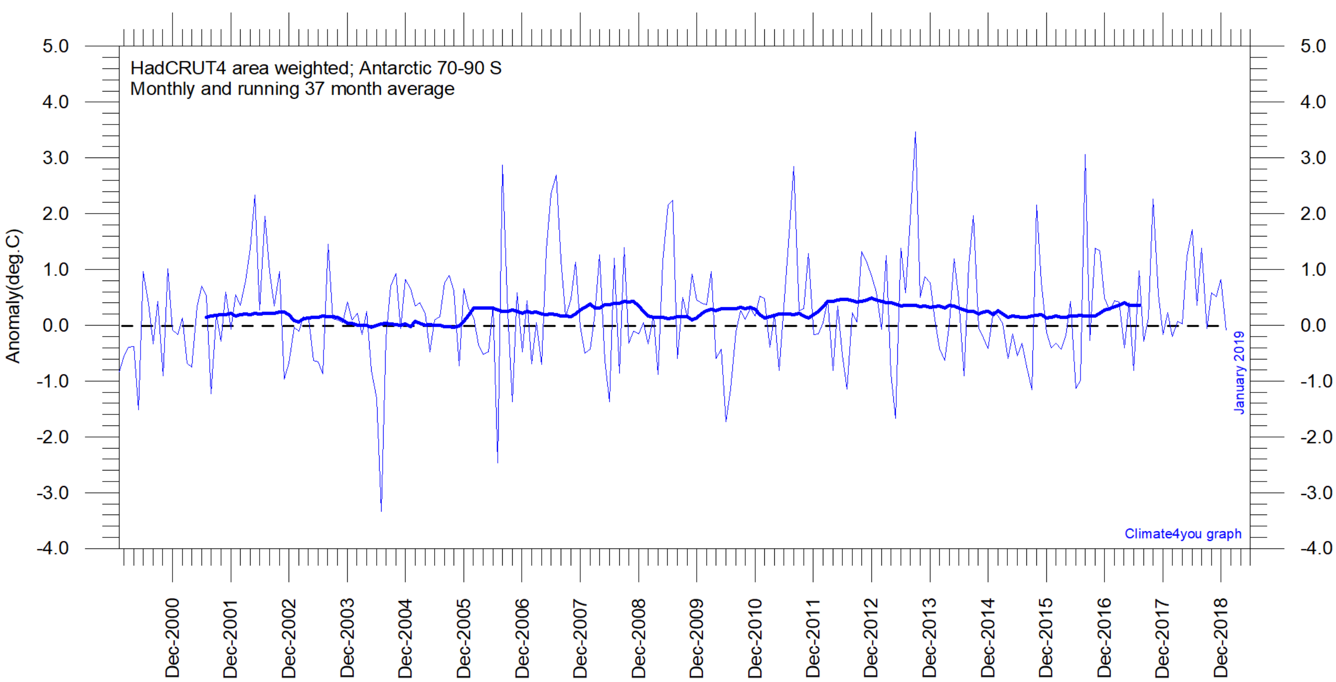

Diagram showing area weighted Antarctic (70-90°N) monthly surface air temperature anomalies ([HadCRUT4]) since January 2000, in relation to the WMO [normal period] 1961-1990. The thin line shows the monthly temperature anomaly, while the thicker line shows the running 37-month (c. 3 year) average.

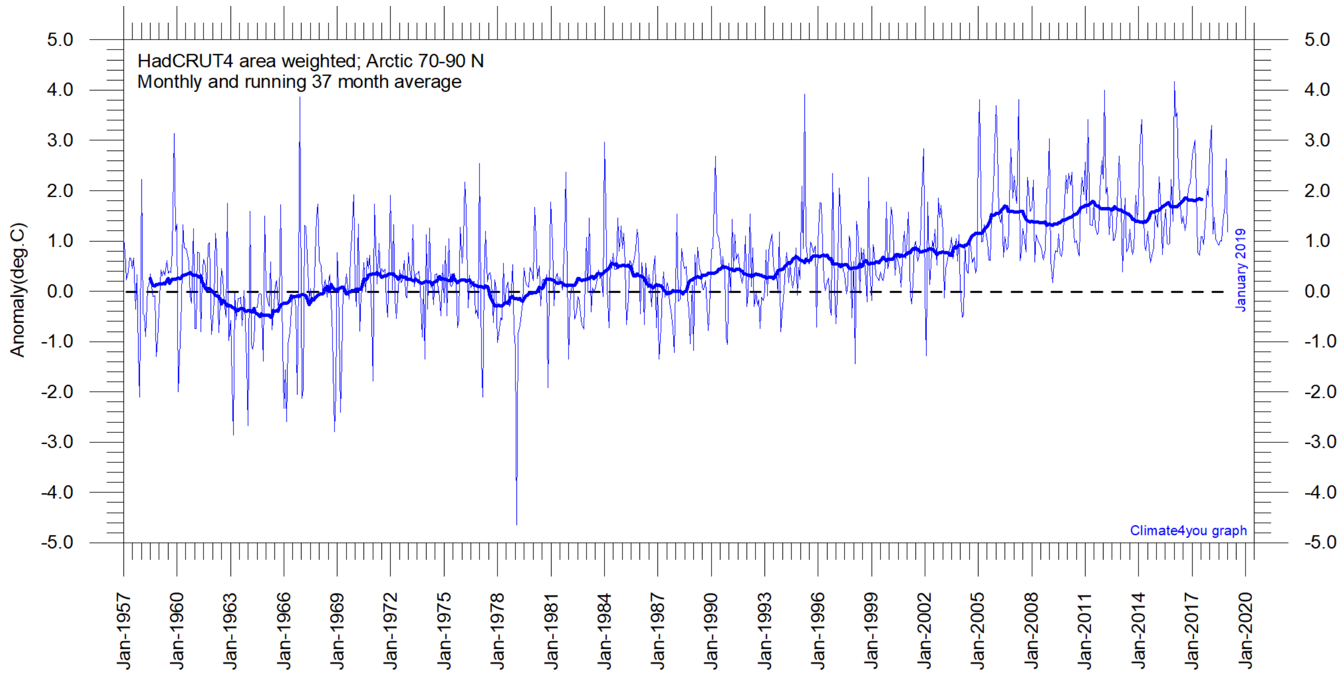

Diagram showing area weighted Arctic (70-90°N) monthly surface air temperature anomalies ([HadCRUT4]) since January 1957, in relation to the WMO [normal period] 1961-1990. The thin line shows the monthly temperature anomaly, while the thicker line shows the running 37-month (c. 3 year) average.

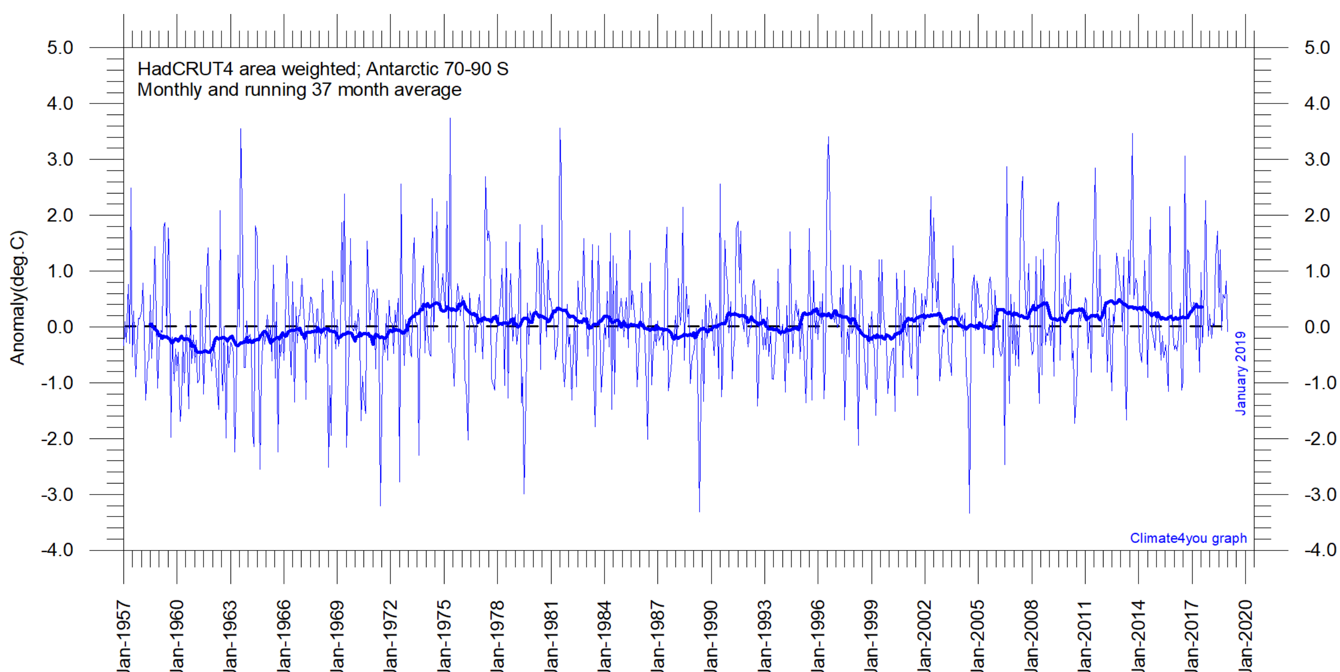

Diagram showing area weighted Antarctic (70-90°N) monthly surface air temperature anomalies ([HadCRUT4]) since January 1957, in relation to the WMO [normal period] 1961-1990. The thin line shows the monthly temperature anomaly, while the thicker line shows the running 37-month (c. 3 year) average.

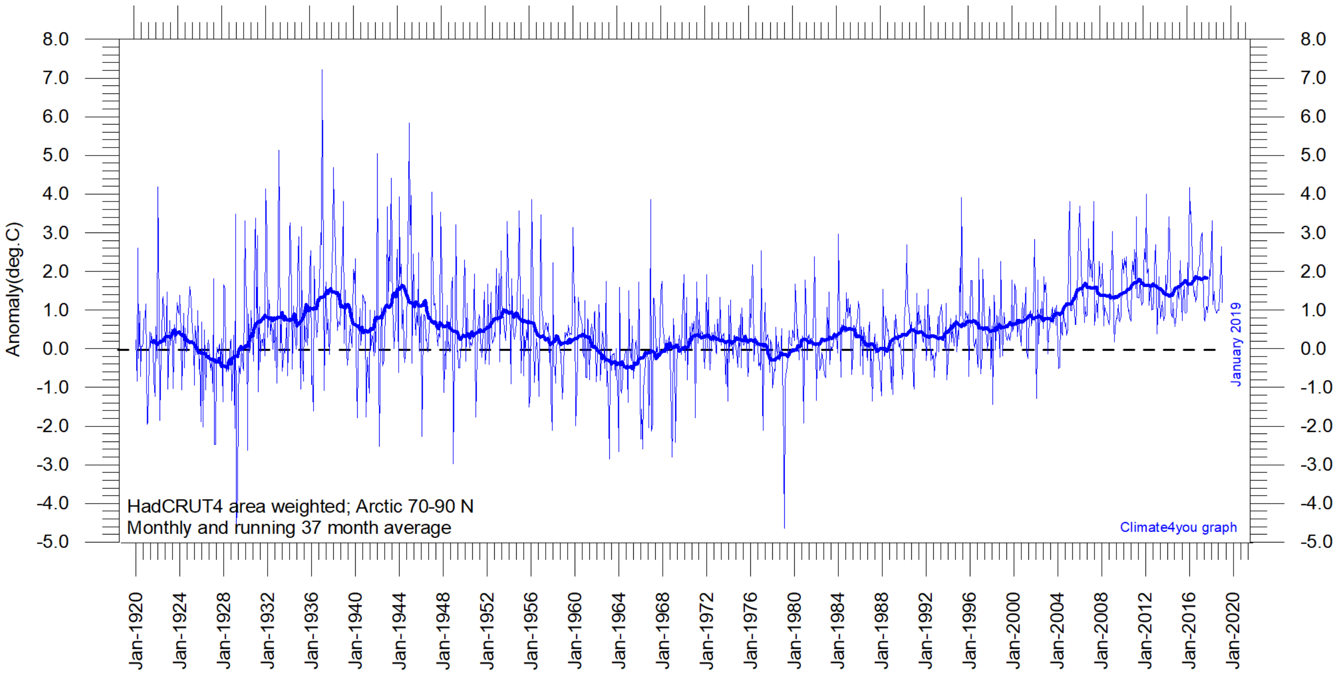

Diagram showing area-weighted Arctic (70-90°N) monthly surface air temperature anomalies ([HadCRUT4]) since January 1920, in relation to the WMO [normal period] 1961-1990. The thin line shows the monthly temperature anomaly, while the thicker line shows the running 37-month (c. 3 year) average.

29

Because of the relatively small number of Arctic stations before 1930, month-to-month variations in the early part of the Arctic temperature record 1920-2018 are larger than later (diagram above).

The period from about 1930 saw the establishment of many new Arctic meteorological stations, first in Russia and Siberia, and following the 2nd World War, also in North America. The period since 2005 is warm, about as warm as the period 1930-1940.

As the HadCRUT4 data series has improved high latitude coverage data coverage (compared to the HadCRUT3 series), the individual 5°x5° grid cells has been weighted according to their surface area. This area correction is especially important for polar regions.

This approach contrasts with that adopted by Gillet et al. 2008, which calculated a simple average, with no correction for the significant surface area effect of latitude in polar regions.

Literature:

Gillett, N.P., Stone, D.A., Stott, P.A., Nozawa, T., Karpechko, A.Y.U., Hegerl, G.C., Wehner, M.F. and Jones, P.D. 2008. Attribution of polar warming to human influence. *Nature Geoscience* 1, 750-754.

Arctic and Antarctic sea ice, updated to February 2019

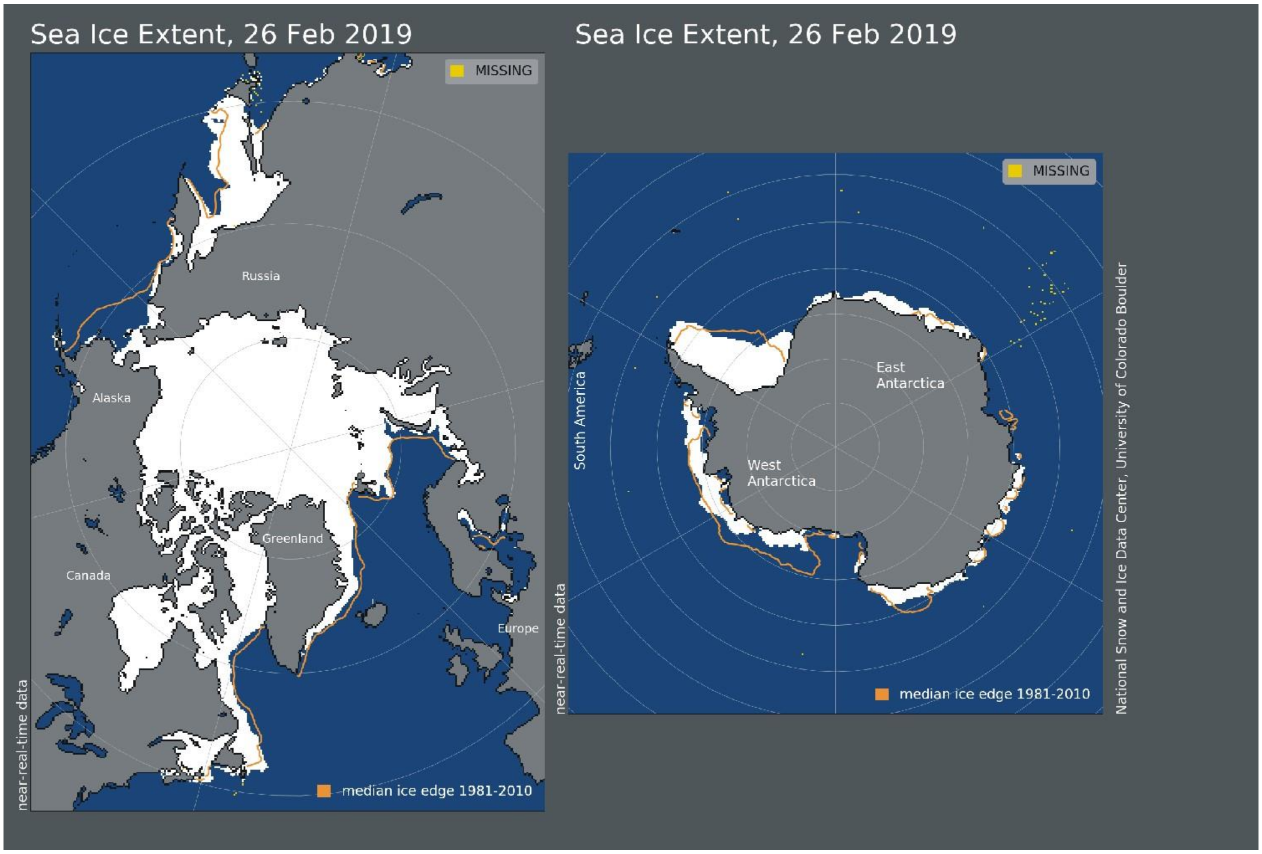

Sea ice extent 26 February 2019. The median limit of sea ice (orange line) is defined as 15% sea ice cover, according to the average of satellite observations 1981-2010 (both years included). Sea ice may therefore well be encountered outside and open water areas inside the limit shown in the diagrams above. Map source: National Snow and Ice Data Center (NSIDC).

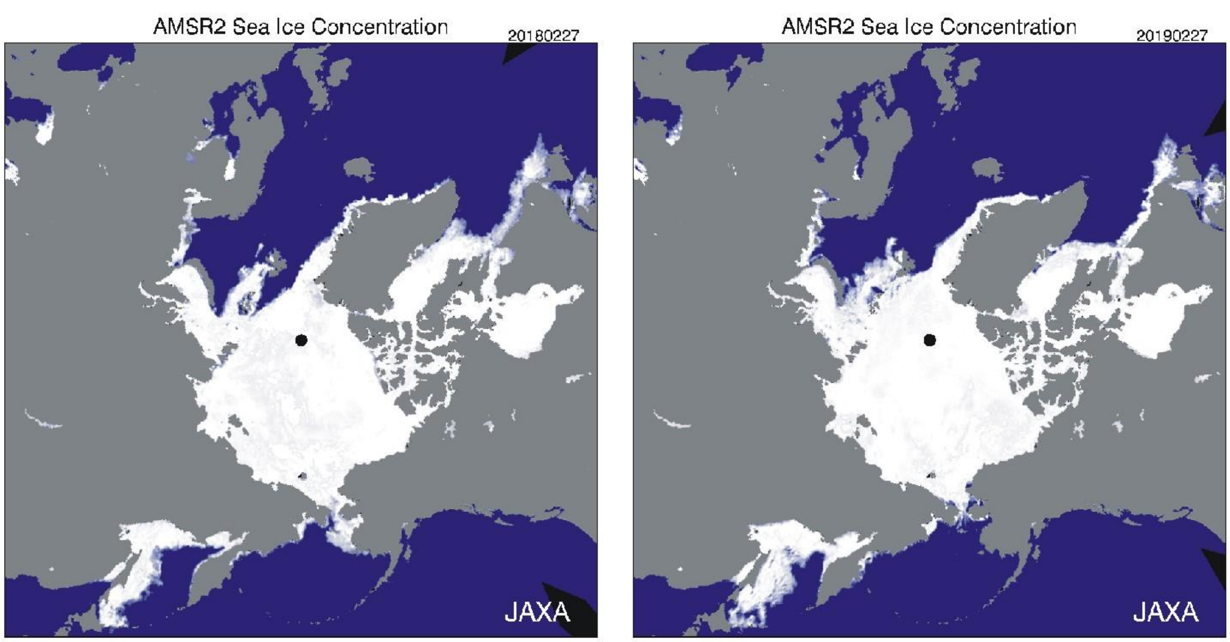

Diagrams showing Arctic sea ice extent and concentration 27 February 2018 (left) and 2019 (right), according to the Japan Aerospace Exploration Agency (JAXA).

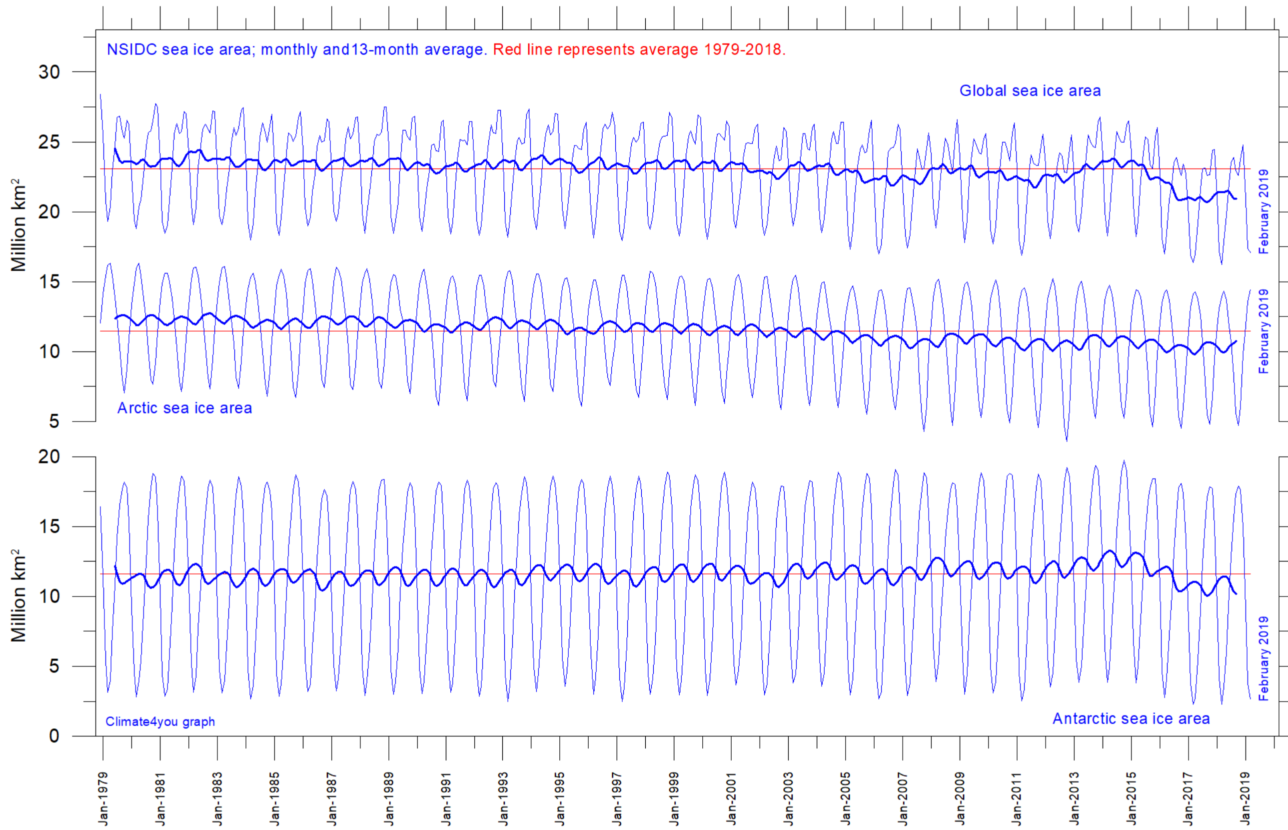

Graphs showing monthly Antarctic, Arctic and global sea ice extent since November 1978, according to the [National Snow and Ice data Center](#) (NSIDC).

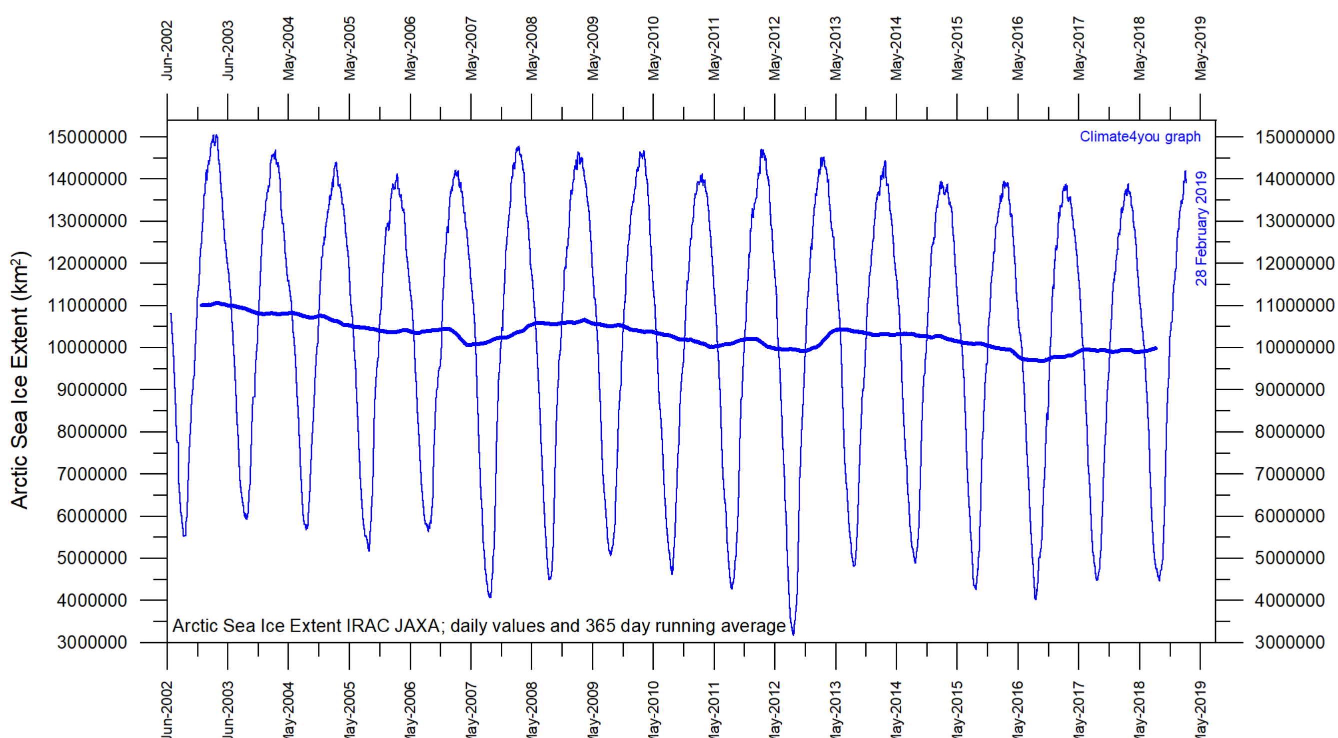

Diagram showing daily Arctic sea ice extent since June 2002, to 28 February 2019, by courtesy of [Japan Aerospace Exploration Agency](#) (JAXA).

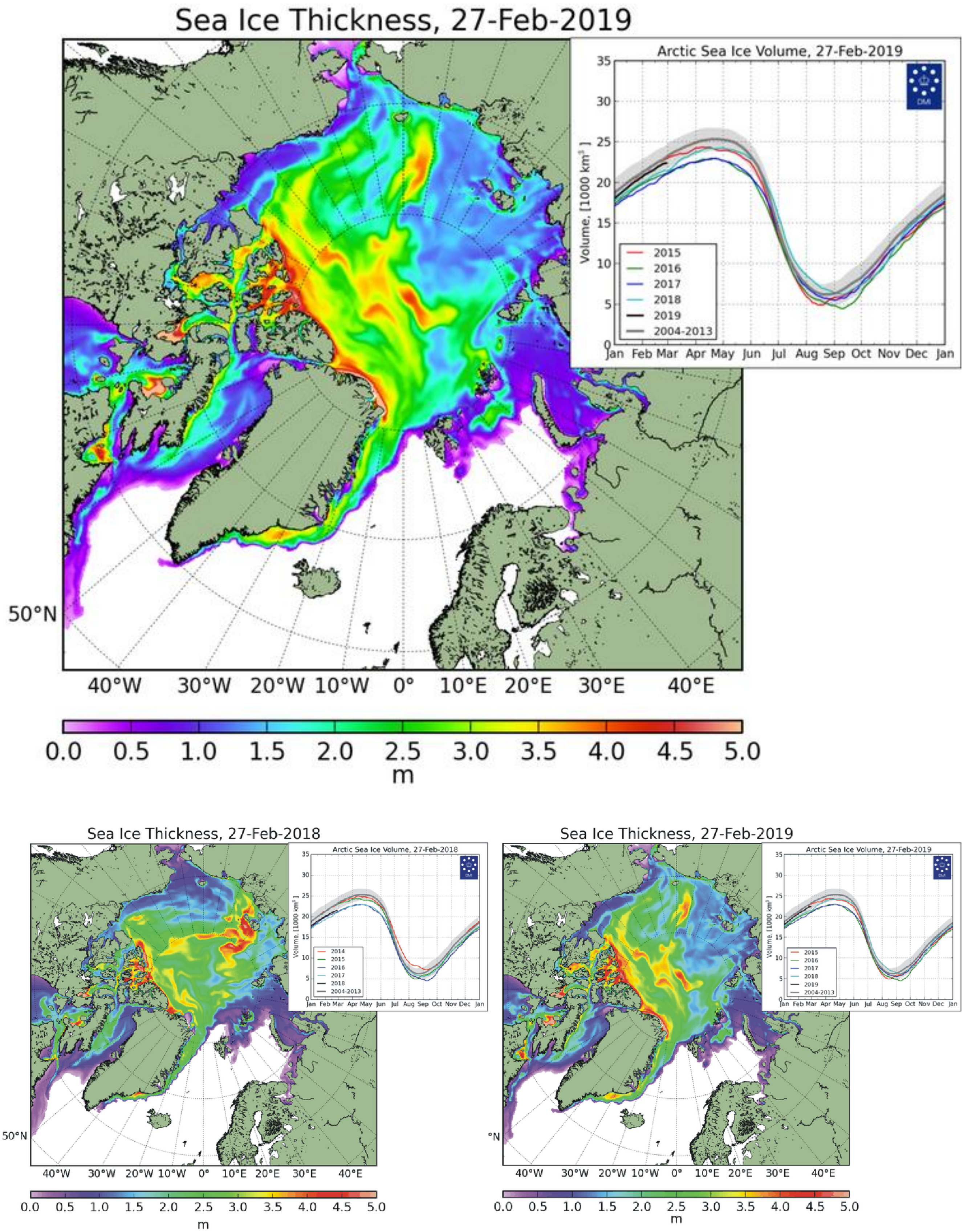

Diagrams showing Arctic sea ice extent and thickness 27 February 2018 (left) and 2019 (right and above) and the seasonal cycles of the calculated total arctic sea ice volume, according to [The Danish Meteorological Institute (DMI)](). The mean sea ice volume and standard deviation for the period 2004-2013 are shown by grey shading.

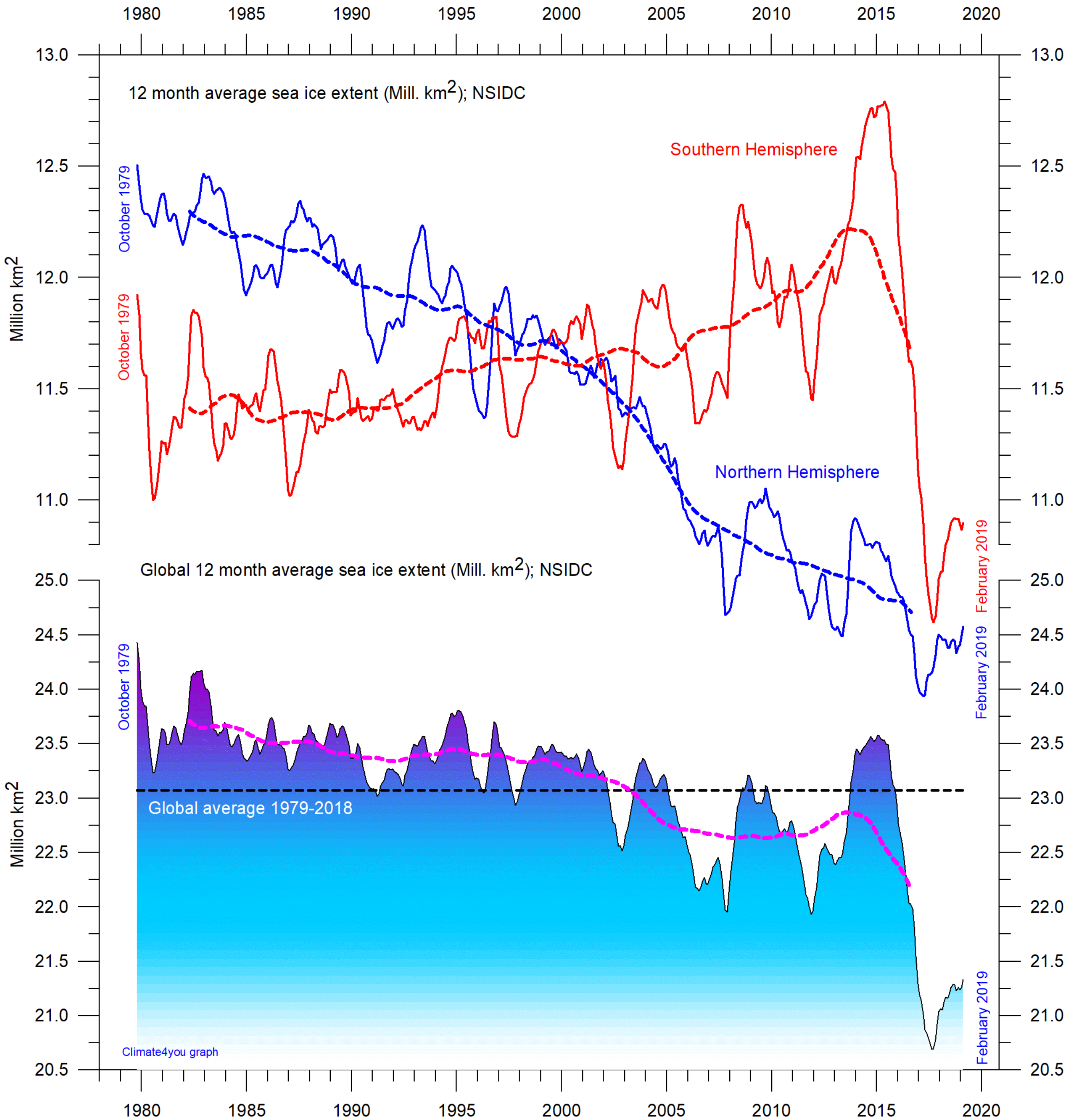

12 month running average sea ice extension, global and in both hemispheres since 1979, the satellite-era. The October 1979 value represents the monthly 12-month average of November 1978 - October 1979, the November 1979 value represents the average of December 1978 - November 1979, etc. The stippled lines represent a 61-month (ca. 5 years) average. Data source: National Snow and Ice Data Center (NSIDC).

Sea level in general

Global (or eustatic) sea-level change is measured relative to an idealised reference level, the geoid, which is a mathematical model of planet Earth's surface (Carter et al. 2014). Global sea-level is a function of the volume of the ocean basins and the volume of water they contain. Changes in global sea-level are caused by – but not limited to - four main mechanisms:

1. Changes in local and regional air pressure and wind, and tidal changes introduced by the Moon.
2. Changes in ocean basin volume by tectonic (geological) forces.
3. Changes in ocean water density caused by variations in currents, water temperature and salinity.
4. Changes in the volume of water caused by changes in the mass balance of terrestrial glaciers.

In addition to these there are other mechanisms influencing sea-level; such as storage of ground water, storage in lakes and rivers, evaporation, etc.

Mechanism 1 is controlling sea-level at many sites on a time scale from months to several years. As an example, many coastal stations show a pronounced annual variation reflecting seasonal changes in air pressures and wind speed. Longer-term climatic changes playing out over decades or centuries will also affect measurements of sea-level changes. Hansen et al. (2011, 2015) provide excellent analyses of sea-level changes caused by recurrent changes of the orbit of the Moon and other phenomena.

Mechanism 2 – with the important exception of earthquakes and tsunamis - typically operates over long (geological) time scales and is not significant on human time scales. It may relate to variations in the sea-floor spreading rate, causing volume changes in mid-ocean mountain ridges, and to the slowly changing configuration of land and oceans. Another effect may be the slow rise of basins due to isostatic offloading by deglaciation after an ice age. The floor of the Baltic Sea and the Hudson Bay are presently rising, causing a slow net transfer of water from these basins into the adjoining oceans. Slow changes of very big glaciers (ice sheets) and movements in the mantle will affect the gravity field and thereby the vertical position of the ocean surface. Any increase of the total water mass as well as sediment deposition into oceans increase the load on their bottom, generating sinking by viscoelastic flow in the mantle below. The mantle flow is directed towards the surrounding land areas, which will rise, thereby partly compensating for the initial sea level increase induced by the increased water mass in the ocean.

Mechanism 3 (temperature-driven expansion) only affects the uppermost part of the oceans on human time scales. Usually, temperature-driven changes in density are more important than salinity-driven changes. Seawater is characterised by a relatively small coefficient of expansion, but the effect should however not be overlooked, especially when interpreting satellite altimetry data. Temperature-driven expansion of a column of seawater will not affect the total mass of water within the column considered and will therefore not affect the potential at the top of the water column. Temperature-driven ocean water expansion will therefore not in itself lead to any lateral displacement of water, but only locally lift the ocean surface. Near the coast, where people are living, the depth of water approaches zero, so no temperature-driven expansion will take place here (Mörner 2015). Mechanism 3 is for that reason not important for coastal regions.

Mechanism 4 (changes in glacier mass balance) is an important driver for global sea-level changes along coasts, for human time scales. Volume changes of floating glaciers – ice shelves – has no influence on the global sea-level, just like volume changes of floating sea ice has no influence. Only the mass-balance of grounded or land-based glaciers is important for the global sea-level along coasts.

Summing up: Mechanism 1 and 4 are the most important for understanding sea-level changes along coasts.

References:

Carter R.M., de Lange W., Hansen, J.M., Humlum O., Idso C., Kear, D., Legates, D., Mörner, N.A., Ollier C., Singer F. & Soon W. 2014. Commentary and Analysis on the Whitehead& Associates 2014 NSW Sea-Level Report. Policy Brief, NIPCC, 24. September 2014, 44 pp. http://climatechangereconsidered.org/wp-content/uploads/2014/09/NIPCC-Report-on-NSW-Coastal-SL-9z-corrected.pdf

Hansen, J.-M., Aagaard, T. and Binderup, M. 2011. Absolute sea levels and isostatic changes of the eastern North Sea to central Baltic region during the last 900 years. Boreas, 10.1111/j.1502-3885.2011.00229.x. ISSN 0300–9483.

Hansen, J.-M., Aagaard, T. and Huijpers, A. 2015. Sea-Level Forcing by Synchronization of 56- and 74-YearOscillations with the Moon's Nodal Tide on the Northwest European Shelf (Eastern North Sea to Central Baltic Sea). Journ. Coastal Research, 16 pp.

Mörner, Nils-Axel 2015. Sea Level Changes as recorded in nature itself. Journal of Engineering Research and Applications, Vol.5, 1, 124-129.

Global sea level from satellite altimetry, updated to January 2018

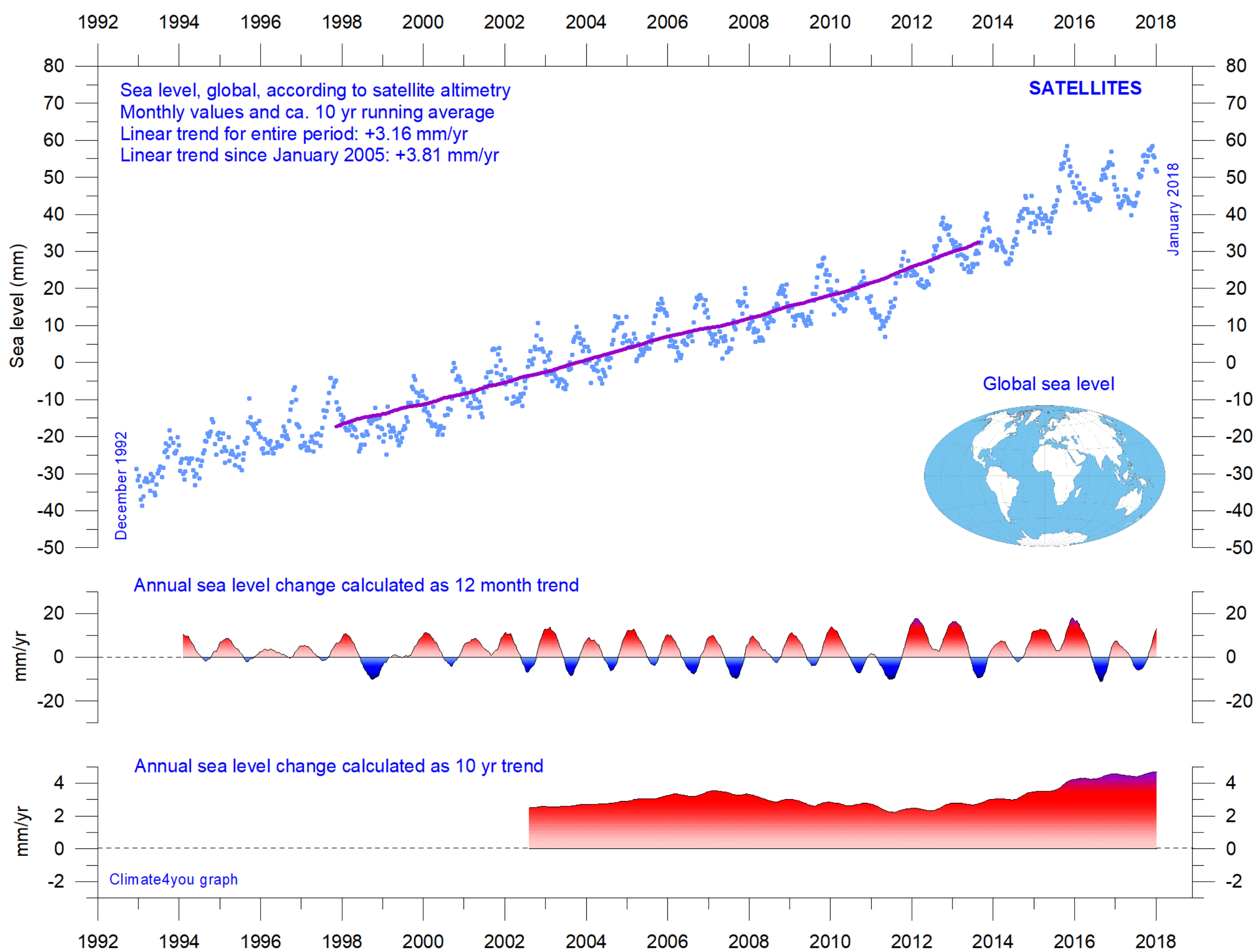

Global sea level since December 1992 according to the Colorado Center for Astrodynamics Research at University of Colorado at Boulder. The blue dots are the individual observations, and the purple line represents the running 121-month (ca. 10 year) average. The two lower panels show the annual sea level change, calculated for 1 and 10-year time windows, respectively. These values are plotted at the end of the interval considered. Data from the TOPEX/Poseidon mission have been used before 2002, and data from the Jason-1 mission (satellite launched December 2001) after 2002.

Global sea level from tide-gauges, updated to December 2017

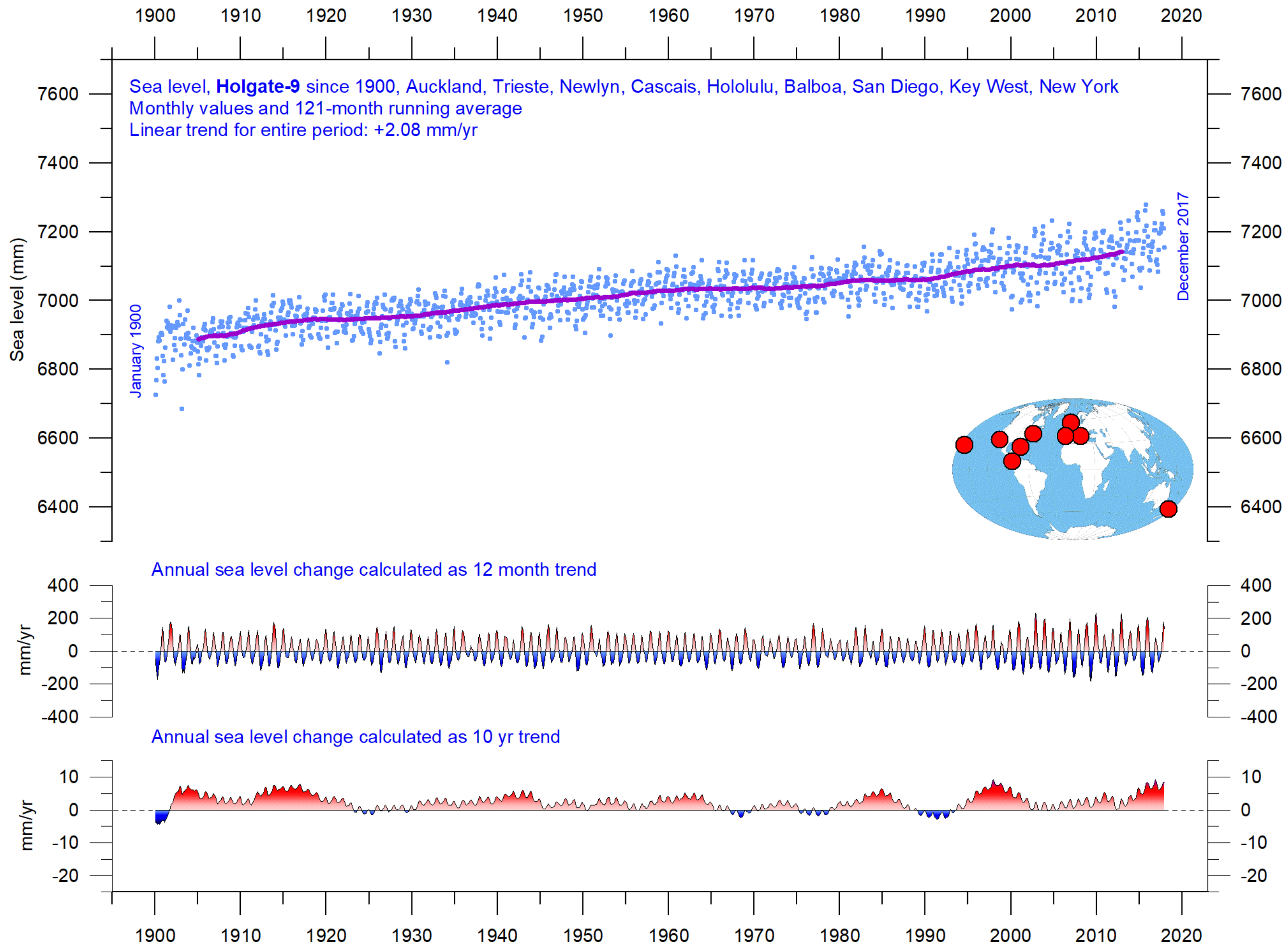

Holgate-9 monthly tide gauge data from PSMSL Data Explorer. Holgate (2007) suggested the nine stations listed in the diagram to capture the variability found in a larger number of stations over the last half century studied previously. For that reason, average values of the Holgate-9 group of tide gauge stations are interesting to follow. The blue dots are the individual average monthly observations, and the purple line represents the running 121-month (ca. 10 year) average. The two lower panels show the annual sea level change, calculated for 1 and 10-year windows, respectively. These values are plotted at the end of the interval considered.

Reference:

Holgate, S.J. 2007. On the decadal rates of sea level change during the twentieth century. Geophys. Res. Letters, 34, L01602, doi:10.1029/2006GL028492

Northern Hemisphere weekly and seasonal snow cover, updated to February 2019

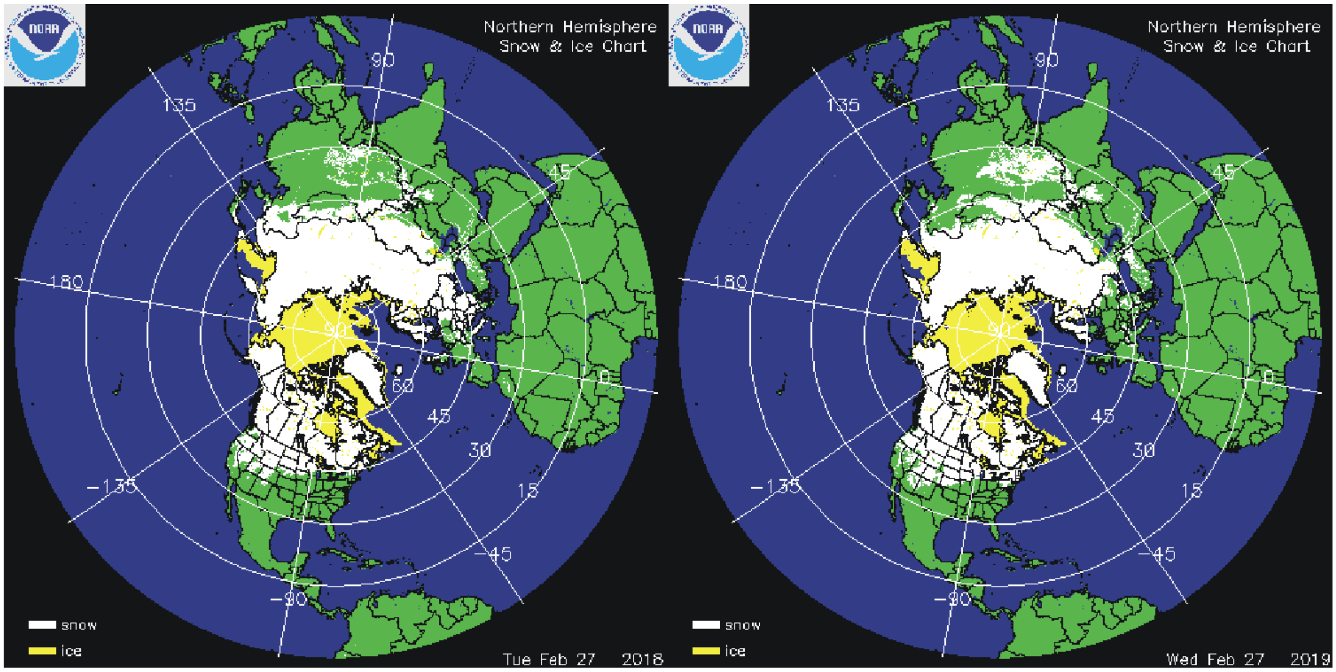

Northern hemisphere snow cover (white) and sea ice (yellow) 27 February 2018 (left) and 2019 (right). Map source: [National Ice Center](#) (NIC).

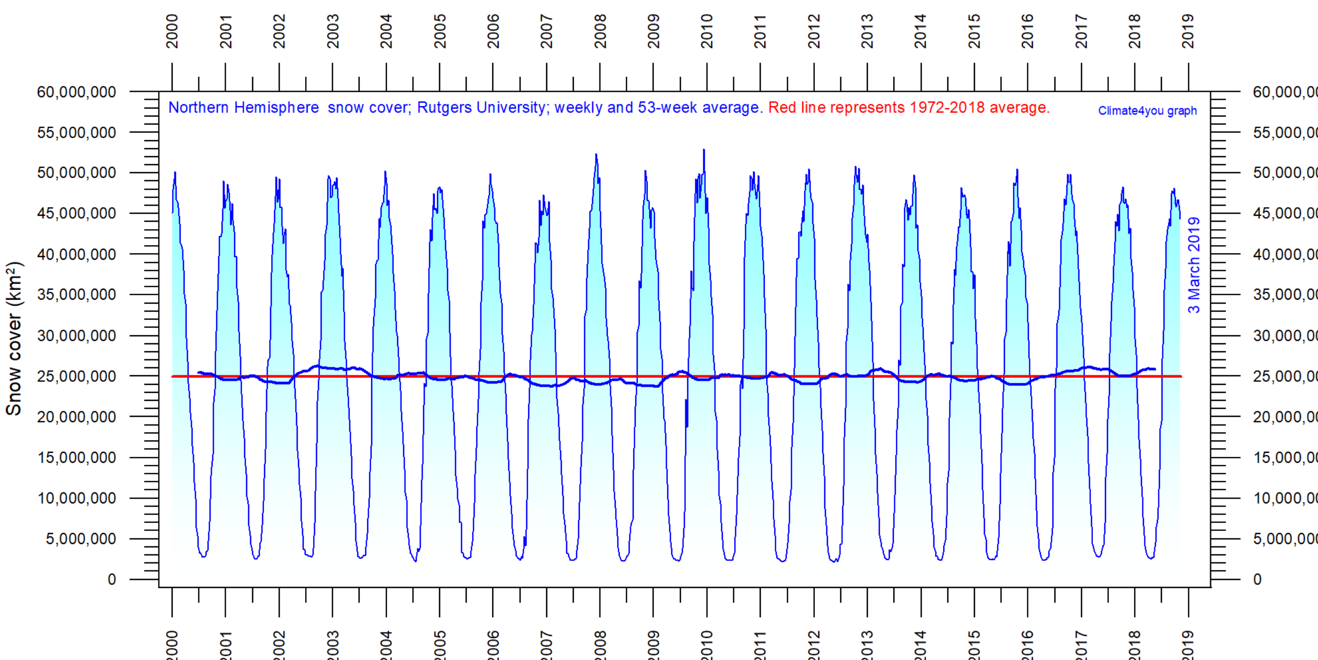

Northern hemisphere weekly snow cover since January 2000 according to Rutgers University Global Snow Laboratory. The thin blue line is the weekly data, and the thick blue line is the running 53-week average (approximately 1 year). The horizontal red line is the 1972-2018 average.

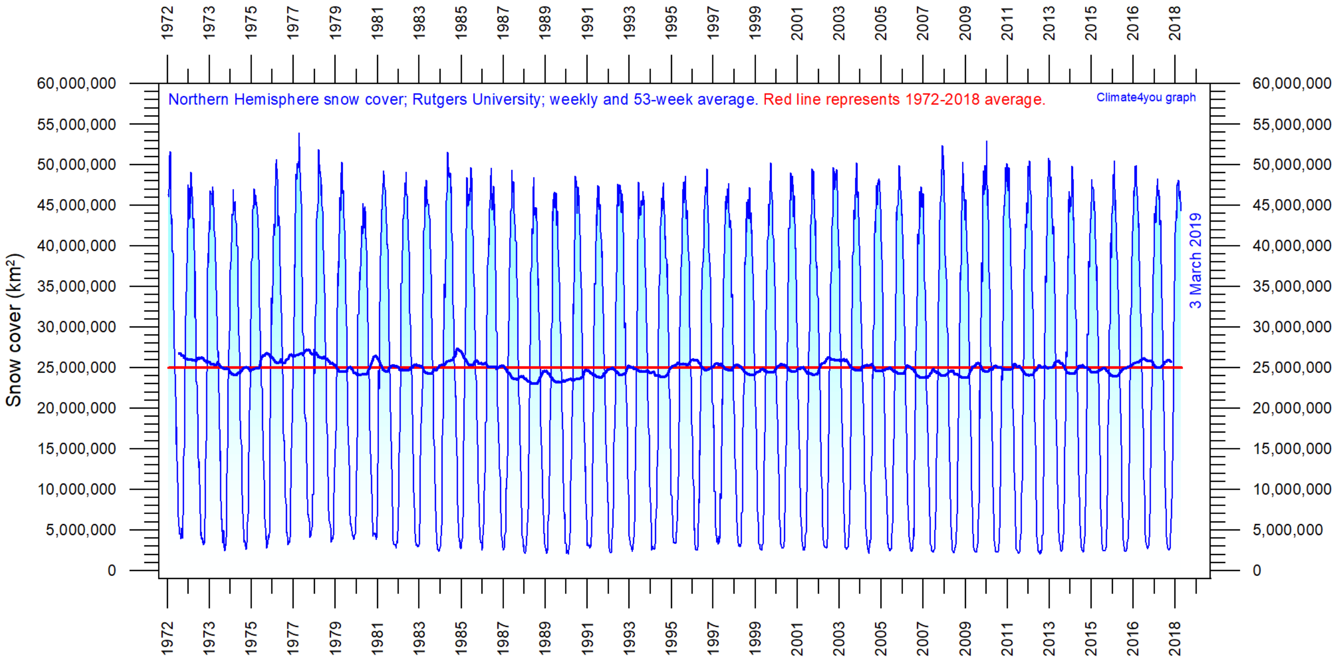

Northern hemisphere weekly snow cover since January 1972 according to Rutgers University Global Snow Laboratory. The thin blue line is the weekly data, and the thick blue line is the running 53-week average (approximately 1 year). The horizontal red line is the 1972-2018 average.

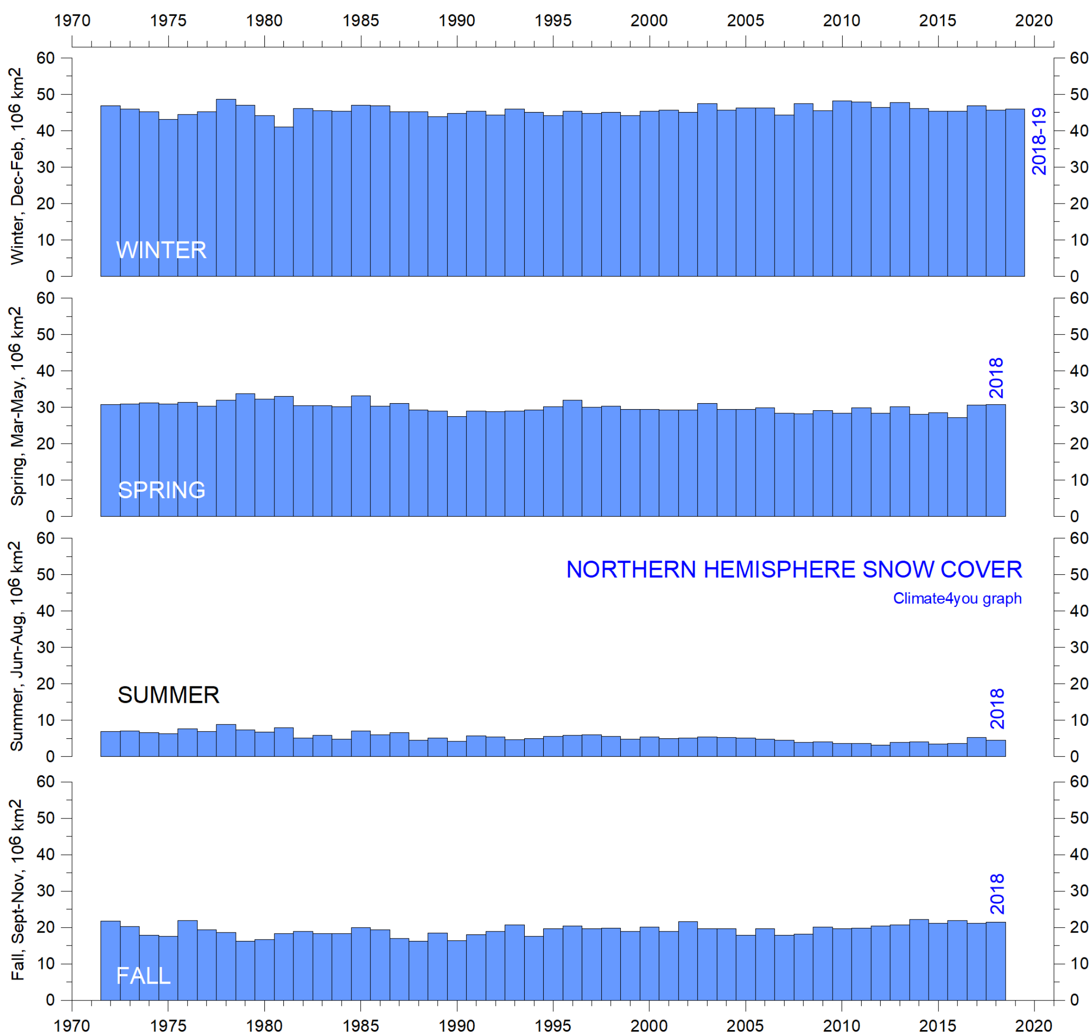

Northern hemisphere seasonal snow cover since January 1972 according to Rutgers University Global Snow Laboratory.

Atmospheric specific humidity, updated to February 2019

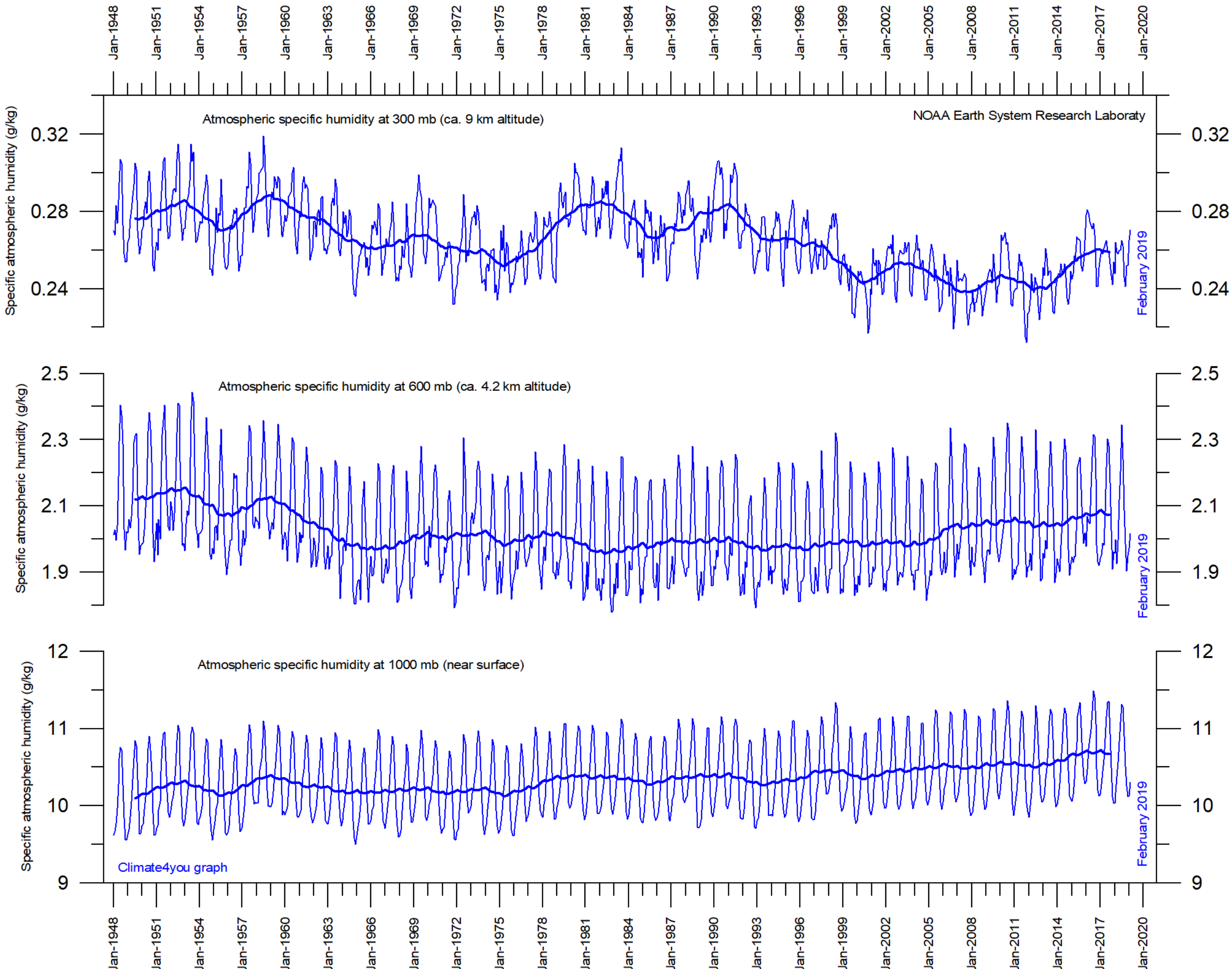

Specific atmospheric humidity (g/kg) at three different altitudes in the lower part of the atmosphere (the Troposphere) since January 1948 (Kalnay et al. 1996). The thin blue lines show monthly values, while the thick blue lines show the running 37-month average (about 3 years). Data source: Earth System Research Laboratory (NOAA).

Note: Water vapour is the most important greenhouse gas in Earth's atmosphere, much more important than CO_2.

Atmospheric CO_2, updated to February 2019

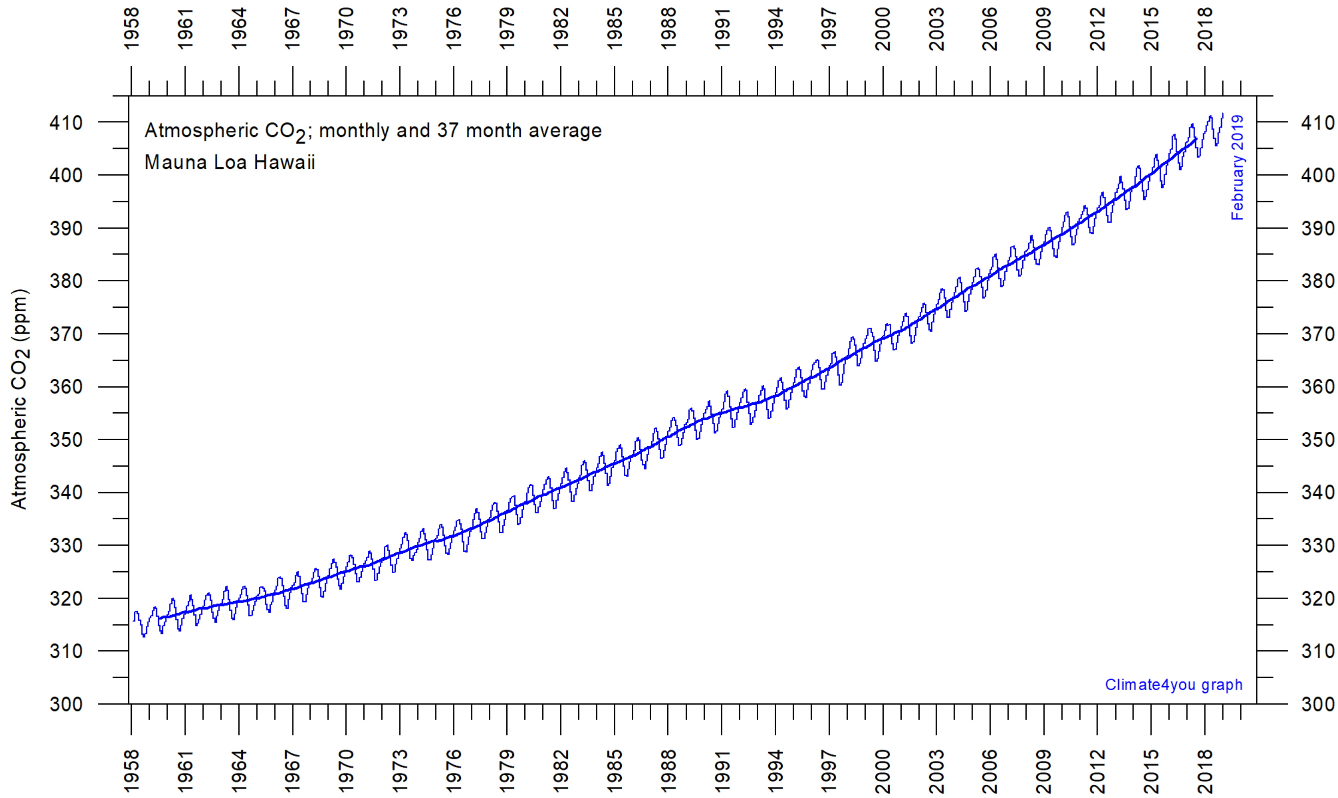

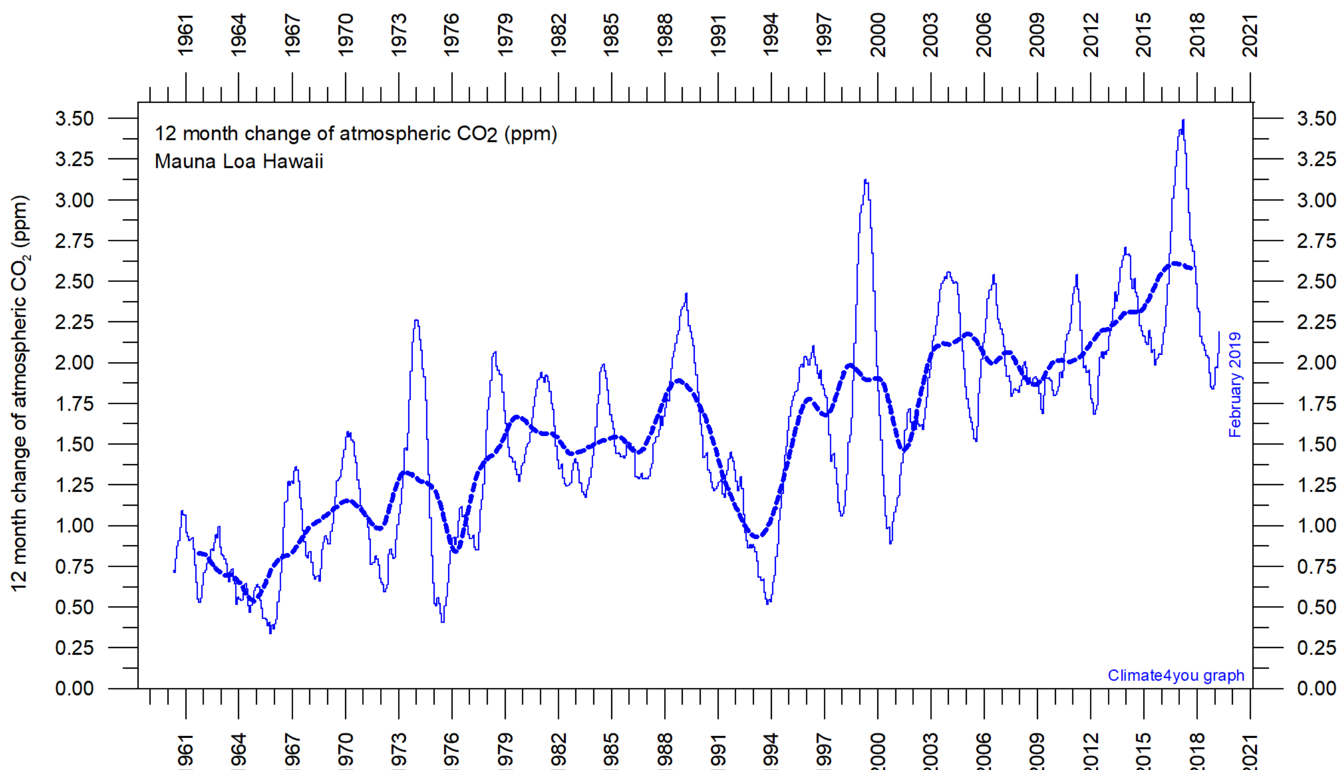

Monthly amount of atmospheric CO_2 (upper diagram) and annual growth rate (lower diagram); average last 12 months minus average preceding 12 months, thin line) of atmospheric CO_2 since 1959, according to data provided by the [Mauna Loa Observatory](), Hawaii, USA. The thick, stippled line is the simple running 37-observation average, nearly corresponding to a running 3-year average.

The relation between annual change of atmospheric CO_2 and La Niña and El Niño episodes, updated to February 2019

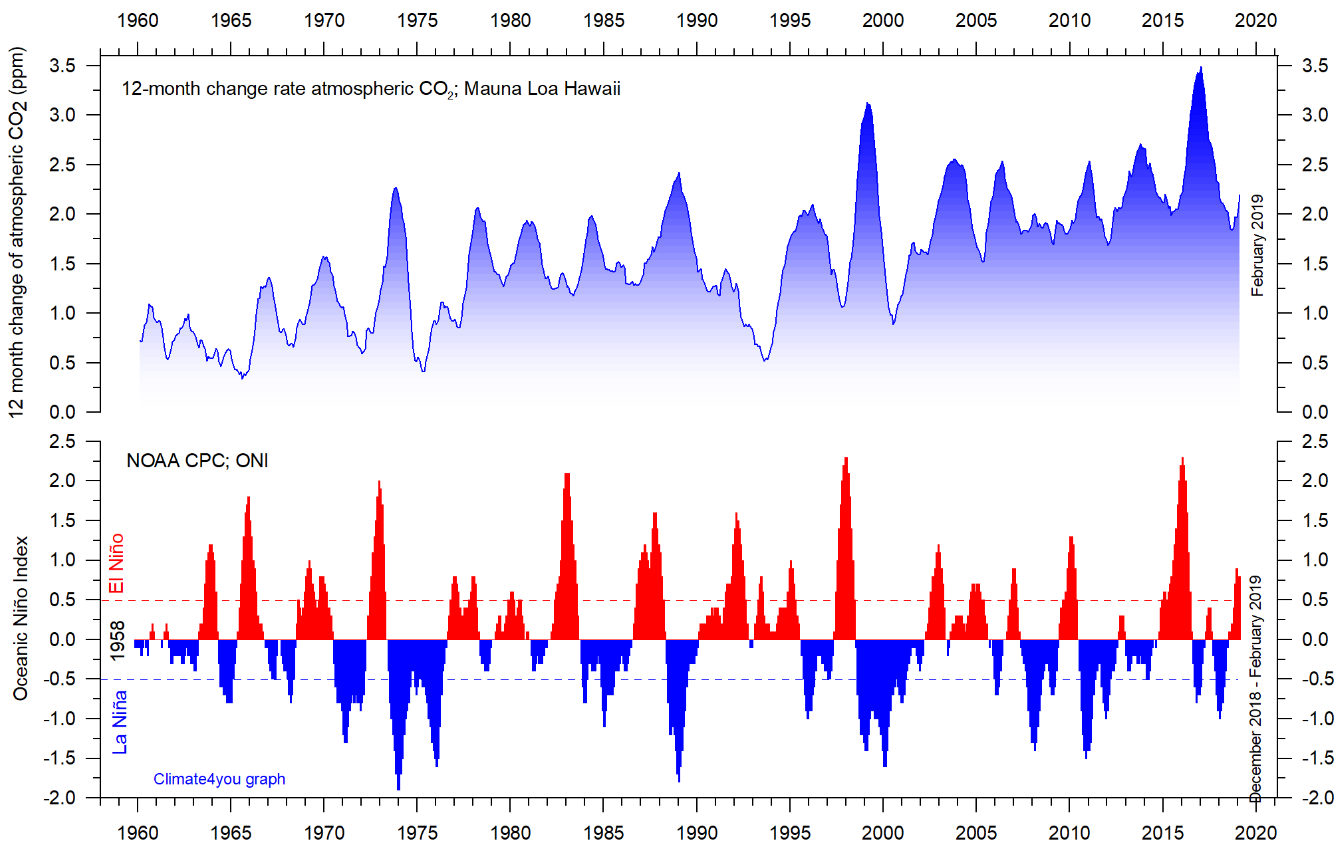

Visual association between annual growth rate of atmospheric CO_2 (upper panel) and Oceanic Niño Index (lower panel). See also diagrams on page 40 and 22, respectively.

<u>Note:</u> Changes in the global atmospheric CO_2 is seen to vary roughly in concert with changes in the Oceanic Niño Index. The typical sequence of events is that changes in the global atmospheric CO_2 <u>follows</u> changes in the Oceanic Niño Index.

The phase relation between atmospheric CO_2 and global temperature, updated to January 2019

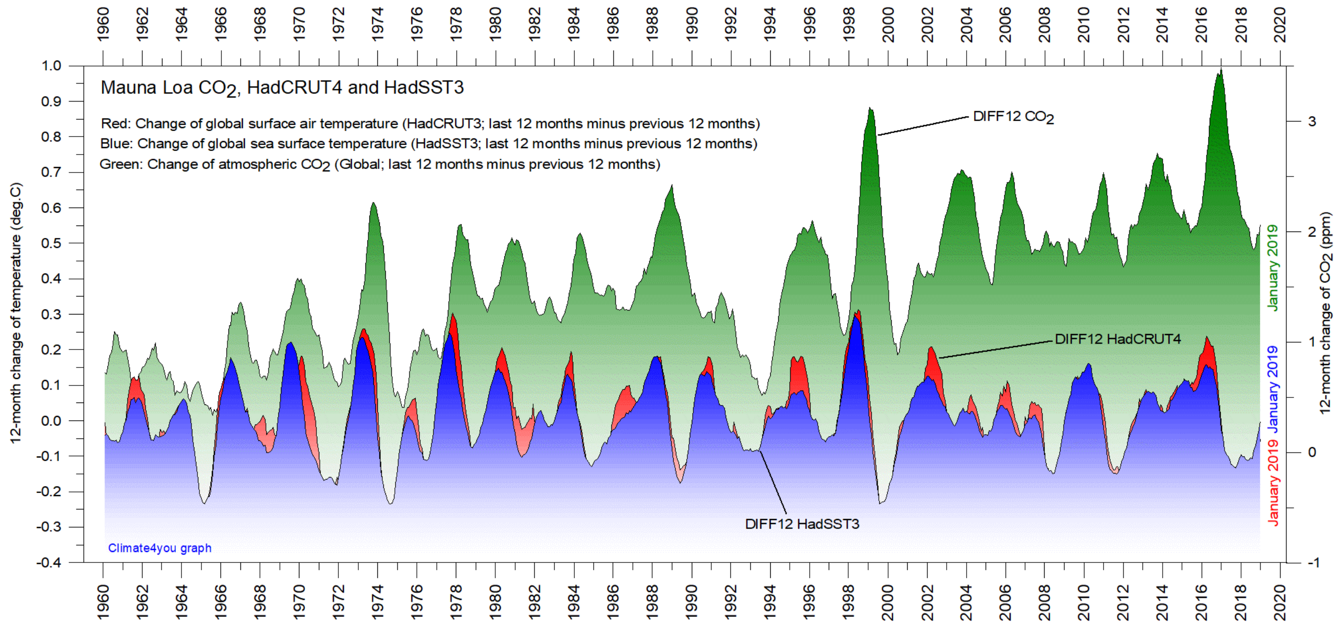

12-month change of global atmospheric CO_2 concentration (Mauna Loa; green), global sea surface temperature (HadSST3; blue) and global surface air temperature (HadCRUT4; red dotted). All graphs are showing monthly values of DIFF12, the difference between the average of the last 12 month and the average for the previous 12 months for each data series.

Note: The typical sequence of events is seen to be that changes in the global atmospheric CO_2 follows changes in global surface air temperature, which again follows changes in global ocean surface temperatures. Thus, changes in global atmospheric CO_2 are lagging 9.5–10 months behind changes in global air surface temperature, and no less than 11–12 months behind changes in global sea surface temperature.

References:

Humlum, O., Stordahl, K. and Solheim, J-E. 2012. The phase relation between atmospheric carbon dioxide and global temperature. Global and Planetary Change, August 30, 2012.
http://www.sciencedirect.com/science/article/pii/S0921818112001658?v=s5

Global air temperature and atmospheric CO_2, updated to February 2019

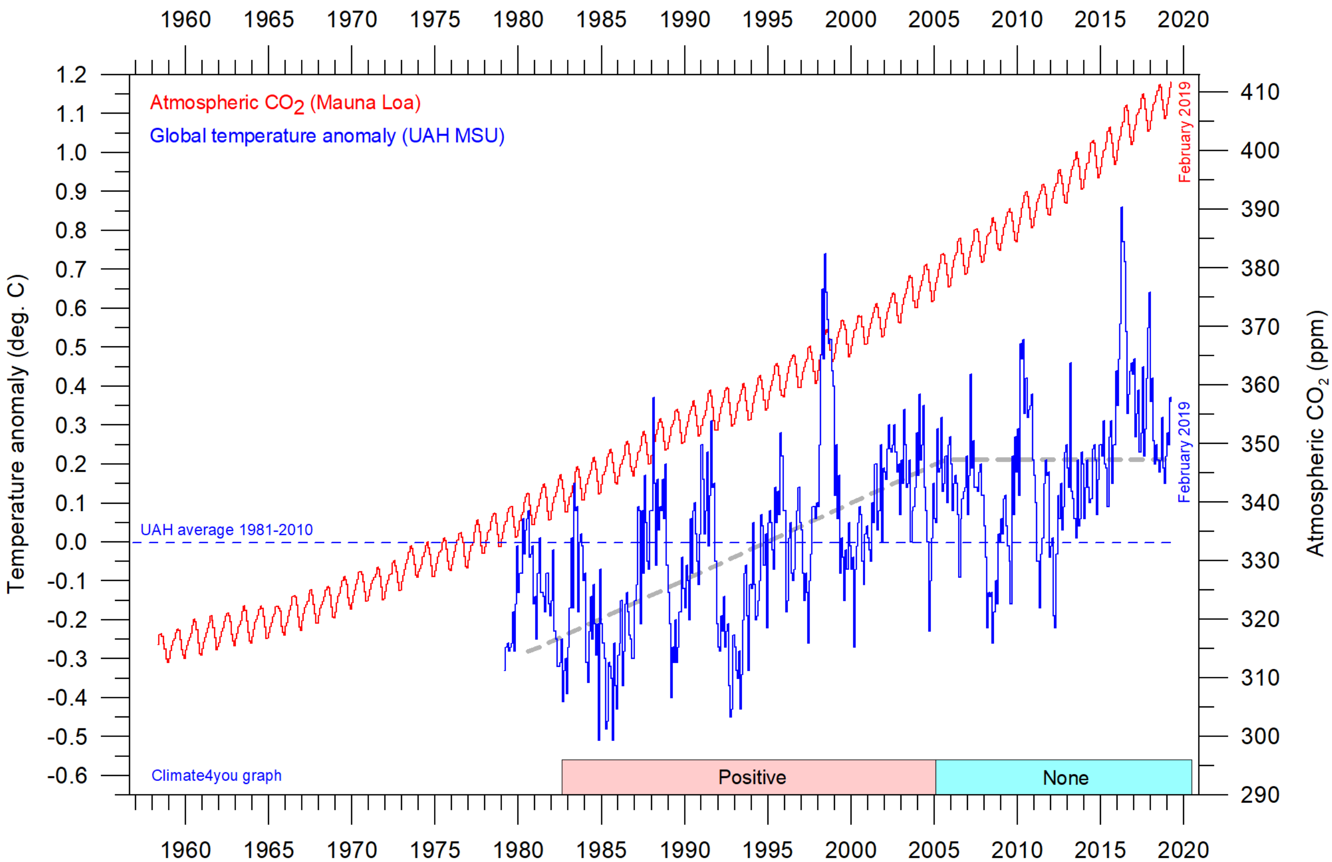

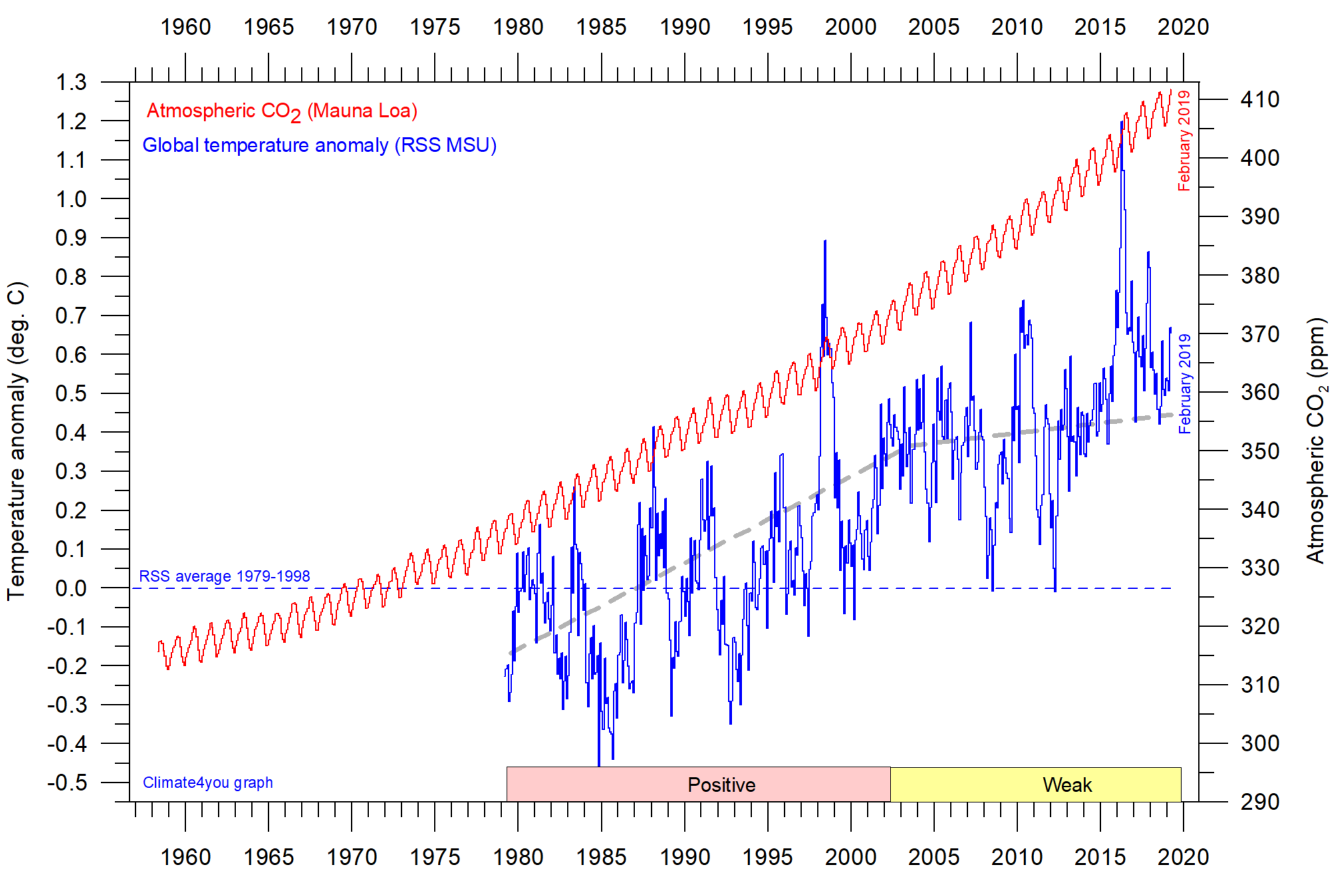

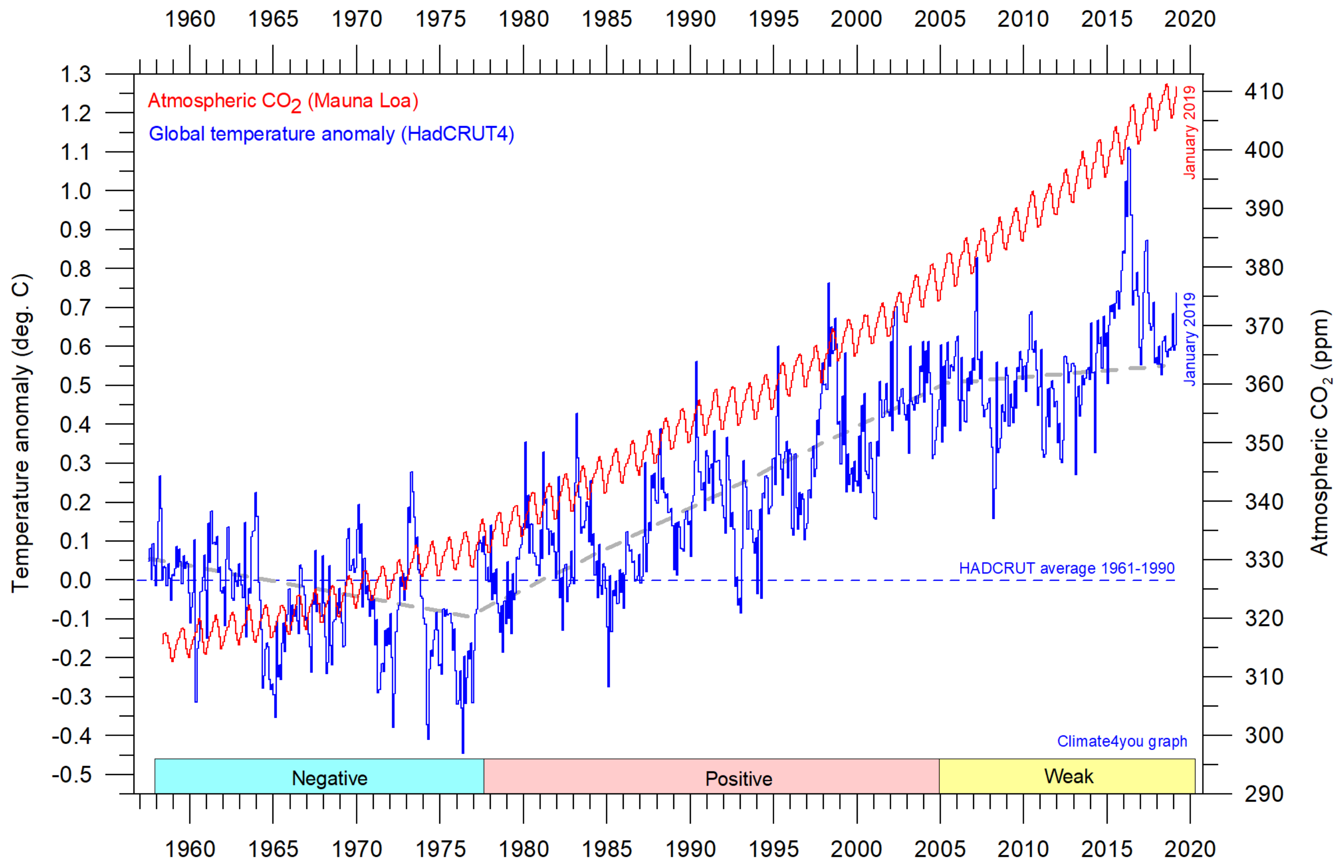
Atmospheric CO2 (Mauna Loa)
Global temperature anomaly (HadCRUT4)
January 2019
January 2019
HADCRUT average 1961-1990
Climate4you graph
Negative
Positive
Weak
Temperature anomaly (deg. C)
Atmospheric CO2 (ppm)

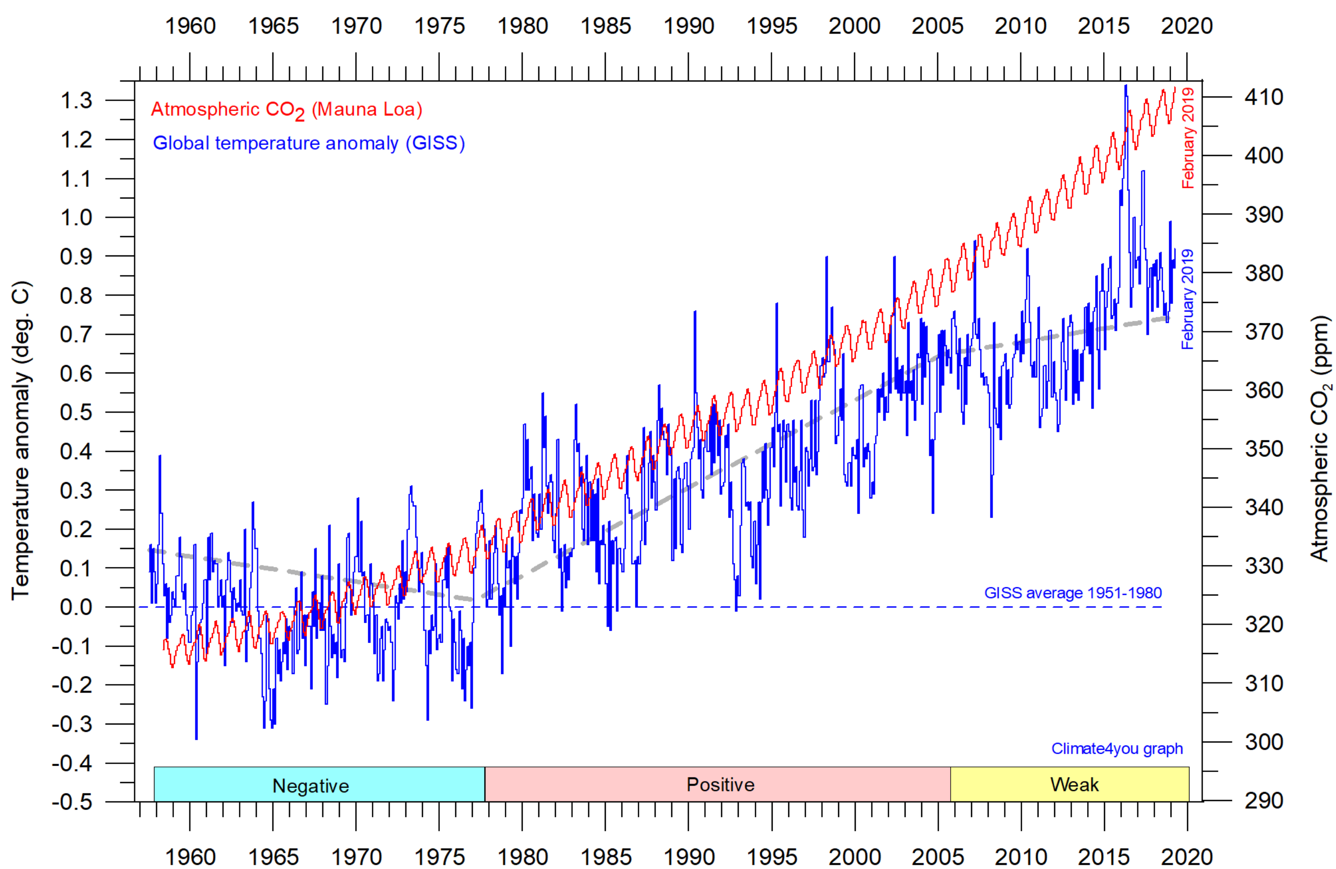
Atmospheric CO2 (Mauna Loa)
Global temperature anomaly (GISS)
February 2019
February 2019
GISS average 1951-1980
Climate4you graph
Negative
Positive
Weak
Temperature anomaly (deg. C)
Atmospheric CO2 (ppm)

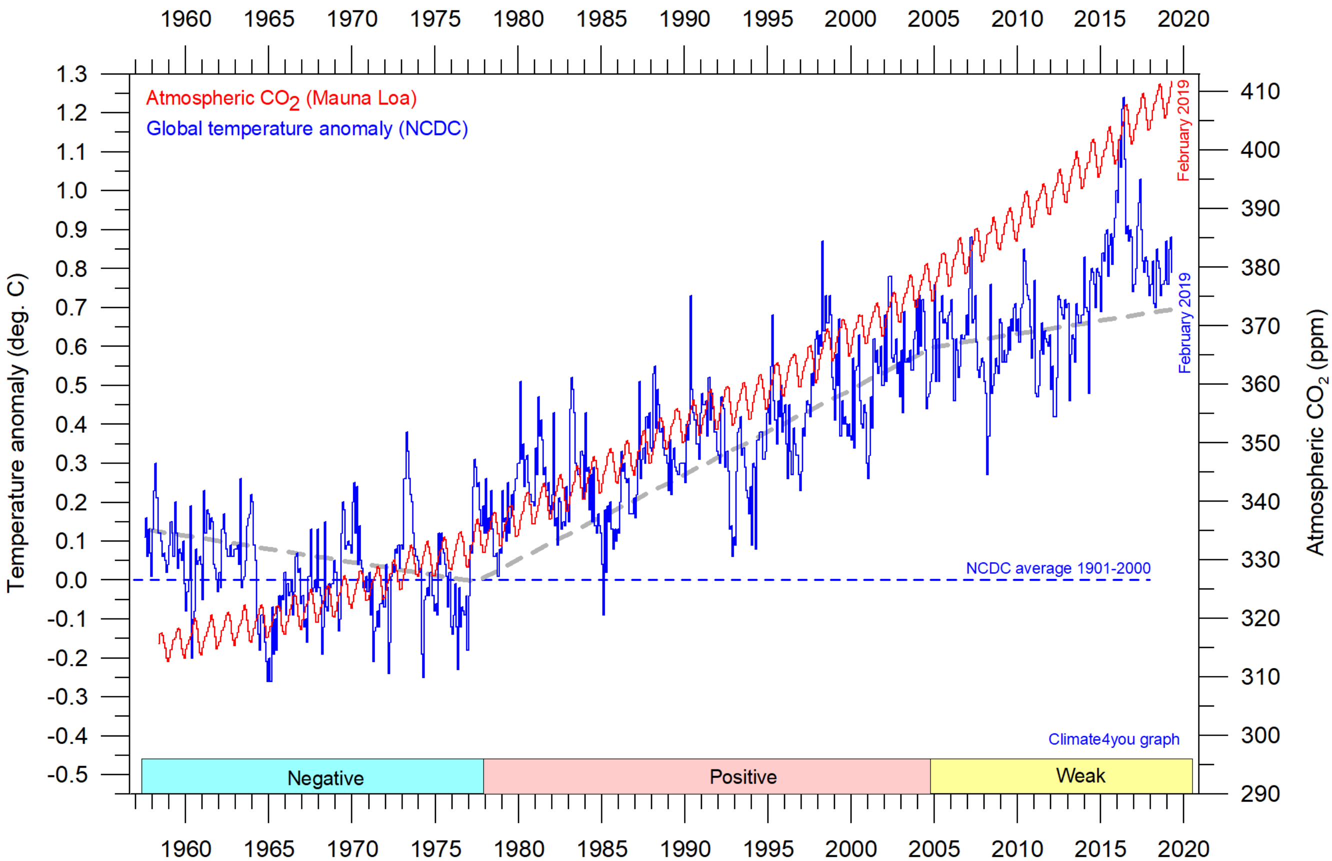

Diagrams showing UAH, RSS, HadCRUT4, GISS, and NCDC monthly global air temperature estimates (blue) and the monthly atmospheric CO_2 content (red) according to the [Mauna Loa Observatory](), Hawaii. The Mauna Loa data series begins in March 1958, and 1958 was therefore chosen as starting year for the all diagrams above. Reconstructions of past atmospheric CO_2 concentrations (before 1958) are not incorporated in this diagram, as such past CO_2 values are derived by other means (ice cores, stomata, or older measurements using different methodology), and therefore are not directly comparable with direct atmospheric measurements. The dotted grey line indicates the approximate linear temperature trend, and the boxes in the lower part of the diagram indicate the relation between atmospheric CO_2 and global surface air temperature, negative or positive.

Most climate models are programmed to give the greenhouse gas carbon dioxide CO_2 significant influence on global temperature. It is therefore relevant to compare different temperature records with measurements of atmospheric CO_2, as shown in the diagrams above.

Any comparison, however, should not be made on a monthly or annual basis, but for a longer time, as other effects (oceanographic, cloud cover, etc.) may override the potential influence of CO_2 on short time scales such as just a few years.

It is of cause equally inappropriate to present new meteorological record values, whether daily, monthly or annual, as demonstrating the legitimacy of the hypothesis ascribing high importance of atmospheric CO_2 for global temperatures. Any such meteorological record value may well be the result of other phenomena. Unfortunately, many news media repeatedly fall into this trap.

What exactly defines the critical length of a relevant period length to consider for evaluating the alleged importance of CO_2 remains elusive and represents a theme for discussion. However, the length of the critical period must be inversely proportional to the temperature sensitivity of CO_2, including feedback effects. Thus, if the net temperature effect of atmospheric CO_2 is strong, the critical period will be short, and vice versa.

However, past climate research history provides some clues as to what has traditionally been considered the relevant length of period over which to compare temperature and atmospheric CO_2. After about 10 years of concurrent global temperature- and CO_2-increase, IPCC was established in 1988. For obtaining public and political support for the CO_2-hyphotesis the 10-year warming period leading up to 1988 most likely was considered important. Had the global temperature instead been decreasing at that time, politic support for the hypothesis would have been difficult to obtain in 1988.

Based on the previous 10 years of concurrent temperature- and CO_2-increase, many climate scientists in 1988 presumably felt that their understanding of climate dynamics was enough to conclude about the importance of CO_2 for global temperature changes. From this it may safely be concluded that 10 years was considered a period long enough to demonstrate the effect of increasing atmospheric CO_2 on global temperatures. The 10-year period is also basis for the anomality diagrams shown on page 2.

Adopting this approach as to critical time length (at least 10 years), the varying relation (positive or negative) between global temperature and atmospheric CO_2 has been indicated in the lower panels of the diagrams above.

Latest 20-year QC1 global monthly air temperature changes, updated to February 2019

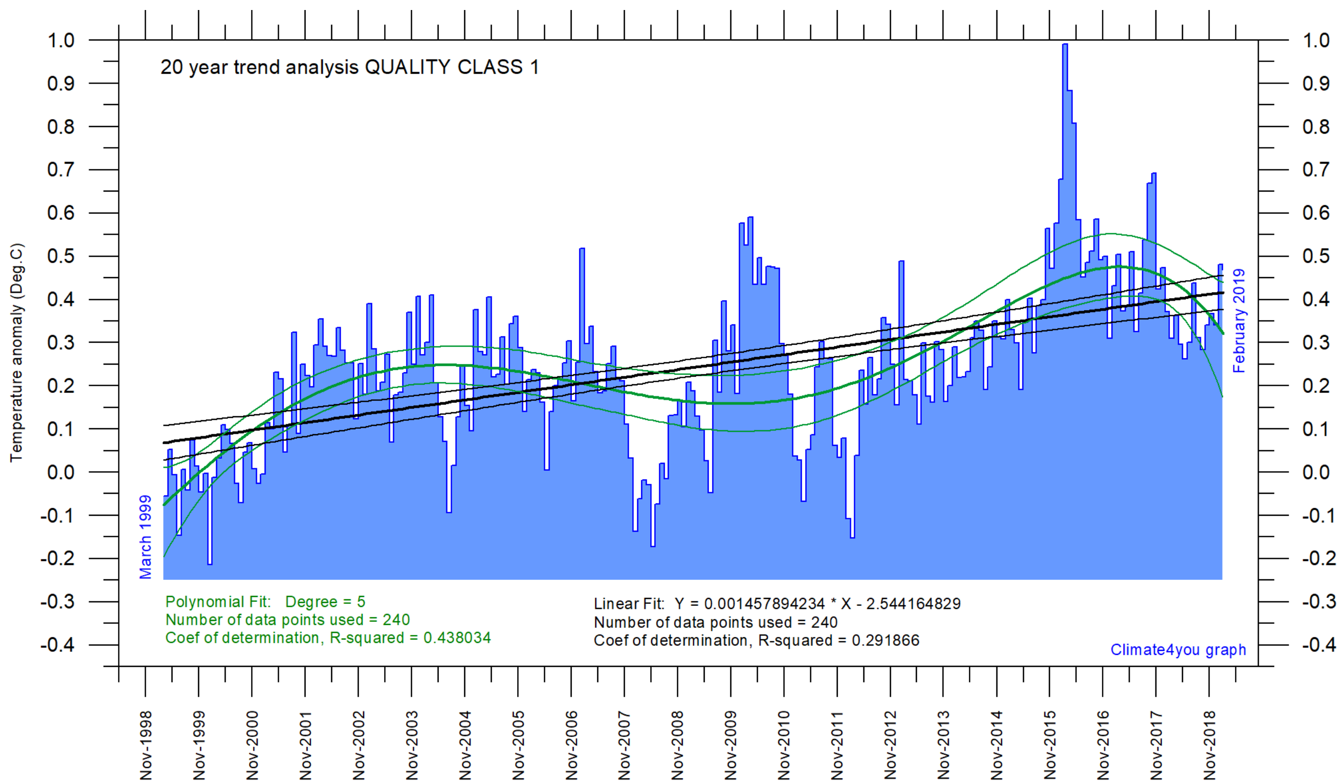

Last 20 years' global monthly average air temperature according to Quality Class 1 (UAH and RSS; see p.10) global monthly temperature estimates. The thin blue line represents the monthly values. The thick black line is the linear fit, with 95% confidence intervals indicated by the two thin black lines. The thick green line represents a 5-degree polynomial fit, with 95% confidence intervals indicated by the two thin green lines. A few key statistics are given in the lower part of the diagram (please note that the linear trend is the monthly trend).

In the still ongoing climate debate the following about the global surface air temperature is often put forward: Is the surface air temperature still increasing or has it basically remained without significant changes during the last about 15 years?

The diagram above may be useful in this context and demonstrates the differences between two often used statistical approaches to determine recent temperature trends. Please also note that such fits only attempt to describe the past, and usually have small, if any, predictive power. In addition, before using any linear trend (or other) analysis of time series a proper statistical model should be chosen, based on statistical justification.

For temperature time series, there is no *a priori* physical reason why the long-term trend should be linear in time. In fact, climatic time series often have trends for which a straight line is not a good approximation, as is clearly demonstrated by several of the diagrams shown in the present report.

For an excellent description of problems often encountered by analyses of temperature time series analyses, please see [Keenan, D.J. 2014: Statistical Analyses of Surface Temperatures in the IPCC Fifth Assessment Report]().

Sunspot activity and QC1 average satellite global air temperature, updated to February 2019

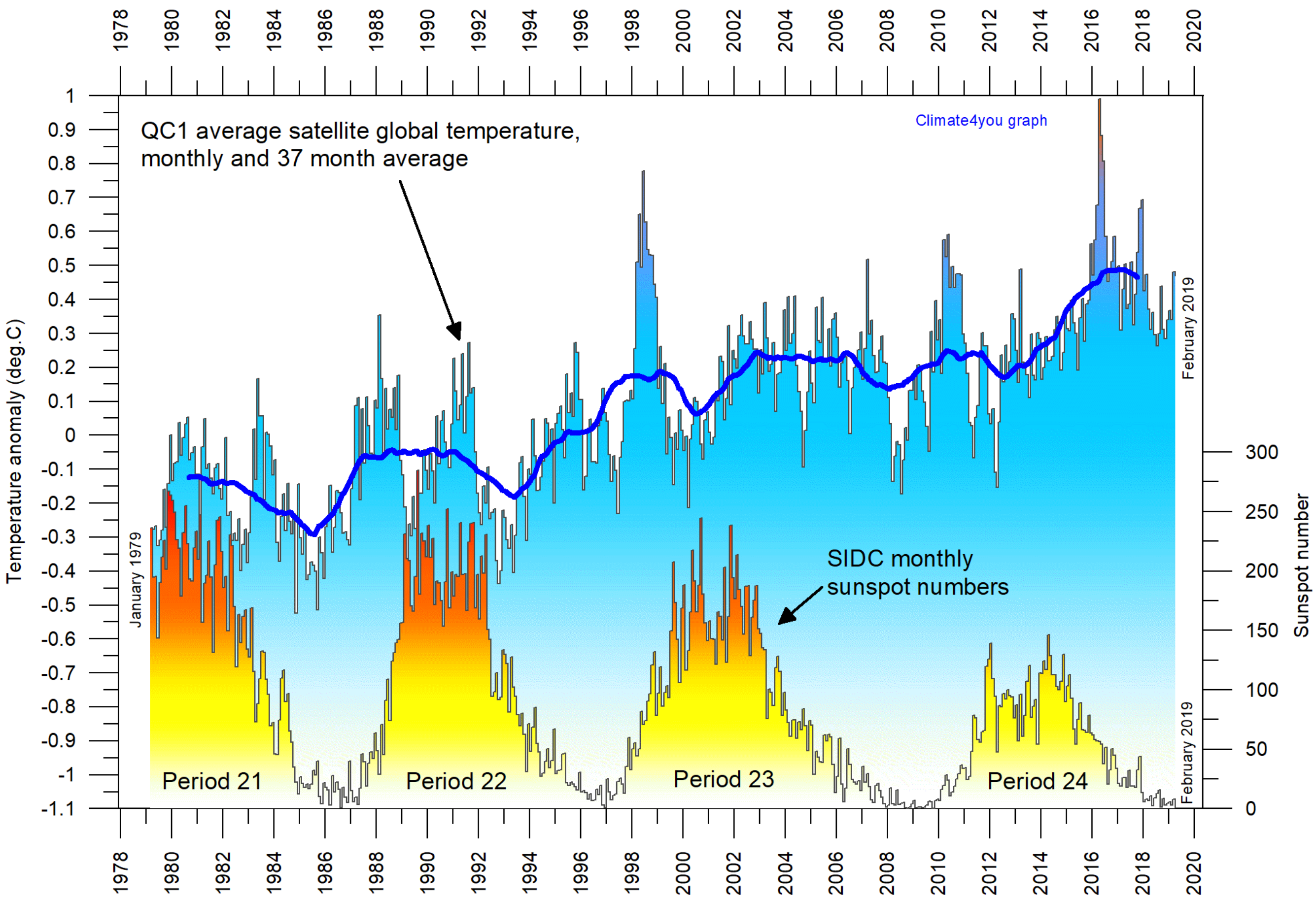

Variation of global monthly air temperature according to Quality Class 1 (UAH and RSS; see p.4) and observed sunspot number as provided by the Solar Influences Data Analysis Center (SIDC), since 1979. The thin lines represent the monthly values, while the thick line is the simple running 37-month average, nearly corresponding to a running 3-year average. The asymmetrical temperature 'bump' around 1998 is influenced by the oceanographic El Niño phenomenon in 1998, as is the case also for 2015-16.

1840: Louis Agassiz visits the Parallel Roads of Glen Roy

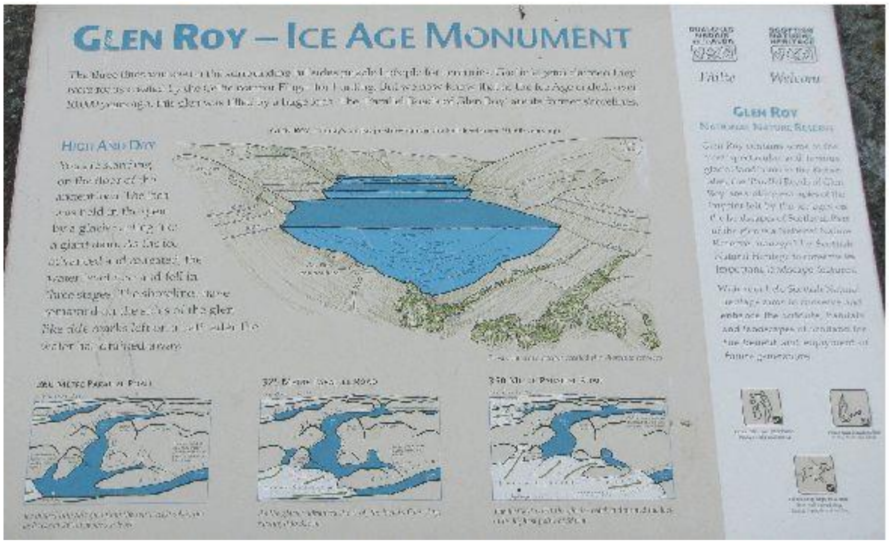

Popular explanation on the origin of the Parallel Roads of Glen Roy as displayed at the main parking lot in Glen Roy, June 2, 2008 (left). The valley Glen Roy is recognized as one of the most important geological sites and arguably the most famous landform in Great Britain. This is the place where the former existence of glaciers outside the Alps for the first time in earnest was recognized by scientists. This, in turn, also lead to the conclusion that Earth had been exposed to large, natural climatic variations. Portrait of Jean Louis Rodolphe Agassiz (right).

Jean Louis Rodolphe Agassiz (1807-1873) was born in Môtier (now part of Haut-Vully) in the canton of Fribourg, Switzerland. He studied at the universities of Zürich, Heidelberg and Munich, extending his knowledge of natural history, especially of botany. Following a subsequent move to the University of Paris, he became interested in geology and zoology, especially fish.

In 1832 he was appointed professor of natural history in the University of Neuchâtel in Switzerland. Here the fossil-rich slates and limestones attracted his interest, although very little previously had been accomplished in the way of scientific study of these deposits. This resulted in a long palaeontological interest in the classification of fossil fish. Under his inspiring leadership, the University of Neuchâtel soon became a leading institution for scientific research.

In the meantime, the glaciers of the Alps had been made an object for scientific studies by naturalists and scientists like De Saussure, Venetz, Charpentier and Schimper. Both Charpentier and Schimper had suggested that fragments of alpine rocks scattered over the slopes and summits of the Jura Mountains in westernmost Switzerland had been transported there by former glaciers.

This scientific issue attracted the attention of Agassiz, and he had the opportunity to discuss it with both Charpentier and Schimper, and subsequently made successive journeys to the alpine regions in company with them. He even had a hut constructed upon one of the Aar glaciers in central Switzerland, to investigate the structure and movement of the glacier. Based on this work, Agassiz in 1837 became the first to scientifically propose that the Earth once had been subject to a past ice age with much cooler climate and more extensive glaciers. At that time this was a bold or even outrageous hypothesis, demanding large climatic changes in the past.

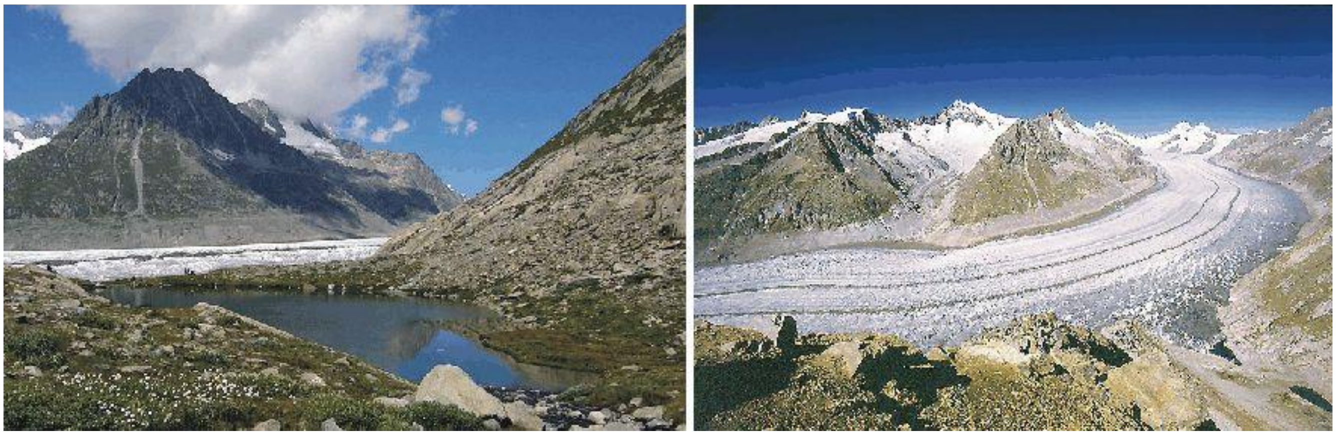

Lake Marjelensee at Grosser Aletschgletscher in Berner Oberland, Switzerland (left). Previously, during the Little Ice Age, Aletschgletscher was thicker and Marjelensee dammed by the glacier and therefore larger and deeper than now. Grosser Aletschgletscher looking NW (right). Lake Marjelensee, including a remnant ice-dammed par, is seen in the lower right corner. The upper limit of the grey zone seen above the glacier indicate the position of the glacier surface and Marjelensee around 1850-60, when the present period of glacier recession began in the Alps.

In 1840 Agassiz published two volumes entitled *Etudes sur les glaciers* ("Study on Glaciers"). Here he discussed glacier movement, formation of moraines, and glacier erosion as demonstrated by striae and roches moutonnées seen in front of many glaciers in the Alps. As many glaciers at that time was growing, he had no difficulty in accepting Charpentier's and Schimper's idea that some of the alpine glaciers previously had extended across the wide plains and valleys, far beyond their contemporary size. However, Agassiz went still farther in his conclusions. He concluded that, in the relatively recent past, Switzerland had been like Greenland, and that one vast sheet of ice, originating in the central Alps, had extended over the entire lowland of northwestern Switzerland, reaching the Jura mountains.

The publication of this work gave a fresh impetus to the study of glacial phenomena in all parts of the world. In addition, it was important to Agassiz to convince the geological community in Britain, then at the forefront of international geological science. For that reason, Agassiz in 1842 visited Scotland.

Following a presentation of his '*outrageous ideas*' at a meeting of the British Association in Glasgow, Agassiz departed on a tour of the West Highlands, accompanied by the Rev. William Buckland, professor of Geology and Mineralogy at Oxford University. North-east of Fort Williams, Agassiz visited the already at that time famous Parallel

Roads of Glen Roy. A few years before, in 1938, Charles Darwin (1839) had interpreted the Parallel Roads as former marine shorelines, suggesting that Scotland since had been exposed to considerable tectonic uplift because of movements of molten rock below the surface (see Climate4you update January 2019). The valley Glen Roy is said to have made a thorough impression on Agassiz. He immediately interpreted the terraces as shorelines formed along a past lake dammed by a now vanished glacier. In Switzerland, he had seen similar terraces around present-day ice dammed lakes, especially at lake Marjelensee at the eastern side of Grosser Aletschgletscher in Berner Oberland (see photos on the previous page).

Upper end of Glen Roy, looking ENE on September 3, 2000. The uppermost of the former lake shorelines (350 m asl.) are seen to fit in altitude with the pass at the head of the valley. During this maximum sea level, water from ice-dammed Loch Glen Roy spilled over in the neighbouring Drummin valley to the east, to continue into the Spey drainage system further east. After the disappearance of the lake, a major landslide has taken place on the southern valley side (to the right), destroying the old shorelines. The age of this landslide is not known, but it has been speculated that this and other landslides in the area may have been released as permafrost thawed after the last glacial period.

After having visited Glen Roy, Agassiz travelled to Fort Augustus 30 km north of Glen Roy, on way to Inverness in NE Scotland, before continuing to Edinburgh. From Fort Augustus Agassiz wrote a letter about his findings to editor Robert Jameson in Edinburgh, intending that it be published in the *Edinburgh New Philosophical Journal* (McKirdy et al. 2007). Jameson immediately recognised the significance of Agassiz' discoveries. As the latest issue of his journal was already in press, Jameson passed the letter on to Charles Maclaren, editor of the still existing newspaper *The Scotsman*. Maclaren was also a geologist by training, and equally rapidly grasped the importance of Agassiz's letter. Thus, on 7 October 1840, under the headline, *'Discovery of former glaciers in Scotland, especially in the Highlands, by Professor Agassiz'*, the Ice Age was first announced to the wider public in a daily Scottish newspaper.

The ice-dammed lake in Glen Roy and in two other valleys in the Lochaber region of western Scotland were produced by the readvance of glaciers from west of the Great Glen (the valley containing Loch Ness) up the lower part of Glen Spean. These valleys today drain west, towards the Atlantic Ocean. The advance of glaciers 12,500-12,000 years ago blocked off the drainage outlet, causing Glen Roy, Glen Glory and Glen Spean to fill with water, until spilling over a threshold at 260 m altitude into valleys draining east into the present North Sea area. Further advance of ice up these glens fragmented this large water body into three separate lakes, forcing the Glen Roy lake to empty over a higher col at 325 m, eventually to empty directly into the Spey drainage system across a col at the valley head at 350 m altitude. At the glaciers later retreated, each of these three outlets was opened in turn, presumably starting with a flood event, a *jökulhlaup*, and then for a time stabilising the level of the lake surface at successively lower altitudes.

Fort Augustus at the south-western end of Loch Ness, looking W on June 2, 2008 (left). The valley bottom is filled with glaciofluvial sediments, deposited by a large river draining meltwater from glaciers further to the SW. A thick layer of the glaciofluvial sediments is very coarse-grained, with individual clasts up to 30-40 cm in size, and may have been derived from a jökulhlaup generated by sudden drainage of the former ice-dammed lake in Glen Roy (right).

The Parallel Roads of Glen Roy themselves presumably were eroded by a combination of wave action and frost weathering of bedrock at lake level, at any time maintained by the lowest available outlet possibility. In Glen Roy there are three main shorelines, at 350 m, 325 and 260 m above sea level. At its maximum size the lake in Glen Roy attained a surface area of c. 73 km^2 and a maximum water volume of c. 5 km^3.

Sissons (1979) suggested that, in common with many present-day ice-dammed lakes, this huge body of water would periodically have emptied in a gigantic flood or *jökulhlaup*, with a discharge of possibly as much as 22,500 m^3/s. The earliest such *jökulhlaup* followed the Great Glen to Inverness in NE Scotland, passing through Loch Ness. At the town Fort Augustus at the SW end of Loch Ness a huge fan of coarse gravel and stones 7 km^2 in area and up to 39 m thick was interpreted by Sissons (1979) as a *jökulhlaup* deposit, produced in a few days some time 11,500-12,000 years ago, as a result of the breaching of the ice dam in lower Glen Roy, some 30 km away (see photos above).

The glacier advance creating the ice-dammed lake in Glen Roy was caused by a sudden period of climatic cooling at the end of the last ice age. This climatic reversal is today known as the Younger Dryas or the Greenland Stadial 1. In Scotland it is locally better known as the Loch Lomond Readvance.

REFERENCES:

Darwin, C.R. 1839. Observations on the parallel roads of Glen Roy, and of other parts of Lochaber in Scotland, with an attempt to prove that they are of marine origin. *Philosophical Transactions of the Royal Society* 129, 39-81. Read before the Society 7 February 1839. http://darwin-online.org.uk/content/frameset?itemID=F1653&viewtype=text&pageseq=1

McKirdy, A., Gordon, J. and Crofts, R. 2007. *Land of mountain and flood. The geology and landforms of Scotland*. Birlinn Limited, Edinburgh, Scotland, 324 pp.

Sissons, J.B. 1979. The limit of the Loch Lomond Advance in Glen Roy and vicinity. *Scottish Journal of Geology* 15, 31-42.

*****

All diagrams in this report, along with any supplementary information, including links to data sources and previous issues of this newsletter, are freely available for download on www.climate4you.com

Yours sincerely,

Ole Humlum (Ole.Humlum@gmail.com)

Arctic Historical Evaluation and Research Organisation, Longyearbyen, Svalbard

March 20, 2019.